

## **Fourth Malmö Conference on Medical Imaging**



## **Optimisation in X-ray and Molecular Imaging 2015**

Gothenburg, Sweden

28-30 May 2015

**Programme and abstracts**

## Welcome to Gothenburg and OXMI 2015!

We are pleased to welcome you to Optimisation in X-ray and Molecular Imaging 2015 – the 4<sup>th</sup> edition of the Malmö Conference on Medical Imaging and the first to be held in Gothenburg, Sweden.

The Malmö Conference on Medical Imaging is a successful series of scientific conferences focusing on optimisation of medical imaging with special emphasis on image quality evaluation and radiation safety.

Six years have passed since the last conference in Malmö in June 2009. The exciting new advances in the imaging field we saw at that time are now in many ways already part of standard hospital procedures and can often be found also outside the doors of the radiological departments. Today, highly advanced imaging equipment is used in operating rooms and for dose planning in radiation therapy. The fast development of methods and equipment and their entry into hospital routine is a true challenge when it comes to resources and methods for optimisation.

The aim of this conference is to adopt this challenge and to contribute to the continuing development of adequate methods and strategies for optimisation. Patients now and tomorrow undergoing imaging procedures should be able to rely on the fact that the image quality is adequate and the radiation dose is reasonably low.

We invite you to three exciting conference days!



*Magnus Båth*

Chair Scientific Committee



*Lars Gunnar Månsson*

Chair Organising Committee

Follow the conference on Twitter!

Twitter account @OXMI2015 (#OXMI2015)

## **Meeting place for the conference**

Conference Center Wallenberg  
Medicinaregatan 20A, Gothenburg, Sweden

Google Map: [Medicinaregatan 20A](#)

## **Information and contact**

Web page: [www.oxmi.org](http://www.oxmi.org)

Twitter account: @OXMI2015 (#OXMI2015)

Email: [info@oxmi.org](mailto:info@oxmi.org)

## **Get-together (Wednesday 27 May)**

Conference Center Wallenberg from 18.00

## **Conference dinner (Friday 29 May)**

Världskulturmuseet (Museum of World Culture) at 19.30

Restaurant Tabla

Södra Vägen 54, Gothenburg

## **Conference bureau**

Demo Meeting

Göteborgsvägen 91A

SE - 431 37 Mölndal, Sweden

+46 70 954 54 37

[info@oxmi.org](mailto:info@oxmi.org)

## Useful telephone numbers

### ***Organising committee***

Cellular phones: +46 70 526 40 25 (Lars Gunnar Månsson, chair)  
+46 73 660 14 91 (Jonny Hansson, co-chair)

### ***Scientific committee***

Cellular phones: +46 73 625 44 99 (Magnus Båth, chair)  
+46 70 526 40 25 (Lars Gunnar Månsson, co-chair)

### ***Taxi***

Taxi Göteborg	+46 31 65 00 00
Taxi Kurir	+46 31 27 27 27

### ***Hotels***

#### [Hotel Gothia Towers](#)

Mässans gata 24  
Gothenburg  
Tel: +46 31 750 88 00  
Tram/Bus stop *Korsvägen*

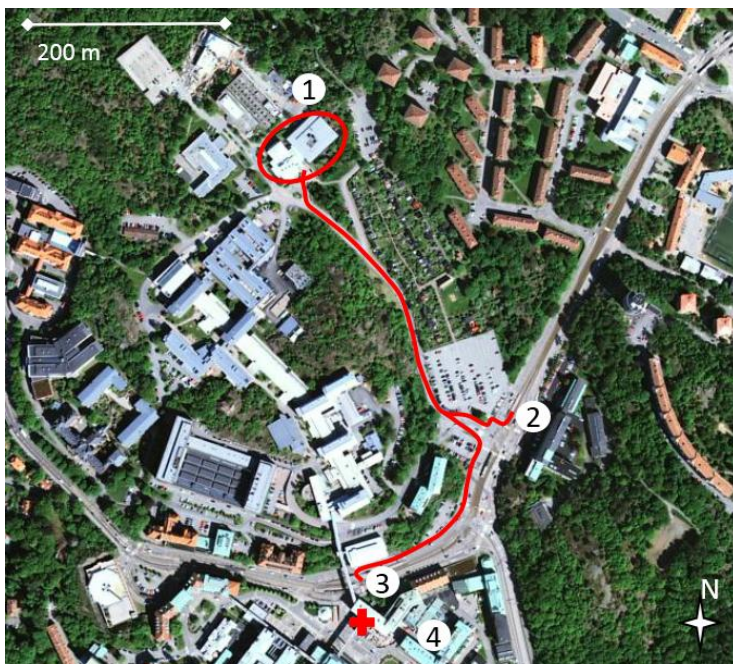
#### [Hotel Panorama](#)

Eklandagatan 51  
Gothenburg  
Tel: +46 31 767 70 00  
Bus stop *Utlandagatan*

#### [Slottsskogens Vandrarhem](#) (Youth Hostel)

Vegagatan 21  
Gothenburg  
Tel: +46 31 42 65 20  
Tram/Bus stop *Olivedalsgatan*

## Map and transportation



- ① **Conference Centre Wallenberg**  
Address: Medicinaregatan 20A
- ② **Tram/Bus stop *Medicinaregatan***  
Trams: 6, 7, 8, 13
- ③ **Tram/Bus stop *Sahlgrenska Huvudentré***  
Trams: 6, 7, 8, 13  
Buses: 16, 52
- ④ **Sahlgrenska University Hospital**

Web page for transportation with tram or bus: [www.vasttrafik.se](http://www.vasttrafik.se)

Transportation to Museum of World Culture (conference dinner) from Conference Centre Wallenberg: trams 6, 8, 13 to *Korsvägen*.

## **Local Organising Committee**

Lars Gunnar Månsson, chair  
Jonny Hansson, co-chair  
Anja Almén  
Magnus Båth  
Emma Eliasson  
Jakobína Grétarsdóttir  
Charlotta Lundh  
Ylva Surać  
Angelica Svalkvist  
Christina Söderman  
Anne Thilander-Klang  
Alexa von Wrangel

## **Scientific Committee**

Magnus Båth, Gothenburg, chair  
Lars Gunnar Månsson, Gothenburg, co-chair  
Anja Almén, Gothenburg, SE  
Peter Bernhardt, Gothenburg, SE  
Hilde Bosmans, Leuven, BE  
Dev Chakraborty, Pittsburgh, US  
David Dance, Guildford, GB  
James T Dobbins III, Durham, US  
Jakobína Grétarsdóttir, Gothenburg, SE  
Christoph Hoeschen, Munich, DE  
Åse Johnsson, Gothenburg, SE  
Charlotta Lundh, Gothenburg, SE  
Sören Mattsson, Malmö, SE  
Michael Moores, Liverpool, GB  
Michael Sandborg, Linköping, SE  
Angelica Svalkvist, Gothenburg, SE  
Anne Thilander-Klang, Gothenburg, SE  
Anders Tingberg, Malmö, SE  
Francis Verdun, Lausanne, CH  
Eleonor Vestergren, Gothenburg, SE

## **Conference organisers**

Sahlgrenska University Hospital, Gothenburg – University of Gothenburg –  
Skåne University Hospital, Malmö – Lund University –  
Helmholtz Zentrum München – IRS Liverpool –  
Swedish Society for Radiation Physics

## **Commercial Exhibitors**

### **GE Healthcare Sverige AB**

Skårs led 3, SE-412 63 Gothenburg, Sweden

[www3.gehealthcare.se](http://www3.gehealthcare.se)

### **Mediel AB**

Box 172, SE-431 22 Mölndal, Sweden

[www.mediel.se](http://www.mediel.se)

### **Mentice**

Odinsgatan 10, SE-411 03 Gothenburg, Sweden

[www.mentice.com](http://www.mentice.com)

### **Nuklex**

Kungsgatan 111, SE-753 18 Uppsala, Sweden

[www.nuklex.se](http://www.nuklex.se)

### **Philips Healthcare**

Knarrarnäsgatan 7, SE-164 85 Stockholm, Sweden

[www.healthcare.philips.com/se](http://www.healthcare.philips.com/se)

### **PTW-Freiburg**

Lörracher Strasse 7, DE-79115 Freiburg, Germany

[www.ptw.de](http://www.ptw.de)

### **Scanflex Medical AB**

Tumstocksvägen 9A, SE-187 66 Täby, Sweden

[www.scanflex.se](http://www.scanflex.se)

### **Sectra AB**

Teknikringen 20, SE-583 30 Linköping, Sweden

[www.sectra.com](http://www.sectra.com)

### **Siemens Healthcare**

Johanneslundsvägen 12-14, SE-194 87 Upplands Väsby, Sweden

[www.siemens.se/healthcare](http://www.siemens.se/healthcare)

### **Toshiba Medical Systems Sverige**

Sisjö Kullegata 8 (plan2), SE-421 32 V. Frölunda, Sweden

[www.toshiba-medical.eu](http://www.toshiba-medical.eu)

### **Unfors RaySafe AB**

Uggledalsvägen 29, SE-427 40 Billdal, Sweden

[www.raysafe.com](http://www.raysafe.com)

## Wednesday, 27 May 2015

18.00-

Get-together and registration

## Thursday, 28 May 2015

08.00-08.30

Registration

*Oral session 1*

08.30-10.00

**Conference opening and introductory session**

Chairs: S Mattsson and L G Månsson

08.30-08.45

**Welcome**

L G Månsson

*Sweden*

08.45-09.00

**[O 1-1] The centre for imaging and intervention at Sahlgrenska University Hospital – a house of possibilities**

J Grétarsdóttir and J Hansson

*Sweden*

09.00-10.00

**Invited speaker**

**[O 1-2] Spectral CT, basic principles, applications, and prospects for molecular imaging**

Norbert J Pelc (Stanford University)

*USA*

10.00-10.30

Coffee

*Oral session 2*

10.30-12.00

**Computed Tomography**

Chairs: H Bosmans and Å A Johnsson

10.30-10.45

**[O 2-1] A study of the image quality of CT brain adaptive statistical iterative reconstructed (ASiR) images using subjective and objective methods**

J Mangat, J Morgan, P Clinch, A Reilly, M Bâth, J Clinch, E Chaloner and M Lewis

*United Kingdom and Sweden*

10.45-11.00

**[O 2-2] The effect of Adaptive Statistical iterative Reconstruction (ASiR) on assessment of diagnostic quality and visualisation of anatomical structures in paediatric head CT examinations**

J Larsson, M Bâth, K Ledelius and A Thilander-Klang

*Sweden*

11.00-11.15

**[O 2-3] Model based iterative reconstruction IMR gives possibility to evaluate thinner slice thicknesses than conventional iterative reconstruction iDose4 – a phantom study**

M-L Aurumskjöld, K Ydström, A Tingberg and M Söderberg

*Sweden*

11.15-11.30

**[O 2-4] Comparison of Adaptive Statistical Iterative Reconstruction (ASiR) and VEO reconstruction for paediatric abdominal CT examinations – an observer performance study of diagnostic image quality**

M Hultenmo, H Caisander, K Mack and A Thilander-Klang

*Sweden*

11.30-11.45

**[O 2-5] Paediatric CT protocol optimisation: Adapting Size Specific Dose Estimates to recalculate CT protocol parameters for five body sizes**

K Rani, A Jahnen, A Noel and D Wolf

*Luxembourg and France*

11.45-12.00

**[O 2-6] Low dose CT of the lumbar spine at about 1 mSv compared with lumbar spine radiography; a phantom and clinical study**

M Alshamari, M Geijer, E Norrman, M Lidén, W Krauss, F Wilamowski and H Geijer

*Sweden*



---

12.00-13.30

Lunch

*Oral session 3*

13.30-15.00

**Image perception by human and model observers**

Chairs: C Hoeschen and M Sandborg

13.30-14.15

*Invited speaker*

**[O 3-1] Medical Image Perception I: The human search engine**

Jeremy M Wolfe (Harvard Medical School)

USA

14.15-14.30

**[O 3-2] Objective task based assessment of low contrast detectability in iterative reconstruction**

D Racine, A H Ba, J G Ott, N Ryckx, F O Bochud and F R Verdun

Switzerland

14.30-14.45

**[O 3-3] Patient exposure optimisation through task-based assessment of a new iterative reconstruction technique: the ADMIRE algorithm**

J G Ott, A H Ba, D Racine, N Ryckx, F O Bochud, H Alkadhi and F R Verdun

Switzerland

14.45-15.00

**[O 3-4] The effect of fixed adaptation on the calibration of medical displays**

P Sund, L G Månsson and M Båth

Sweden

---

15.00-15.30

Coffee

*Oral session 4*

15.30-16.45

**Segmentation and classification**

Chairs: D Dance and E Vestergren

15.30-15.45

**[O 4-1] Improved detection rate and visualization of liver uptake foci in diagnostic <sup>111</sup>In-octreotide SPECT/CT investigations with a novel segmentation analysis**

T Magnander, E Wikberg, J Nilsson, J Svensson, P Gjertsson, B Wångberg, M Båth and P Bernhardt

Sweden

15.45-16.00

**[O 4-2] Pulmonary nodule segmentation by mean-shift and quantum clustering**

A Chodorowski and Q Mahmood

Sweden

16.00-16.15

**[O 4-3] Volumetric localization of dense breast tissue using breast tomosynthesis data**

M Dustler, H Pettersson and P Timberg

Sweden

16.15-16.30

**[O 4-4] Volumetric breast density in spectral tomosynthesis**

K Berggren, M Lundqvist, M Wallis, M Danielsson and E Fredenberg

Sweden

16.30-16.45

**[O 4-5] Characterisation of benign and malignant calcifications**

L M Warren, D R Dance, S Astley and K C Young

United Kingdom

---

16.45-17.00

Break

---

*Oral session 5*

**17.00-18.00**

**Mammography**

Chairs: A Tingberg and A Thilander Klang

- 17.00-17.15 **[O 5-1] Does the image quality measured using the CDMAM test object relate to cancer detection in mammography**  
A Mackenzie, L M Warren, M G Wallis, J Cooke, R M Given-Wilson ,D R Dance,  
D P Chakraborty, M D Halling-Brown, P T Looney and K C Young  
*United Kingdom and USA*
- 17.15-17.30 **[O 5-2] The use of PMMA to simulate local dense areas to assess automatic exposure control in digital mammography**  
R W Bouwman, J Binst, D R Dance, K C Young, W J H Veldkamp, H Bosmans and  
R E van Engen  
*The Netherlands, Belgium and United Kingdom*
- 17.30-17.45 **[O 5-3] How well do digital mammography systems in the UK breast screening programme meet European Guidelines?**  
K C Young  
*United Kingdom*
- 17.45-18.00 **[O 5-4] Estimates of breast cancer growth rate from mammograms and its relation to histopathology**  
D Förnvik, K Lång, I Andersson, M Dustler, S Borgqvist and P Timberg  
*Sweden*

**Poster session**

**18.00-20.00**

see separate list at the end of the programme

**The poster session includes a Welcome Reception by the City of Gothenburg**

## Friday, 29 May 2015

08.00-08.30

Registration

*Oral session 6*

08.30-10.00

**Knowledge development, challenge of expertise, education and training**

Chairs: C Hoeschen and B M Moores

08.30-09.15

*Invited speaker*

**[O 6-1] Medical Image Perception II: How much of my time is this image worth?**

Jeremy M Wolfe (Harvard Medical School)

*USA*

09.15-09.30

**[O 6-2] Arranging for better learning opportunities in radiology**

J Ivarsson, H Rystedt, S Asplund, Å Johnsson and M Båth

*Sweden and Finland*

09.30-09.45

**[O 6-3] Video as a tool for optimization of radiological protection in image-guided interventions - possibilities and limitations**

A von Wrangel, A Almén, M Båth, H Rystedt and C Lundh

*Sweden*

09.45-10.00

**[O 6-4] Basic radiation protection education and training for medical professionals, Georgian experience and future perspectives**

F Todua, D Nadareishvili, G Ormotsadze and T Sanikidze

*Georgia*

10.00-10.30

Coffee

*Oral session 7*

10.30-12.00

**Modelling and Monte Carlo simulation**

Chairs: D Dance and P Bernhardt

10.30-10.45

**[O 7-1] Organ dose estimation and quality image assessment in computed tomography**

C Adrien, C Le Loirec, J C Garcia-Hernandez, S Dreuil and J M Bordy

*France*

10.45-11.00

**[O 7-2] Computed Tomography dose calculations using a radiation Treatment Planning System**

H-E Källman, R Holmberg, J Andersson, L Kull, E Traneus and A Ahnesjö

*Sweden*

11.00-11.15

**[O 7-3] A Monte-Carlo simulation framework for joint optimisation of image quality and patient dose in digital paediatric radiography**

B Menser, D Manke, D Mentrup and U Neitzel

*The Netherlands and Germany*

11.15-11.30

**[O 7-4] Dual-lattice anthropomorphic voxel models for image quality optimization**

N Petoussi-Hens, J Becker, M Greiter, H Schlattl, M Zankl and C Hoeschen

*Germany*

11.30-11.45

**[O 7-5] Customization of a Monte Carlo dosimetry tool for dental Cone Beam CT systems**

A Stratis, G Zhang, R Jacobs, R Bogaerts and H Bosmans

*Belgium*

11.45-12.00

**[O 7-6] A method for simulation of spiculated mammographic lesions**

P Elangovan, A Rashidnasab, R Ferrari Pinto, D R Dance, K C Young and K Wells

*United Kingdom and Belgium*

12.00-13.30

Lunch

*Oral session 8*

13.30-15.00

**Patient dose benchmarking**

Chairs: P Bernhardt and C Lundh

13.30-14.00 *Invited speaker*

**[O 8-1] The use of diagnostic reference levels in optimisation**

Colin J Martin (University of Glasgow)

*United Kingdom*

14.00-14.15 **[O 8-2] Diagnostic dose levels in paediatric CT at the Queen Silvia Children's Hospital, Gothenburg, Sweden**

A Thilander-Klang, M Hulthenmo, S Johansson and H Caisander

*Sweden*

14.15-14.30 **[O 8-3] Multicentre comparison of patient dose for X-ray guided embolizations of arteriovenous malformations in the brain**

J E M Mourik, M L Overvelde, D Zweers and K Geleijns

*The Netherlands*

14.30-14.45 **[O 8-4] Updated estimations of effective dose for PET radiopharmaceuticals recently published by the ICRP**

M Andersson, L Johansson, D Minarik, S Mattsson and S Leide Svegborn

*Sweden*

14.45-15.00 **[O 8-5] Managing patient's dose in digital x-ray chest screening examinations using an anthropomorphic phantom: comparison between a Russian and a Swedish hospital**

A V Vodovatov, A A Drozdov and C Bernhardsson

*Russia and Sweden*

---

15.00-15.30

**Coffee**

*Oral session 9*

15.30-16.45

**Physical evaluation of technologies**

Chairs: A Svalkvist and A Thilander Klang

15.30-15.45 **[O 9-1] Iterative scatter correction for grid-less bedside chest radiography: Performance for a chest phantom**

D Mentrup, S Jockel, B Menser and U Neitzel

*Germany and The Netherlands*

15.45-16.00 **[O 9-2] Influence of scout acquisition and scan direction on the dose reducing effect of automatic tube current modulation**

C Franck and K Bacher

*Belgium*

16.00-16.15 **[O 9-3] Characterising the EOS™ slot scan imaging system with using effective Detective Quantum Efficiency**

A H Clavel, P Monnin, J M Létang, F R Verdun and A Darbon

*Switzerland and France*

16.15-16.30 **[O 9-4] System upgrade on Philips Allura FD20 angiography systems: Effects on patient skin dose and static image quality**

N Ryckx, M Sans-Merce and F R Verdun

*Switzerland*

16.30-16.45 **[O 9-5] Comparison of wireless detectors for digital radiography systems: Image quality and dose**

J E M Mourik, P van der Tol, W J H Veldkamp and J Geleijns

*The Netherlands*

---

16.45-17.00

**Break**

---

*Oral session 10*

**17.00-18.00**

**Strategies in research and optimisation**

Chairs: G Alm Carlsson and L G Månsson

- 17.00-17.15 **[O 10-1] The process of optimisation of radiological protection – the significance of diagnostic reference levels**  
A Almén and M Båth  
*Sweden*
- 17.15-17.30 **[O 10-2] Cost-risk-benefit analysis in diagnostic radiology – an economic basis for radiation protection of the patient**  
B M Moores  
*United Kingdom*
- 17.30-17.45 **[O 10-3] Need for individual cancer risk estimations in X-ray and nuclear medicine imaging?**  
S Mattsson  
*Sweden*
- 17.45-18.00 **[O 10-4] A strategic research agenda for radiation protection research related to medical applications of ionising radiation – a common proposal of EANM, EFOMP, EFRS, ESR and ESTRO**  
C Hoeschen, S Combs, J Damilaks, W Dörr, G Frija, G Glatting, J McNulty, G Paulo, W Stiller, V Tsapaki and J F Verzijlbergen  
*Germany, Greece, Austria, France, Ireland, Portugal and The Netherlands*

*Discussion*

**18.00-18.30**

**OPERRA Workshop Part II – Chance for stakeholder input for medical radiation protection Strategic Research Agenda**

Chairs: C Hoeschen and N J Pelc

**19.30-**

**Conference dinner**

The Museum of World Culture, Södra Vägen 54

## Saturday, 30 May 2015

---

08.00-08.30

Registration

*Oral session 11*

08.30-09.45

**Occupational exposure**

Chairs: J Grétarsdóttir and S Mattsson

08.30-09.15

*Invited speaker*

**[O 11-1] Eye lens dosimetry for interventional radiologists and cardiologists: Practical approaches to protection and dose monitoring**

Colin J Martin (University of Glasgow)  
*United Kingdom*

09.15-09.30

**[O 11-2] Optimisation of radiological protection in a complex hybrid environment using detailed dose rate information**

C Lundh, M Båth and A Almén  
*Sweden*

09.30-09.45

**[O 11-3] The effect of low kV on staff dose during CT guided interventions**

P van der Tol, J E M Mourik, K Y E Leung and J Geleijns  
*The Netherlands*

---

09.45-10.00

**Announcements**

---

10.00-10.30

**Coffee**

*Oral session 12*

10.30-12.00

**Quality assurance**

Chairs: H Bosmans and B M Moores

10.30-10.45

**[O 12-1] Accurate KAP meter calibration as a prerequisite for optimization in projection radiography**

A Malusek, M Sandborg and G Alm Carlsson  
*Sweden*

10.45-11.00

**[O 12-2] Effect on relative KAP meter energy dependence of heavily filtered beams used in X-ray systems**

L Herrnsdorf and H Petersson  
*Sweden*

11.00-11.15

**[O 12-3] Benchmarking of CT to patient exposure optimization**

D Racine, A H Ba, J G Ott, N Ryckx, F O Bochud and F R Verdun  
*Switzerland*

11.15-11.30

**[O 12-4] Dosimetry on a mobile intraoperative CT system**

P van der Tol, J E M Mourik and J Geleijns  
*The Netherlands*

11.30-11.45

**[O 12-5] Clinical audit of image quality in radiology using visual grading characteristics analysis**

E Tesselaar, N Dahlström and M Sandborg  
*Sweden*

11.45-12.00

**[O 12-6] Dutch quality control of Radiology imaging equipment: a unified approach for protocols and software**

A A Becht, W K J Renema and J E M Mourik  
*The Netherlands*

---

12.00-13.30

**Lunch**

---

13.30-15.00

**Tomosynthesis**

Chairs: A Svalkvist and P Timberg

- 13.30-13.45 **[O 13-1] Individualized calculation of tissue imparted energy in breast tomosynthesis**  
N Geeraert, R Klausz, S Muller, I Bloch and H Bosmans  
*Belgium and France*
- 13.45-14.00 **[O 13-2] Thoracic spine imaging: A comparison between radiography and tomosynthesis using visual grading characteristics**  
E Ceder, B Danielson, P Kováč, H Fogel and M Båth  
*Sweden*
- 14.00-14.15 **[O 13-3] Visibility of structures of relevance for patients with cystic fibrosis in chest tomosynthesis – influence of anatomical location and observer experience**  
C Meltzer, M Båth, S Kheddache, H Ásgeirsdóttir, M Gilljam and Å A Johnsson  
*Sweden*
- 14.15-14.30 **[O 13-4] Effect of radiation dose on pulmonary nodule size measurements in chest tomosynthesis**  
C Söderman, Å A Johnsson, J Vikgren, R Rossi Norrlund, D Molnar, A Svalkvist, L G Månsson and M Båth  
*Sweden*
- 14.30-14.45 **[O 13-5] Finding role for Digital Tomosynthesis (DTS) in chest imaging**  
Á Horváth, G Horváth and K Szondy  
*Hungary*
- 14.45-15.00 **[O 13-6] Clinical use of chest tomosynthesis - after five years with the new modality**  
C Petersson, M Båth, J Vikgren and Å A Johnsson  
*Sweden*

---

15.00-15.05

**Conference closing**

---

## Poster session – Thursday, 28 May 2015, 18.00-20.00

**[P-1] Iterative reconstruction: different solutions - different effects**

M A Staniszewska and D Chruściak

*Poland*

**[P-2] Assessment of clinical image quality in paediatric abdominal CT examinations – dependency on level of Adaptive Statistical iterative Reconstruction (ASiR) and type of convolution kernel**

J Larsson, M Båth, K Ledenius, H Caisander and A Thilander-Klang

*Sweden*

**[P-3] Overview, practical tips and potential pitfalls using automatic exposure control in CT – Siemens CARE Dose 4D**

M Söderberg

*Sweden*

**[P-4] Methods for determination of CTDI**

E Bąbel and M A Staniszewska

*Poland*

**[P-5] Implications of patient centering on organ dose in Computed Tomography examinations - A comparison between TLD measurements and CT Expo simulation**

B Kataria, M Sandborg and J Nilsson-Althén

*Sweden*

**[P-6] Dosimetric measurements using the TG 200 phantom – a comparison of dosimetric techniques with application in CT and CBCT**

M Gunnarsson, L Herrnsdorf, P Törnqvist and M Söderberg

*Sweden*

**[P-7] Comparison of effective dose estimates of paediatric conventional X-ray and computed tomography examinations of the cervical spine**

M Hultenmo and A Thilander-Klang

*Sweden*

**[P-8] Computed tomography dose index and dose length product for 4-slice scanner at a densely populated city of northern Nigeria**

I Garba, M Yahuza, M Barde and M Abba

*Nigeria*

**[P-9] A first step to defining DRLs for CT-examinations in Russia**

L Chipiga

*Russia*

**[P-10] Exposure of the Swiss population by X-ray diagnostic imaging: Results of the 2013 intermediate survey**

R LeCoultre, J Bize, M Champendal, D Wittwer, N Ryckx and F R Verdun

*Switzerland*



**[P-11] Exploring Dual Energy CT images for radiotherapy treatment planning of patients with metal implants**

E Petterson, U Lindencrona, N Drugge and A Thilander-Klang

*Sweden*

**[P-12] Quantitative dual-energy computed tomography using the base material decomposition in projection and image space**

M Magnusson, D Ballesterio, M Sandborg, G Alm Carlsson and A Malusek

*Sweden*

**[P-13] Parallelization of the model-based iterative reconstruction algorithm DIRA**

A Örtenberg, M Magnusson, M Sandborg, G Alm Carlsson and A Malusek

*Sweden*

**[P-14] Patient dose assessment after interventional cardiology procedures: A multi-centric approach to trigger optimization**

N Ryckx, J J Goy, J C Stauffer and F R Verdun

*Switzerland*

**[P-15] Skin dose, effective dose and related risk in TAVI procedures– Is the cancer risk acceptable for younger patients?**

A Karambatsakidou, A Omar, B Chehrazi, A Rück and J Scherp Nilsson

*Sweden*

**[P-16] Skin doses of the patients undergoing interventional radiological examinations**

S Sarycheva and V Golikov

*Russia*

**[P-17] Withdrawn**

**[P-18] Verification of indicated skin entrance air kerma in cardiac x-ray guided intervention using Gafchromic film**

J Nilsson Althén and M Sandborg

*Sweden*

**[P-19] Correlation between scatter radiation dose at the height of the operator's eye and dose to patient for different angiographic projections**

F Leyton, M S Nogueira, E Vano, L Gubolino, Maycon and C Ubeda

*Chile, Brazil and Spain*

**[P-20] Assessing the usefulness of the quasi-ideal observer for quality control and dose optimisation in fluoroscopy and interventional radiology**

E Tesselaar and M Sandborg

*Sweden*

**[P-21] Multicentre comparison of image quality for low contrast objects and micro-catheter tips in X-ray guided treatment of arteriovenous malformation in the brain**

J E M Mourik, M L Overvelde, I Hernandez Giron, W J H Veldkamp, D Zweers and K Geleijns

*The Netherlands and Spain*

**[P-22] Breast density assessment in breast tomosynthesis using the central projection image**

P Timberg, K Lång, H Sartor, M Dustler and S Zackrisson

*Sweden*

**[P-23] Validation of a simulation procedure for generating breast tomosynthesis projection images**

H Petersson, L M Warren, A Tingberg, M Dustler and P Timberg  
*Sweden and United Kingdom*

**[P-24] Influence of in-plane artifact on pulmonary nodule size measurements in chest tomosynthesis**

C Söderman, Å A Johnsson, J Vikgren, R Rossi Norrlund, D Molnar, A Svalkvist, L G Månsson and M Båth  
*Sweden*

**[P-25] Evaluation of an improved implementation of a method of simulating pulmonary nodules in chest tomosynthesis**

F Svensson, C Söderman, A Svalkvist, R Rossi Norrlund, J Vikgren, Å A Johnsson and M Båth  
*Sweden*

**[P-26] Image fusion of two FBP-reconstructed digital tomosynthesis volumes from frontal and lateral acquisitions**

J Arvidsson, C Söderman and M Båth  
*Sweden*

**[P-27] Effective dose to patients from thoracic spine examinations with tomosynthesis**

A Svalkvist, C Söderman and M Båth  
*Sweden*

**[P-28] Retrospective estimation of patient dose-area product in thoracic spine tomosynthesis performed using VolumeRAD**

M Båth, C Söderman and A Svalkvist  
*Sweden*

**[P-29] Image quality assessment in chest x-ray using an anthropomorphical phantom**

A A Drozdov, A V Vodovatov and C Bernhardsson  
*Russia and Sweden*

**[P-30] Evaluation of dose reduction potentials of a novel scatter correction software for bedside chest X-ray imaging**

V Toth, C Brieskorn, B Renger, D Mentrup, S Jockel, F Lohöfer, M Schwarz, E J Rummeny and P B Noël  
*Germany*

**[P-31] Estimation of organ doses for the patients undergoing X-ray examination by use of physical human phantoms**

V Golikov, A Barkovsky, E Wallström and Å Cederblad  
*Russia and Sweden*

**[P-32] Withdrawn**

**[P-33] Comparison of the accuracy in kidney activity concentration estimates by the conjugate view and posterior view method**

T Magnander, J Svensson, M Båth, P Gjertsson, E Forssell-Aronsson and P Bernhardt  
*Sweden*

**[P-34] Evaluation of image quality parameters in PET/CT using the MADEIRA and NEMA NU-2 2001 phantoms**

L Chipiga, M Sydoff, I Zvonova and C Bernhardsson  
*Russia and Sweden*

**[P-35] Portable scintillation detector for lung activity measurements prior to V/P<sub>SPECT</sub>**

M Larsson, J Himmelman and J Dalmo  
*Sweden*

**[P-36] A phantom for determination of calibration coefficients and minimum detectable activities using a SPECT/CT for internal contamination monitoring following radiation emergency situations**

Ü Ören, M Andersson, C L Rääf and S Mattsson  
*Sweden*

**[P-37] Can an energy compensated solid-state x-ray detector be used for radiation protection applications at higher energies?**

Ü Ören, L Herrnsdorf, M Gunnarsson, S Mattsson and C L Rääf  
*Sweden*

**[P-38] Evaluation of the ionization chamber and solid state detector for a radiometric survey at radiodiagnostic facilities. Preliminary results metrology laboratory.**

F Leyton, M Navarro, E Matos and I Garcia  
*Brazil*

**[P-39] Noninvasive method for the calibration of the peak voltage (kVp) meters**

E Matos, C de Navarro, M Navarro, F Leyton and I Garcia  
*Brazil*

**[P-40] Variations of optical properties of photon irradiated nPAG, nMAG and VIPET polymer dose gels**

N Vaiciunaite and D Adliene  
*Lithuania*

**[P-41] Simple surface plasmon resonance based dosimeter**

D Adliene and B G Urbonavicius  
*Lithuania*

**[P-42] Automatic segmentation of male pelvis for brachytherapy of prostate**

M Kardell, M Magnusson, M Sandborg, G Alm Carlsson and A Malusek  
*Sweden*

**[P-43] Image guided radiotherapy with heavy elements: proofs of concept**

C Le Loirec, D Chambellan and D Tisseur  
*France*

**[P-44] Optimisation conventional spin echo sequence for echo-planar diffusion-weighted (SE-EPI-DW) MRI of the Achilles tendon using high-field 3T MR scanner in clinical setting**

M Al-Mulla, L A Rainford and A McGee  
*Ireland*

**[P-45] VGC Analyzer – a software for statistical analysis of multiple-reader multiple-case visual grading characteristics (VGC) studies**

M Båth and J Hansson  
*Sweden*

**[P-46] Reanalysis of visual grading characteristics (VGC) data using VGC Analyzer**

J Hansson, L G Månsson and M Båth

*Sweden*

**[P-47] MedXViewer: An extensible web-enabled software package for flexible, collaborative and remote medical imaging viewing, perception studies and reader training**

P Looney, K C Young and M D Halling-Brown

*United Kingdom*

**[P-48] ViewDEX: a status report**

A Svålvik, S Svensson, M Håkansson, M Båth and L G Månsson

*Sweden*

**[P-49] Determining the chronological age of breast cancer with  $^{14}\text{C}$  bomb-pulse dating and its correlation to collagen SAXS-pattern**

K Lång, A Rosso, M Bech, S Zackrisson, D Graubau, K Eriksson-Stenström and S Mattsson

*Sweden*

**[P-50] Introducing the silicon photomultiplier (SiPM) technology: A flexible, modular kit for sensor testing and education at postgraduate level**

L Herrnsdorf and S Mattsson

*Sweden*

## **The centre for imaging and intervention at Sahlgrenska University Hospital – a house of possibilities**

**J Grétarsdóttir<sup>1</sup> and J Hansson<sup>1</sup>**

*<sup>1</sup>Department of Medical Physics and Biomedical Engineering, Sahlgrenska University Hospital, Gothenburg, Sweden*

Sahlgrenska University Hospital in Gothenburg, Sweden, has been preparing for the construction of a new Imaging and Intervention Center for almost ten years. The building is planned to be ready for use in 2016 and will host the most advanced equipment for diagnostics and treatments in a suitable environment for modern medical care with departments for radiology, nuclear medicine incl. cyclotron, catheter intervention, hybrid surgery and a center for sterilisation of medical goods.

From the beginning of the project, medical physicists and biomedical engineers have been engaged in the planning and the execution of the construction. Having a role of internal expertise in the hospital organisation, the medical physicist and biomedical engineers need to be flexible and proactive in order to catch up the important tasks the hospital is facing during the process. This is especially important in projects where a large amount of advanced medical equipment are to be installed, requiring the correct choice for safety and quality to be made in every moment. The hospital management, medical departments, the builder, external consultants and the construction entrepreneur are parties with their own agenda, hopefully with a common goal. However, changes during the project easily make previous decisions to be forgotten or skipped when new considerations are prioritized.

The department of medical physics and biomedical engineering has during the project had the main focus on the core tasks that are considered to be the responsibility of the organisation to solve and for which it will be accountable when the construction is finished and the building is in use. The work has in this aspect been altered from generation of supporting documents in the beginning via support to the medical departments in their planning to direct project management of the installation of medical equipment. The presentation will enlighten the strategic set up for the work of the department of medical physics and biomedical engineering and the critical moments during the project that have been identified as important for the success of commissioning the project.

***Invited speaker*****Spectral CT, basic principles, applications, and prospects for molecular imaging****N J Pelc<sup>1</sup>***<sup>1</sup>Departments of Bioengineering and Radiology, Stanford University, Stanford, CA, USA*

The purpose of this presentation is to discuss the basic principles and implementations for material characterization with spectral x-ray measurements and the prospects for "molecular" imaging.

Conventional CT images the linear attenuation coefficient at one and cannot uniquely identify materials. The energy dependence of x-ray attenuation depends on atomic number; spectral imaging measures attenuation at multiple energies to more fully characterize materials. One might assume that N energies would enable separation into N components. However, in the diagnostic energy range x-ray attenuation is dominated by Compton scattering and photoelectric absorption, and, unless there is an absorption edge within the measured spectrum, the two mechanisms have the same energy dependence for all materials and there are two "basis functions" and spectral CT can only measure effective atomic number and electron density, or the amount of two "basis materials". For elements with an absorption edge (*e.g.*, K-edge) within measured spectrum it is possible to quantitate that material as well as the two basis functions.

There are several implementations available. The system can obtain measurements at multiple kVp and/or filtration. Other methods use energy discrimination at the detector. These include layered detectors and photon counting energy discriminating systems. These approaches have different dose efficiency and sensitivity to subject motion. Analysis of the spectral data can be performed in the image domain from images reconstructed for each spectral band, or on the measured projections prior to reconstruction. The latter is more complicated but provides additional benefits.

Material decomposition amplifies measurement noise. Also, fundamentally, x-ray absorptiometry is relatively insensitive. Measurement noise limits the ability to detect small changes in atomic number or small amounts of any material. Thus, while spectral CT provides more material specificity than conventional CT and while K-edge methods can depict specific elements, the sensitivity is not high. If it is to be used for "molecular" imaging, it will require high amounts of the molecular probe, orders of magnitude more than radionuclide methods and even MRI.

## A Study of the Image Quality of CT Brain Adaptive Statistical Iterative Reconstructed (ASIR) Images Using Subjective and Objective Methods

J Mangat<sup>1</sup>, J Morgan<sup>2</sup>, P Clinch<sup>3</sup>, A Reilly<sup>4</sup>, M Båth<sup>5</sup>, J Clinch<sup>6</sup>, E Chaloner<sup>7</sup> and M Lewis<sup>8</sup>

<sup>1</sup>CT Dept/ London Chest hospital, London, United Kingdom

<sup>2</sup>School of Health Sciences/ City University, London, United Kingdom

<sup>3</sup>Medical Engineering and Physics Dept/ Kings College Hospital, London, United Kingdom

<sup>4</sup>Physics Dept/ The Clatterbridge Cancer Centre, Cheshire, United Kingdom

<sup>5</sup>Department of Medical Physics and Biomedical Engineering, Sahlgrenska University Hospital, Gothenburg, Sweden

<sup>6</sup>Medical Engineering and Physics Dept/ Kings College Hospital, London, United Kingdom

<sup>7</sup>Medical Engineering and Physics Dept/ Kings College Hospital, London, United Kingdom

<sup>8</sup>Medical Physics Dept/ Guy's & St. Thomas' Hospital, London, United Kingdom

**Purpose:** The aim of this study was to investigate the image quality of ASIR reconstructed brain images using subjective, observer-based assessment and objective metrics to elucidate trends and possible alternatives to the current standard protocol featuring 40%ASIR and a noise index of 11.20, possibly facilitating a dose decrease.

**Method:** An audit of image quality of patient brain scans (n=55) was performed using Visual Grading Assessment (VGA) by two radiologist-observers, using CEC image criteria of retrospectively reconstructed images at 0% -70% & 100% ASIR-levels originally scanned using the standard protocol. Analysis was conducted using Visual Grading Characteristics (VGC). Empirical phantom-based assessments of high-contrast spatial resolution (HCSR) and Noise Power Spectrum (NPS) with 0-100%ASIR increments and decremting tube currents (565-235mA), were also conducted.

**Results:** VGC analysis showed that the mid-range increments (50%-70%ASIR) were not significantly different to 40%ASIR ( $p>0.05$ ). Low-contrast spatial resolution (LCSR) showed slight, non-significant improvement with 70% and 60%ASIR increments compared with 40%ASIR ( $p>0.05$ ). Subjective image noise remained constant across this range, but was slightly worse than 40%ASIR ( $p>0.05$ ). However, 70%ASIR reconstructions were found to be overly susceptible to artefact appearance. Hence pairwise-analysis was performed using 60% & 50%ASIR, which showed 60%ASIR was the preferred increment. Phantom-based HCSR investigations showed  $MTF_{50}$  and  $MTF_{10}$  increases of up-to 4.1% and 3.0%, respectively ( $p<0.05$ ) for ASIR reconstructed images as compared to those produced using FBP.  $MTF_{50}$  and  $MTF_{10}$  showed a linearly improving relationship with increasing %ASIR. With tube current, MTF behaviour was more complex with a rapid increase up to 305mA, a plateau between 305 and 420mA and then a rapid fall off. The NPS study revealed peak-frequency decreased linearly with increasing %ASIR and remained constant with tube current. Peak-variance decreased non-linearly with %ASIR and tube current. Empirical ranges for  $MTF_{50}$ ,  $MTF_{10}$ , peak frequency NPS & peak variance NPS of (0.370- 0.375 $mm^{-1}$ ), (0.617- 0.622 $mm^{-1}$ ), (0.199- 0.176 $mm^{-1}$ ) & (99.28- 84.92 $mm^{-1}$ ) respectively, were obtained for the standard protocol for the mid-range ASIR increments.

**Conclusion:** This study demonstrated the trends for objective and subjective image quality metrics with ASIR increment and tube-current. 60%ASIR with a tube current of 305mA (NI=12.20) was proposed as an alternative to the current standard, as it was the best fit with these empirical ranges, producing a possible dose saving of 16.1%.

## The effect of Adaptive Statistical iterative Reconstruction (ASiR) on assessment of diagnostic quality and visualisation of anatomical structures in paediatric head CT examinations

J Larsson<sup>1, 2</sup>, M Båth<sup>1, 3</sup>, K Ledenius<sup>4</sup> and A Thilander-Klang<sup>1, 3</sup>

<sup>1</sup>*Department of Radiation Physics, Institute of Clinical Sciences, Sahlgrenska Academy, University of Gothenburg, Gothenburg, Sweden*

<sup>2</sup>*Section of Diagnostic Imaging and Functional Medicine, NU-Hospital Group, Trollhättan, Sweden*

<sup>3</sup>*Department of Medical Physics and Biomedical Engineering, Sahlgrenska University Hospital, Gothenburg, Sweden*

<sup>4</sup>*Department Radiology, Skaraborg Hospital, Skövde, Sweden*

**Purpose:** The purpose of this study was to investigate the effect of different levels of Adaptive Statistical iterative Reconstruction (ASiR) on diagnostic quality and visualisation of anatomical structures for paediatric head CT examinations.

**Materials and Methods:** Forty patients from infants to an age of 17 years-old undergoing routine head CT on a 64 slice MDCT scanner (Discovery CT750 HD, GE Healthcare) were included in the study and divided into age dependent sub groups (0-2, 3-5 and 6-17 years-old). Scanning raw data, acquired within tube current range 190 to 400 mA, was retrospectively reconstructed into 5 mm thick axial image stacks at levels of 0%, 20%, 30%, 40%, 50%, 60%, 70%, 80% and 100% ASiR with convolution kernel Soft. In a blinded randomized visual grading study, three paediatric radiologists with different experience rated a question of diagnostic quality (For what diagnostic situation is this image quality sufficient?) and 6 questions related to anatomical structures, using a four point rating scale. Data were analysed in comparison with 30 % ASiR with kernel Soft (the ASiR level and kernel used clinically prior to the study) using a method for paired ordinal data that identifies and measures systematic shift in rating distributions.

**Results:** In all sub groups, 50%, 60% and 70% ASiR demonstrated a statistically significant negative Relative Position (RP) for diagnostic quality, indicating a higher diagnostic quality compared to 30% ASiR. All trends of the assessed anatomical structures, except the cerebrospinal fluid space around the brain, demonstrated enhancement in visibility with increased level of ASiR. The visibility of the cerebrospinal fluid space around the brain was degraded at ASiR levels above 60% ASiR. Diagnostic quality at 0% ASiR (100% filtered back projection) was significantly lower than 30% ASiR.

**Conclusion:** This study shows that the commonly used 30% ASiR may not always be the optimal level of ASiR. The investigated effect of ASiR showed, in this study, that 60% ASiR was the optimal ASiR level for a paediatric head CT examinations at the tube current range 190 to 400 mA, when reconstructing 5 mm thick images with convolution kernel Soft.



## **Model based iterative reconstruction IMR gives possibility to evaluate thinner slice thicknesses than conventional iterative reconstruction iDose<sup>4</sup> – a phantom study**

**M-L Aurumskjöld<sup>1</sup>, K Ydström<sup>2</sup>, A Tingberg<sup>1</sup> and M Söderberg<sup>1</sup>**

<sup>1</sup>*Medical Radiation Physics, Department of Translational Medicine, Lund University, Malmö, Sweden*

<sup>2</sup>*Philips Healthcare, Malmö, Sweden*

Computed tomography (CT) is one of the most important modalities in a radiological department, which produces images with high diagnostic quality and it is often available all hours of the day. CT provides valuable diagnostic information, but in some cases radiation dose to the patient can be relatively high. One of the actions made to reduce the radiation dose is to use advanced image reconstruction algorithms.

The purpose of this study was to investigate the effect of slice thickness combined with model-based iterative reconstruction method (IMR) on the improvement of the image quality and diagnostic confidence compared to standard slice thickness with iterative reconstruction (iDose<sup>4</sup>). The study was performed on a Philips Brilliance iCT scanner. Image quality was both objectively and subjectively assessed. Objective measurements of noise and contrast-to-noise ratio were performed using an image quality phantom, an anthropomorphic phantom and clinical cases. A subjective evaluation of low-contrast resolution was performed by three observers using the low-contrast resolution module in the image quality phantom.

Thinner slice thickness combined with IMR compared to standard slice thickness with iDose<sup>4</sup> can improve image quality and diagnostic confidence. IMR gives strong noise reduction and enhanced low contrast thereby enables selection of thinner slices. Objective evaluation of image noise shows that thinner slice thickness with IMR provides lower noise than thicker slice thickness with iDose<sup>4</sup>. Results from the subjective assessment show that the highest level of iDose<sup>4</sup> with 5 mm slice thickness got the same result as lowest level of IMR and 1 mm slice thickness. IMR is not dependent on the slice thickness in the same manner as iDose<sup>4</sup>. Higher level of IMR, the less important is the slice thickness.

In conclusion, there is great potential to reduce slice thickness and maintain the same or reduce the noise level with model-based iterative reconstruction as with thicker slices which has to be used with iDose<sup>4</sup> reconstruction. This will subsequently result in an improvement of image quality for images reconstructed with IMR.

## Comparison of Adaptive Statistical Iterative Reconstruction (ASiR) and VEO reconstruction for paediatric abdominal CT examinations – an observer performance study of diagnostic image quality

M Hultenmo<sup>1</sup>, H Caisander<sup>2</sup>, K Mack<sup>2</sup> and A Thilander-Klang<sup>1,3</sup>

<sup>1</sup>Department of Medical Physics and Biomedical Engineering, Sahlgrenska University Hospital, Gothenburg, Sweden

<sup>2</sup>Department of Paediatric Radiology and Physiology, The Queen Silvia Children's Hospital, Gothenburg, Sweden

<sup>3</sup>Department of Radiation Physics, Institute of Clinical Sciences, Sahlgrenska Academy, University of Gothenburg, Gothenburg, Sweden

**Purpose:** The aim of the study was to compare the Adaptive Statistical Iterative Reconstruction (ASiR) with the model based iterative reconstruction algorithm VEO for paediatric abdominal CT examinations, focusing on visibility of abdominal structures and diagnostic image quality.

**Materials and Methods:** In this study raw data from 82 paediatric patients (1-17 years-old), undergoing abdominal CT examinations on a 64 slice CT scanner (Discovery CT750 HD, GE Healthcare) at Queen Silvia Children's Hospital, were collected. Age dependent tube voltage (kV) and Noise Index (NI, i.e. level of dose modulation) were used. From raw data, 2.5 or 5 mm axial and coronal images were reconstructed with both the routinely used 70% ASiR with soft kernel and the VEO algorithm. The reconstructed images were anonymized and randomized in an observer performance study using the software ViewDEX. Four experienced paediatric radiologists graded the delineation of six crucial abdominal structures, the diagnostic use of the image quality and the level of artefacts. The results were analysed by using Svensson's method for paired ordinal data.

**Results:** VEO reconstruction significantly improved the visibility of several structures compared to ASiR in both axial and coronal 2.5 mm images. Comparison of diagnostic image quality between the coronal 2.5 mm ASiR and the corresponding VEO images resulted in a statistically significant negative Relative Position (RP) value representing a systematic improved grading of the VEO images by all radiologists (e.g. RP = -0.37; 95% CI -0.48 to -0.20 for age group 1-10 years-old). For the 2.5 mm axial images in the same age group, two radiologists graded the diagnostic use of the image quality of VEO as significantly better than ASiR and one radiologist graded the algorithms in the opposite way (i.e. ASiR as significantly better than VEO). One radiologist graded the two methods without any significant difference. For the 5 mm images no statistically significant difference in diagnostic use of image quality was seen between the two iterative reconstruction algorithms.

**Conclusions:** The VEO reconstruction can be used instead of 70% ASiR to improve diagnostic image quality of paediatric abdominal CT examinations with thinner slices (~2.5 mm). Coronal images benefit more from VEO reconstruction than axial images do.

## **Paediatric CT protocol optimisation: Adapting Size Specific Dose Estimates to recalculate CT protocol parameters for five body sizes**

**K Rani<sup>1,2</sup>, A Jahnen<sup>1</sup>, A Noel<sup>2</sup> and D Wolf<sup>2</sup>**

<sup>1</sup>Luxembourg Institute of Science and Technology, ITIS Dept, Luxembourg

<sup>2</sup>Université de Lorraine, CRAN, Nancy, France

**Purpose:** Developing size-based paediatric CT protocols for abdominal examination and comparing them with age-based protocols. A new calculation methodology has been developed to adapt the CT protocol parameters to five paediatric sizes.

**Methodology:** Using Size Specific Dose Estimates (SSDE) calculation, we developed a methodology to recalculate the appropriate values of CT protocol parameters (tube current, tube voltage and level of iterative reconstruction). The weight and the effective diameter of the patient were used to define the size of the paediatric patients. The technical image quality indicators like the noise, the contrast-to-noise ratio and the low contrast detectability (LCD) were evaluated. The entire experiments were carried out on the Discovery™ CT750 HD (General Electric Healthcare) multi-slice (64-slices) MSCT scanner.

**Results:** Recalculated CT protocol parameters have been realized for five sizes of patients (from 4kg/11, 8 cm effective diameter to 54kg/23, 5 cm effective diameter). A total of 50 images were compared, five for each size compared to age-based examinations. Low tube voltage (80 kV) procedures can be performed for several paediatric sizes using the appropriate recalculation of CT protocol parameters. From the technical image evaluation, we can observe that size-based configuration of protocols allow us to improve image quality (decrease of noise up to 20% ,improving CNR up to 30% and improving LCD up to 20%) while lowering the delivered dose for all studied sizes.

**Conclusion:** An innovative approach has been applied to adapt the SSDE calculation in order to obtain size-based protocols resulting in an improvement of the image quality and the delivered dose. Our study demonstrates that it's possible to adapt CT protocols parameters for several sizes of paediatric patients. The results of this study will serve as a basis for adapting the abdominal CT protocol parameters to any size of paediatric patients.

## Low dose CT of the lumbar spine at about 1 mSv compared with lumbar spine radiography; a phantom and clinical study

M Alshamari<sup>1</sup>, M Geijer<sup>2</sup>, E Norrman<sup>3</sup>, M Lidén<sup>1</sup>, W Krauss<sup>1</sup>, F Wilamowski<sup>1</sup> and H Geijer<sup>1</sup>

<sup>1</sup>Department of Radiology, Faculty of Medicine and Health, Örebro University, Örebro, Sweden.

<sup>2</sup>Department of Medical Imaging and Physiology, Skåne University Hospital, Lund University, Lund, Sweden

<sup>3</sup>Department of Medical Physics, Faculty of Medicine and Health, Örebro University, Örebro, Sweden

**Purpose:** Despite recent abundant evidence of the limited value of lumbar spine radiography, it is still the most common radiologic investigation. Low dose CT of the lumbar spine at about 1 mSv may be an alternative to increase the diagnostic value without increasing radiation exposure. A phantom study was performed to determine optimal settings for low dose CT of the lumbar spine at about 1 mSv, combined with a clinical study to compare the image quality of low dose CT with radiography.

**Method:** An ovine phantom was scanned repeatedly with various technical settings. Five radiologists scored each scan on four image quality criteria. The best settings were then used to perform low dose CT in a clinical study. Fifty-one patients were examined with low dose CT and radiography. Evaluation of image quality was performed by five reviewers who scored all examinations on eight image quality criteria and assessed some common pathologic changes. Statistical analysis was performed according to visual grading regression.

**Major findings:** A tube potential at 120 kV with reference mAs 30 and medium/medium-smooth convolution filter gave the best image quality at the 1-mSv level according to the phantom study. In the clinical study, image quality was rated significantly higher for CT compared with radiography for most of the criteria. According to visual grading regression, a proportional odds model, odds ratio with 95% CI limits were 2.61 (1.84, 3.70) for disc profile, 7.48 (5.09, 10.97) for intervertebral foramina and pedicles, 130 (67.3, 251) for intervertebral joints, 9.88 (6.79, 14.4) for spinous and transverse processes, 3.65 (2.63, 5.07) for adjacent soft tissues, 5.82 (4.06, 8.35) for sacro-iliac joints and 308 (120, 792) for absence of superimposed gastrointestinal gas and contents. Only one criterion (cortical and trabecular bone) was better on radiography, odds ratio 0.30 (0.22, 0.42). Reviewers visualized degenerative changes more clearly and were more certain with low dose CT. Effective dose for CT was 1.0 mSv and 0.6 mSv for radiography.

**Conclusions:** Low dose CT, at 1 mSv, has superior image quality to radiography and gives more anatomical information compared with radiography without substantial increase in radiation dose.

***Invited speaker*****Medical Image Perception I: The human search engine****J M Wolfe<sup>1,2</sup>**<sup>1</sup>*Visual Attention Lab, Brigham and Women's Hospital, Cambridge, MA, USA*<sup>2</sup>*Departments of Ophthalmology and Radiology, Harvard Medical School, Boston, MA, USA*

For some medical images, the primary perceptual task is evaluation: Did this tumor shrink? Is that fracture healing? In many other situations, the first task is to find something: Are there signs of lung cancer? Did that accident cause internal injuries? These visual search tasks are performed by clinicians using the same human “search engine” that would be used in more mundane tasks: Where is my coffee mug? Are there any typos in this abstract? In this talk, I will discuss the fundamental limits on human visual processing that make search necessary. I will also show how human search is “guided search”: even though we need to search, we do not search the world at random. We are guided by a combination of basic feature such as, for example, the known size and shape of the target. We are also guided by our understanding of the world we are searching. A major part of becoming a domain expert, like a radiologist, is the development of this ability to guide search to likely target locations. Eye tracking and other methods can reveal how radiologists search. Moreover, these methods can reveal pitfalls in medical image search that may lead to errors.

## Objective task based assessment of low contrast detectability in iterative reconstruction

D Racine<sup>1</sup>, A H Ba<sup>1</sup>, J G Ott<sup>1</sup>, N Ryckx<sup>1</sup>, F O Bochud<sup>1</sup> and F R Verdun<sup>1</sup>

<sup>1</sup>Institute of Radiation Physics, CHUV, Lausanne, Switzerland

Simple binary tasks, such as discrimination between the presence and absence of a pathology are usually characterized by the use of Receiver Operating Curve (ROC) studies. Unfortunately, these studies are time-consuming and difficult to implement. Therefore, it is necessary to develop tools such as model observers which allow image quality quantification under a similar paradigm. This work assesses a new iterative reconstruction algorithm using an anthropomorphic phantom and a Channelized Hotelling Observer (CHO).

An anthropomorphic abdomen phantom (QRM 401, Moehrendorf, Germany) was scanned at 3 CTDI<sub>vol</sub> levels (5, 10 and 15 mGy) on a GE Revolution CT. In a uniform background, it contained spheres of different sizes and contrasts (6 and 8 mm; 10 and 20 HU at 120 kVp) which simulate nodules. Images were reconstructed using adaptive statistical iterative reconstruction (ASIR-V) at 0% and 50% and a slice thickness of 2.5 mm. The target detectability was computed by applying an anthropomorphic CHO with dense difference of Gaussian channels and internal noise. Both CHO and human observers were compared based on a four alternative forced choice (4-AFC) test and using the Percent Correct (PC) as a figure of merit (FOM).

Our results showed accordance between CHO and human performance; indeed, the Spearman's rank correlations were all 1. For the 6 mm/20HU target at 15mGy, human's PC were  $0.972 \pm 0.010$  and  $0.978 \pm 0.002$  with ASIR-V at respectively 0 and 50%. Under the same conditions the CHO gave  $0.989 \pm 0.005$  and  $0.985 \pm 0.011$ . At 10 mGy with ASIR-V 0% the PC were  $0.960 \pm 0.008$  and  $0.951 \pm 0.011$  for respectively humans and CHO. As a consequence, the overall PC root mean square error equals 0.0156.

This work shows that the human observers' performances can be accurately predicted by the CHO with internal noise. We thus provided an objective tool to assess image quality when dealing with iterative reconstruction. In our case, when the dose decreases by 33%, the image quality (PC) is only reduced by 5%. This opens the way for proposing a tool to optimize clinical protocols by ensuring that dose reduction does not impair diagnosis.

## Patient exposure optimisation through task-based assessment of a new iterative reconstruction technique: the ADMIRE algorithm

J G Ott<sup>1</sup>, A H Ba<sup>1</sup>, D Racine<sup>1</sup>, N Ryckx<sup>1</sup>, F O Bochud<sup>1</sup>, H Alkadhi<sup>2</sup> and F R Verdun<sup>1</sup>

<sup>1</sup>*Institute of Radiation Physics, CHUV, Lausanne, Switzerland*

<sup>2</sup>*Institute of diagnostic and interventional radiology, USZ, Zürich, Switzerland*

Over the last decade, Computed Tomography (CT) technology has improved and iterative reconstruction (IR) algorithms have led to drastic changes in image perception. In such a context, ensuring an adequate level of image quality while keeping patient exposure as low as reasonably achievable represents a new challenge that has to be addressed using clinically relevant tasks. The goal of this study is to report and investigate the performances of a new IR algorithm using a model observer that mimics human detection of low contrast targets.

A dedicated low contrast phantom (QRM, Moehrendorf, Germany) containing different targets (6 and 8 mm diameter; 10 and 20 HU at 120 kVp) was scanned at various  $CTDI_{vol}$  levels (1 to 15 mGy) on a Siemens SOMATOM Force CT. Images were reconstructed with a nominal slice thickness of 2.0 mm, using Advanced Modelled Iterative Reconstruction (ADMIRE) with 0 and 3 iterations. The images were assessed by three human observers, who performed a 4-alternative forced-choice detection experiment. Then, a Channelized Hotelling Observer (CHO) model with dense difference of Gaussian channels was applied on the same set of images. The comparison between the two was performed using their percentage of correct responses (PC) as a figure of merit.

Our results indicated a strong agreement between human and model observer as well as a slight improvement in the low contrast detection when switching from 0 to 3 iterations. Indeed, for a 6 mm and 10 HU target at 3 mGy of CTDI and without any iteration performed, the PC for human reached  $92.5 \pm 1.4\%$ . CHO gave  $91.5 \pm 4.4\%$ . Under the same conditions with three iterations, the values reached  $95.8 \pm 1.7\%$  for humans and  $95.6 \pm 2.9\%$  for CHO.

This investigation showed the ability of the CHO model observer to reproduce human detection for a low contrast detection task, thus establishing its reliability for image quality assessment. Good results in term of PC were also observed even in situations where the target was harder to detect (i.e. lower  $CTDI_{vol}$  and contrast level). All those elements suggest that patient dose could be further optimised and reduced thanks to the use of this new CT unit.

## The effect of fixed adaptation on the calibration of medical displays

P Sund<sup>1,2</sup>, L G Månsson<sup>1,2</sup> and M Båth<sup>1,2</sup>

<sup>1</sup>*Department of Radiation Physics, Institute of Clinical Sciences, Sahlgrenska Academy at University of Gothenburg, Gothenburg, Sweden*

<sup>2</sup>*Department of Medical Physics and Biomedical Engineering, Sahlgrenska University Hospital, Gothenburg, Sweden*

**Purpose:** Medical displays are normally calibrated according to the DICOM part 14 calibration method, the grayscale standard display function (GSDF). Based on the assumption of variable adaptation, calibration according to the GSDF results in a perceptually linearized display, for which the perceived contrast is equally distributed at all luminance levels. However, the assumption of variable adaptation is questionable and recently a method of calibration of medical displays that instead is based on the assumption of fixed adaptation was presented (Sund et al, Med Phys 2015). The new calibration method results in a fixed-adaptation compensated grayscale standard display function (GSDF<sub>FAC</sub>), for which the contrast perceived at fixed adaptation is equally distributed. The purpose of the present work was to investigate the effect of the choice of the adaptation level on the GSDF<sub>FAC</sub>.

**Material and methods:** Based on the formulation of the GSDF<sub>FAC</sub>, theoretical calibration curves for fictitious medical displays with different luminance ranges were determined. The calibrations were performed at different assumed adaptation levels. For comparison, the original GSDF was determined for each type of display.

**Results:** For fixed adaptation at a luminance level close to the logarithmic average of the minimum and maximum luminance levels, a small but significant difference between the GSDF and the GSDF<sub>FAC</sub> was obtained. The more the adaptation level deviated from this average, the larger the difference between the two calibrations. For example, for adaptation at a luminance level given by the linear average of the luminance levels corresponding to all digital driving levels (DDLs) – corresponding to fixed adaptation at a histogram-equalized image – the contrast enhancement at low luminance levels was substantially higher with the GSDF<sub>FAC</sub> than with the GSDF.

**Conclusions:** The present study shows that the GSDF<sub>FAC</sub> is strongly dependent on the adaptation level. The study indicates that although an improvement in terms of even distribution of contrast compared with the GSDF can be expected with the GSDF<sub>FAC</sub>, knowledge of the correct adaptation level is crucial.



## Improved detection rate and visualization of liver uptake foci in diagnostic $^{111}\text{In}$ -octreotide SPECT/CT investigations with a novel segmentation analysis

T Magnander<sup>1,2</sup>, E Wikberg<sup>2</sup>, J Svensson<sup>3</sup>, P Gjertsson<sup>4</sup>, B Wängberg<sup>5</sup>, M Båth<sup>1,2</sup> and P Bernhardt<sup>1,2</sup>

<sup>1</sup>Department of Radiation Physics, Institute of Clinical Sciences, Sahlgrenska Academy at University of Gothenburg, Gothenburg, Sweden

<sup>2</sup>Department of Medical Physics and Biomedical Engineering, Sahlgrenska University Hospital, Gothenburg, Sweden

<sup>3</sup>Department of Oncology, Institute of Clinical Sciences, Sahlgrenska Academy at University of Gothenburg, Gothenburg, Sweden

<sup>4</sup>Department of Clinical Physiology, Institute of Medicine, Sahlgrenska Academy at University of Gothenburg, Gothenburg, Sweden

<sup>5</sup>Department of Surgery, Institute of Clinical Sciences, Sahlgrenska Academy at University of Gothenburg, Gothenburg, Sweden

**Purpose:** Detection of liver tumors will change the course of treatment of neuroendocrine tumours. In nuclear medicine  $^{111}\text{In}$ -octreoscan is of high value for detection of neuroendocrine tumours. However, neuroendocrine tumours disseminated to the livers is often challenging to detect from  $^{111}\text{In}$ -octreoscan SPECT images due to low uptake, high noise, poor resolution and low contrast. The aim of the present study was to develop a segmentation analysis method for increased diagnostic accuracy of neuroendocrine liver tumours.

**Methods:** For the SPECT reconstruction 120 projections are acquired with 3 degrees spacing around the patient injected with  $^{111}\text{In}$ -octreoscan. The projections are reconstructed into a 128x128x128 voxel matrix using OSEM with CT based attenuation correction. The liver is segmented from the SPECT or CT using either an isosurface, region growing or a GPU accelerated level set algorithm. Manual editing finishes the segmentation of the liver. The segmented liver volume of interest, liver VOI, is thresholded at 125 equidistant threshold values between 0 and the maximum voxel value. At each threshold value a connected component labeling algorithm is used to calculate the number of uptake foci (NUF). The normalized NUF (nNUF) is then plotted against the threshold index (ThI), defined as  $\text{ThI} = (C_{\text{max}} - C_{\text{thr}}) / C_{\text{max}}$ , where  $C_{\text{max}}$  is the maximal voxel value in the VOI, and  $C_{\text{thr}}$  is the voxel threshold value. The method is named nNUFTI - normalized Number of Uptake Foci vs ThI. The ThI at 0.25 nNUF was used for analysis of liver tumour involvement. SPECT images from 53 patients without tumour involvement (i.e SPECT negative) in the liver were analysed with nNUFTI. A three year follow up with MRI, SPECT, PET/CT and CT was used to separate the patients into two groups: the healthy group, with still no liver tumours, and the malignant group, shown to have developed tumours in the liver.

**Results:** 40 patients ended up in the healthy group and 13 in the malignant group. The ThI at 0.25 nNUF was significantly different between the groups ( $p < 0.01$ ). A probability function for the ThI values was constructed from the obtained data. This relationship might be a useful guide in the diagnostic decision making.

**Conclusions:** Our new developed method nNUFTI has been shown to perform well. More studies on the nNUFTI method are needed.

## Pulmonary Nodule Segmentation by Mean-Shift and Quantum Clustering

A Chodorowski<sup>1</sup> and Q Mahmood<sup>1</sup>

<sup>1</sup>*Department of Signals and Systems, Chalmers University of Technology, Göteborg, Sweden*

**Purpose:** The purpose was to develop an automated segmentation method for pulmonary nodules in CT images. The segmented volumes are commonly used for nodule shape characterization and play a significant role in differential diagnosis between malignant and benign nodules at early stages of pulmonary lesion development. A successful segmentation is thus very important for diagnostic purpose.

**Method:** The segmentation method is based on the mean-shift algorithm and quantum clustering. The mean-shift method is applied simultaneously in both range and spatial domain using adaptive Bayesian bandwidth. The resulting oversegmented volume is divided into two regions by quantum clustering which takes into account the potentials in the range domain.

Data used in this research were obtained from The Cancer Imaging Archive (TCIA) sponsored by the SPIE, NCI/NIH, AAPM and The University of Chicago. Currently we have applied the method on 10 test CT images from the nodule classification challenge (LUNGx Lung Nodule Classification Challenge: <http://spie.org/x110838.xml>) and we plan to evaluate the method on the remaining 60 test images.

**Major findings:** The mean-shift with adaptive bandwidth can lead to a better image segmentation and quantum clustering produces clusters in a natural way found in physical systems (D. Horn and A. Gottlieb, Physical Review Letters, 2002).

**Conclusion:** We present an alternative way for CT image segmentation that can potentially improve the 3-D nodule delineation to be used in nodule classification systems.

## **Volumetric localization of dense breast tissue using breast tomosynthesis data**

**M Dustler<sup>1</sup>, H Pettersson<sup>1</sup> and P Timberg<sup>1</sup>**

*<sup>1</sup>Medical Radiation Physics, Department of Translational Medicine, Lund University, Malmö, Sweden*

Breast tomosynthesis (BT) has the ability to generate 3D mammographic images but – in contrast to e.g. CT – it is not a “true” 3D-technique as the limited angle does not allow a complete volumetric determination of the Hounsfield values of the imaged volume. The value of a voxel in a BT volume can thus not be used to determine whether it consists of dense or fatty tissue.

Methods to estimate the volume of dense tissue in the breast using the 2D mammogram are available, based on the assumption that the breast is binary, i.e. consisting of dense and fatty tissue.

This paper attempts to use combined data from reconstructed BT volumes and density estimation of projection images to localize dense tissue inside the breast.

To be able to verify results, a software breast phantom was used. Projection images were created using the PENELoPE Monte Carlo package. Dense tissue volume was estimated from the central projection image at  $\sim 0^\circ$  using a simulated polychromatic spectrum and NIST attenuation data to determine an effective attenuation coefficient. The resulting density image and the reconstructed BT stack were scaled to match the size of the phantom. The density image was used to determine the number of dense voxels at each location, with the highest valued corresponding BT voxels set to dense tissue, and the rest set to fatty tissue.

Visibly, the volumetric breast model was found to be close to the imaged software phantom, although with added high-frequency noise. The total dense tissue volume was found to be within 10% of the true value.

Locating dense tissue is useful for a number of applications. When adding simulated lesions to already acquired images, knowledge of the type of tissue being replaced at a certain insertion coordinate makes it possible to attain more realistic images. Also, the method can be used to construct software breast phantoms from images of real breasts, e.g. for Monte Carlo simulations.

## **Volumetric breast density in spectral tomosynthesis**

**K Berggren<sup>1,2</sup>, M Lundqvist<sup>1</sup>, M Wallis<sup>3</sup>, M Danielsson<sup>2</sup> and E Fredenberg<sup>1</sup>**

<sup>1</sup>*Philips Healthcare, Solna, Sweden*

<sup>2</sup>*Dept. of Physics, Royal Institute of Technology (KTH), Stockholm, Sweden*

<sup>3</sup>*Cambridge Breast Unit and NIHR Cambridge Biomedical Research Centre, Addenbrookes Hospital, Cambridge, United Kingdom*

Breast density is an indicator of breast cancer risk and diagnostic accuracy in mammography. Traditionally, breast density refers to the fractional area covered by fibro-glandular tissue in a mammogram. However, measures of the volumetric fraction of fibro-glandular tissue, i.e. volumetric breast density (VBD), may improve risk estimates, enhance personalized screening, enable treatment monitoring, and improve dose estimation. Methods to measure VBD in standard mammograms are emerging. With the introduction of breast tomosynthesis (tomo), there is a need and opportunity for implementation of VBD methods also in tomo, which may improve the VBD precision and offer local three-dimensional (3D) risk and sensitivity estimates. To investigate this, a prototype spectral photon-counting tomo system developed (Philips Healthcare) was calibrated using tissue-equivalent material. The material calibration allowed a single image acquisition to produce two sets of projection data corresponding to fibro-glandular and adipose thicknesses, respectively. The two data sets were reconstructed using filtered back-projection and combined to generate a 3D voxel map of breast densities. Such 3D density maps were generated from phantom images and a limited number of clinical images acquired within the HighReX EU project. Detection in the density maps was limited by photon noise. The VBD calculated over the maps showed an accuracy of 3 percentage points and a precision of 5.9 percentage points. These initial results indicate that the spectral tomo method performs on par with current methods for measuring VBD in conventional mammography, but also provides additional information that can potentially be used to improve the performance. Several potential improvements to reduce noise and increase accuracy and precision were identified.

## Characterisation of benign and malignant calcifications

L M Warren<sup>1</sup>, D R Dance<sup>1,2</sup>, S Astley<sup>3</sup> and K C Young<sup>1,2</sup>

<sup>1</sup>National Coordinating Centre for the Physics of Mammography, Royal Surrey County Hospital, Guildford, United Kingdom

<sup>2</sup>Department of Physics, University of Surrey, Guildford, United Kingdom

<sup>3</sup>Centre for Imaging Sciences, University of Manchester, Manchester, United Kingdom

**Aim:** We aim to develop tools to categorise calcifications by their features. Here the tools are used to distinguish benign and malignant calcification clusters. In a national audit of the breast screening programme in the UK for the years 2011/12 it was found that 2397 diagnostic open biopsies were performed on screen detected lesions. Of these 69% were benign and 31% were malignant. If it were possible to determine which cancers were benign or malignant from the mammogram it would be possible to reduce the benign biopsy rate.

**Method:** Ninety-nine malignant and 38 benign calcification clusters were randomly selected from our database of digital mammography images, and were segmented using a region-growing technique. An experienced radiologist confirmed the accuracy of the segmentation. The ground truth (whether the cluster was benign or malignant) was determined from the biopsy results. A feature vector of 120 features was calculated for the individual calcifications and 5 features for the clusters as a whole. Six different classifiers – K Nearest Neighbor, Decision Tree, Random Forest, Adaboost, Naïve Bayes and Linear Discriminate Analysis were applied to the data. The performance of the classifiers were compared using the f-score, overall accuracy and area underneath the receiver characteristic curve (ROC AUC).

**Results:** The classifier with the best overall performance at distinguishing benign and malignant calcification clusters was the AdaBoost classifier. This had an f-score of 0.81 ( $\pm 0.04$ ) and 0.56 ( $\pm 0.15$ ) for malignant and benign clusters respectively. The overall accuracy was 0.74 ( $\pm 0.05$ ) and the ROC AUC was 0.76 ( $\pm 0.06$ ).

**Conclusions:** We have developed tools to characterise calcifications according to their features. Here we have used the tools on a sample of images to classify benign and malignant calcification clusters. We have available a database of 523 malignant and 118 benign calcification clusters on which to apply these tools.

## Does the image quality measured using the CDMAM test object relate to cancer detection in mammography

A Mackenzie<sup>1</sup>, L M Warren<sup>1</sup>, M G Wallis<sup>2</sup>, J Cooke<sup>3</sup>, R M Given-Wilson<sup>4</sup>, D R Dance<sup>1,5</sup>, D P Chakraborty<sup>6</sup>, M D Halling-Brown<sup>7</sup>, P T Looney<sup>1</sup> and K C Young<sup>1,5</sup>

<sup>1</sup>National Coordinating Centre for the Physics in Mammography, Royal Surrey County Hospital, Guildford, United Kingdom

<sup>2</sup>Cambridge Breast Unit, Cambridge University Hospitals NHS Foundation Trust, Cambridge & NIHR Cambridge Biomedical Research Centre, Cambridge, United Kingdom

<sup>3</sup>Jarvis Breast Screening and Diagnostic Centre, Guildford, United Kingdom

<sup>4</sup>Department of Radiology, St George's Healthcare NHS Trust, London, United Kingdom

<sup>5</sup>Department of Physics, University of Surrey, Guildford, United Kingdom

<sup>6</sup>Department of Radiology, University of Pittsburgh, Pittsburgh, USA

<sup>7</sup>Scientific Computing, Department of Medical Physics, Royal Surrey County Hospital, Guildford, United Kingdom

**Purpose:** The EU guidelines set minimum and achievable standards for the threshold gold thickness for images of the CDMAM test object. This study evaluates the relationship between measured image quality and cancer detection.

**Method:** A novel method of converting images to appear as if acquired using different detectors was used. Mammograms acquired from seven systems using amorphous-selenium (a-Se) detectors were selected containing subtle malignant non-calcification lesions, biopsy-proven benign lesions, simulated malignant calcification clusters and normals. The images were adapted to simulate four types of detector: a-Se (Arm1) and caesium iodide (Arm2) converters, and two computed radiography detectors with a needle phosphor (Arm3) and a powder phosphor (Arm4). There were no differences in doses between the study arms. The mean glandular dose (MGD) of the simulated images was 1.18mGy for compressed breast thickness (CBT) between 55 and 65mm. Seven observers marked the location of suspected lesions along with a malignancy score. Analysis was undertaken using jackknife alternative free-response receiver operating characteristics (JAFROC) weighted figure of merit (*FoM*). Sixteen images of the CDMAM test object were also acquired from each system used for the acquisition of clinical images. The images were adapted to appear with the same dose and image quality as used for clinical images at the MGD equivalent to 60mm CBT.

**Results:** The *FoMs* for the calcification clusters were 0.782, 0.760, 0.707, 0.671 and for non-calcification lesions 0.697, 0.689, 0.648, 0.644 for arms 1 to 4 respectively. The threshold gold thicknesses of the 0.1mm disk were 0.790, 0.978, 1.28, 1.75 mm for Arms 1 to 4 respectively. Only Arm4 failed the minimum standards for the CDMAM at MGD of 1.18mGy. The *p*-value for a non-zero slope linear relationship between *FoM* and threshold gold thickness for 0.1mm diameter disk was 0.017 and 0.090 for calcification clusters and non-calcification lesions respectively. There was only a significant relationship between the detection of calcification clusters and measured image quality.

**Conclusions:** Cancer detection is correlated with image quality assessment using the CDMAM test object. Systems should be optimized to meet the EU guidelines achievable image quality level or cancer detection may be adversely affected.

## The use of PMMA to simulate local dense areas to assess automatic exposure control in digital mammography

R W Bouwman<sup>1</sup>, J Binst<sup>2</sup>, D R Dance<sup>3</sup>, K C Young<sup>3</sup>, W J H Veldkamp<sup>1,4</sup>, H Bosmans<sup>2</sup> and R E van Engen<sup>1</sup>

<sup>1</sup>Dutch reference centre for screening, LRCB, Nijmegen, The Netherlands

<sup>2</sup>Department of Radiology, UZ Gasthuisberg, Leuven, Belgium

<sup>3</sup>National coordinating centre for physics in mammography, NCCPM, Guildford, United Kingdom

<sup>4</sup>Leiden university medical centre, LUMC, Leiden, The Netherlands

**Purpose:** Current digital mammography (DM) X-ray systems are equipped with advanced automatic exposure control (AEC) devices. These devices control the exposure factors depending on breast composition. In the supplement of the European guidelines a test is included to evaluate the response of the AEC to local dense areas. In this test local dense areas are simulated by adding extra layers of polymethyl methacrylate (PMMA) to a standard dosimetry phantom. This study evaluates the test by estimating the glandular fraction of the local dense area and by comparing the range of doses found in the test with clinical data.

**Method:** The European guidelines states that this evaluation is performed by positioning a 30 mm thickness of PMMA on the bucky with 10 mm spacers so the breast thickness reading is 40 mm. Subsequently 11 exposures are initiated and after each exposure an additional 20x40x2 mm<sup>3</sup> PMMA plate is added at a specified position. This test was performed on four types of DM system and a further configuration giving a 50 mm breast thickness reading was also evaluated. The exposure data for patient images were collected and the distribution of the patient AGDs for breasts of 35 to 45 mm and 45 to 55 mm were compared with the phantom AGDs. In addition, the glandular fractions of the simulated dense areas were calculated analytically.

**Major findings:** The calculations showed that the proposed local dense area test simulates a total attenuation from fatty to glandular tissue and higher. The ranges of phantom and patient AGDs for breasts of 35 to 45 mm and 45 to 55 thickness were well matched.

**Conclusions:** The test which has recently been added in the supplement of the European guidelines works well and is valuable for estimating the range of patient doses for a given breast thickness. The larger thickness is suggested for a future version of the guidelines since it is closer to the standard thickness.

## How well do digital mammography systems in the UK breast screening programme meet European Guidelines?

K C Young<sup>1,2</sup>

<sup>1</sup>*National Coordinating Centre for the Physics of Mammography, Royal Surrey County Hospital, Guildford, United Kingdom*

<sup>2</sup>*Department of Physics, University of Surrey, Guildford, United Kingdom*

**Aim:** Previous work has shown how dose and detector type in mammography affect cancer detection and has demonstrated the link to image quality (IQ) measurements in European Guidelines. This study reviews how well the digital mammography systems in the UK Breast Screening Programme (NHSBSP) perform in terms of the standards in the Guidelines, with a particular emphasis on image quality and dose and whether the systems needed further optimization.

**Method:** Quality control (QC) measurements are made throughout the UK by medical physicists according to a standard protocol based on EU guidelines. Each physics centre was asked to return a spreadsheet with the most recent QC data for each system. 557 systems are currently used in the NHSBSP and data were returned for 489 digital systems. The data were loaded into a database for analysis. IQ measurements were generally made using software provided by our centre for analyzing CDMAM test object images.

**Results:** 98% of systems met the minimum IQ standard and 61% of systems exceeded the achievable standard. 100% of systems were below the mean glandular dose (MGD) limit of 2.5 mGy for a 53mm thick standard breast with MGDs ranging from 0.57 - 2.47 mGy, with a mean of 1.24 mGy. Threshold gold thickness for the CDMAM images were plotted against the MGD for an equivalent thickness of breast (60mm) for different models of X-ray set. This showed that there were marked variations in both performance and dose setting for the different models. Thus some models always exceeded the achievable IQ level while others never did. Many more systems could reach the achievable IQ level by increasing doses within existing limits.

**Conclusions:** While almost all systems met the minimum standards there was considerable scope to increase doses and to update models so that a greater proportion would exceed the achievable limits. The image quality standards in EU Guidelines seem to be practical and appropriate but too many systems are failing to meet the achievable level due to a lack of optimisation.



## Estimates of breast cancer growth rate from mammograms and its relation to histopathology

D Förnvik<sup>1,2</sup>, K Lång<sup>3</sup>, I Andersson<sup>3</sup>, M Dustler<sup>1</sup>, S Borgqvist<sup>4</sup> and P Timberg<sup>1</sup>

<sup>1</sup>Medical Radiation Physics, Lund University, Malmö, Sweden

<sup>2</sup>Oncology and Radiation Physics, Skåne University Hospital, Lund, Sweden

<sup>3</sup>Diagnostic Radiology, Lund University, Malmö, Sweden

<sup>4</sup>Division of Pathology, Skåne University Hospital, Malmö, Sweden

Mammography contains potentially useful prognostic information on the growth rate of malignant tumours, information that is rarely used in treatment planning. This is particularly true for patients participating in screening programs that implies repeated examinations at regular intervals. This study aimed to investigate the growth rate of 60 consecutive invasive breast cancers based on volume measures on at least two mammograms and its relation to histopathological findings. The average time for doubling of the tumour volume in all invasive breast cancer subtypes was  $328 \pm 172$  days (46-749 days). The mean tumour volume doubling time was 313 days (187-531 days) in grade I, 379 days (135-749 days) in grade II, and 98 days (46-151 days) in grade III tumours. Grade III breast cancers had a significantly shorter tumour volume doubling time compared to grade I & II tumours ( $P < 0.05$ ). There was a trend that invasive lobular carcinomas had a longer tumour volume doubling time compared to ductal types (508 days compared to 274 days) regardless of tumour grade. Multiple linear regression identified that tumour volume doubling time was associated with tumour stage, axillary lymph node involvement, histological grade, oestrogen and Ki-67 expression ( $P < 0.01$ ).

In conclusion, tumour volume doubling time as estimated on serial mammography often carries important prognostic information. This may be especially important regarding very slow growing and very fast growing breast cancers and thus it may contribute to proper treatment planning.

Results are preliminary and may be subject to change.

***Invited speaker*****Medical Image Perception II: How much of my time is this image worth?****J M Wolfe<sup>1,2</sup>**<sup>1</sup>*Visual Attention Lab, Brigham and Women's Hospital, Cambridge, MA, USA*<sup>2</sup>*Departments of Ophthalmology and Radiology, Harvard Medical School, Boston, MA, USA*

Clinicians are awash in medical images. How long should a clinician spend on a given image? There may be more to see in the current image but there are many more waiting to be viewed. Of course, this problem is not limited to medical image perception. How much time should I spend looking through the sale items on this website? Have I picked all the berries that I want from this bush? Should I move on to the next one? One source of information that may contribute to our answer to these questions is the “gist” of the scene or image. “Gist” refers to the information that can be extracted from an exceedingly brief glimpse of an image. For instance, with a 250 msec exposure to a mammogram, a radiologist can classify the image as normal or abnormal at above chance levels. A second factor with a powerful effect on the decision to abandon a search is the perceived prevalence of a target. Observers will tend to leave a search more readily if the target item is perceived to be rare. This is reasonable: you should probably spend less time searching the room for lost gold than for lost car keys. However, many expert search tasks (e.g. cancer screening) are designed as searches for very rare targets. In these cases, this otherwise adaptive “prevalence effect” becomes a source of error. Computer Aided Detection (CAD) seems like a potential solution, but the interactions of experts with CAD systems are not as successful as one might hope, a problem that may also be related to prevalence effects.

## Arranging for better learning opportunities in radiology

J Ivarsson<sup>1</sup>, H Rystedt<sup>1,2</sup>, S Asplund<sup>3</sup>, Å Johansson<sup>5,6</sup> and M Båth<sup>3,4</sup>

1) Department of Education, Communication and Learning, University of Gothenburg, Sweden

2) Teacher Education Department, University of Turku, Finland

3) Department of Radiation Physics, Institute of Clinical Sciences, Sahlgrenska Academy, University of Gothenburg, Sweden

4) Department of Medical Physics and Biomedical Engineering, Sahlgrenska University Hospital, Gothenburg, Sweden

5) Department of Radiology, Institute of Clinical Sciences, Sahlgrenska Academy, University of Gothenburg, Sweden

6) Department of Radiology, Sahlgrenska University Hospital, Gothenburg, Sweden

**Purpose:** The study provides an example on how it is possible to design environments at the workplace that could meet learning demands implied by the introduction of novel imaging technologies in radiology (in this case tomosynthesis). The innovative aspect of this design does not result from the implementation of any specific tool for learning. Instead, advancement is achieved by a novel set-up of existing imaging technologies. Based on a number of pedagogical principles, we developed what we call a *Technology enhanced Learning Session* (TLS), an interactive format that allows for focused discussions between learners with different levels of expertise.

**Method:** Interactions during a TLS were videotaped and later analysed using interaction analysis. We did not seek to explain factors affecting learning, but rather identify qualities of the arrangement that presented opportunities for professionally meaningful forms of action, i.e. enabling conditions of the TLS for displaying knowledge on how to judge radiological section images produced by the novel technology.

**Results:** Based on the analysis we propose three principles to be considered when designing learning environments for teaching professional modes of reasoning in radiology: First, the ways in which participants with different levels of experience interact and communicate have a large impact on the outcome of the activity. By publicly displaying records of the participants' individual assessments everyone can become involved and mistakes become dissected rather than hidden. Second, experts working on authentic cases give prominence to case specific details, disambiguation practices, and several dimensions of variation (in representations, anatomy, pathology etc.). Professional modes of reasoning, when being made publically visible, operate as instructions. Third, participants should be given shared access to visual materials: Given different setups, participants will have different possibilities of establishing shared references and partake in reasoning that build on visual details. As we have seen, the observers' ability to notice, discuss, and investigate particular features of the radiological images became a necessary requirement for the accomplishment of their collaborative work.

**Conclusions:** The study points to what we see as the underexplored possibilities of tailoring basic and specialist training that meets the new demands given by novel imaging technologies in radiology.

## **Video as a tool for optimization of radiological protection in image-guided interventions - possibilities and limitations**

**A von Wrangel<sup>1,2</sup>, A Almén<sup>1,2</sup>, M Båth<sup>1,2</sup>, H Rystedt<sup>3</sup> and C Lundh<sup>1,2</sup>**

<sup>1</sup>Department of Radiation Physics, Institute of Clinical Sciences, Sahlgrenska Academy at University of Gothenburg, Gothenburg, Sweden

<sup>2</sup>Department of Medical Physics and Biomedical Engineering, Sahlgrenska University Hospital, Gothenburg, Sweden

<sup>3</sup>Department of Education, Communication and Learning, University of Gothenburg, Gothenburg, Sweden

In healthcare, the highest patient and staff doses are received in image-guided intervention. This area includes a large variation of procedures with various prerequisites for performing radiological protection. Traditionally, radiation protection has mainly consisted of monitoring staff dose and providing personal radiation shielding in addition to education and training. New strategies have to be developed to achieve an optimized radiation protection in these changing environments. It could be anticipated that video could be a useful tool for optimization. The aim of this work was to develop video as a tool for optimization of radiological protection in image-guided interventions.

Video recordings of the staff during image-guided abdominal interventions have been performed. Three cameras were used. Camera one was placed to get an overview of the room. The second camera was placed on the monitor facing the staff and camera three was recording the live monitor from the x-ray system. The video recordings were visually analyzed. Technical parameters were additionally collected from the x-ray system. Dose rate data was also collected during the procedures.

So far, three procedures have been analysed in order to develop the optimization tool. The most important camera angle was the one over viewing the room. It was with the chosen angles, however, difficult to see what the staff members were looking at during the procedures.

In developing the tool the following has been identified as important issues to consider; the number and position of cameras, the sound quality, editing of video material and safety issues. Furthermore, it is important to consider the competence of the evaluating team, which need to be multidisciplinary. Above all, ethical aspects of recording patients and staff have to be addressed. The present study combines video recordings of the interventional staff with information of the variation of dose rates during the procedure. This is a novel approach for education and training strategies.

## **Basic radiation protection education and training for medical professionals, Georgian experience and future perspectives**

**F Todua<sup>1</sup>, D Nadareishvili<sup>2</sup>, G Ormotsadze<sup>2</sup> and T Sanikidze<sup>3</sup>**

<sup>1</sup>*The Georgian National Academy of Science; Radiological Society of Georgia, Scientific-Research Center of Clinical Medicine, Tbilisi, Georgia*

<sup>2</sup>*LEPL Beritashvili Experimental Biomedicine Center of Ministry of Education and Science of Georgia, Tbilisi, Georgia*

<sup>3</sup>*Tbilisi State Medical University, Tbilisi, Georgia*

In order to make it compatible with new European and International BSS, in 2012 a new law about "Nuclear and radiation Safety" was passed in Georgia. In 2014, safety guides in medical exposure were entered into force. From this point of view, medical and healthcare professionals' education and training in conformity with new International and National safety standards is an urgent task.

For the purpose of solving this problem, I. Beritashvili Center of Experimental Biomedicine and Tbilisi State Medical University in collaboration with IOMP, EFOMP and US HPA, with the support of the Ministry of Education and Science of Georgia and the National Academy of Science, carried out a number of projects, including:

- "Radiobiology and Radiogenic Health Risk" as an elective course in the Faculty of Medicine;
- Summer and winter schools in Medical Physics. Radiobiology and Radiation Protection.

The level of knowledge in medical students was evaluated in field of the radiation exposure in medicine. Namely:

- 1) The health effects of low radiation doses;
- 2) Radiogenic cancerogenic risk assessment and management;
- 3) Physical principles and technological aspects of medical visualization;
- 4) Health risks associated with them and the issues regarding their minimization.

The results of the research in this field showed the necessity of the educational curriculum improvement, namely:

- 1) The inclusion of basic radiobiological course in the curriculums of the faculties of medicine and public health;
- 2) Amplification of the Medical Physics course through more detalisation of through medical visualization issues.

## Organ dose estimation and quality image assessment in computed tomography

C Adrien<sup>1</sup>, C Le Loirec<sup>1</sup>, J C Garcia-Hernandez<sup>1</sup>, S Dreuil<sup>2</sup> and J M Bordy<sup>1</sup>

<sup>1</sup>CEA, LIST, F-91191 Gif-sur-Yvette, France

<sup>2</sup>Institut Gustave Roussy, Villejuif, France

Due to the significant rise of computed tomography (CT) exams in the past few years and the increase of the collective dose due to medical exams, dose estimation in CT imaging has become a major public health issue. However dose optimization cannot be considered without taking into account the image quality which has to be good enough for radiologists. However, in clinical practice, dose is estimated by empirical index and image quality by measurements performed on specific phantoms like the CATPHAN<sup>®</sup>. Based on this kind of information it is thus difficult to correctly optimize protocols regarding organ doses and radiologist criteria.

Therefore our goal is to develop a tool optimizing the patient dose while preserving the image quality needed for diagnosis. The work is divided into two main parts: *(i)* the development of a Monte Carlo dose simulator, and *(ii)* the assessment of an objective image quality criterion. In this paper, developments of the Monte Carlo dose simulator are mainly discussed. For this end, a Monte Carlo tool, based on the PENELOPE code is used. This tool should ultimately enable CT exam simulations in a voxelized numerical phantom mimicking the human anatomy. For that purpose the GE Lightspeed VCT 64 CT tube was modelled by adapting the method proposed by Turner *et al* (Med. Phys. 36: 2154-2164). The axial and helical movements of the X-ray tube were then implemented into the MC tool. Each step of the modelling was then validated with experimental measurements. The MC tool was after all validated for dosimetric purposes.

In parallel the SNR of the CTP 404 inserts from the CATPHAN<sup>®</sup> 600 was computed by using several model observers: the classical Rose model and the recent Ott model (Phys. Med. Biol. 59: 4047-4064). A comparison has been performed between the two models to estimate the detectability of small inserts into a pre-clinical phantom.

The first results of the dose estimation tool performed in anthropomorphic phantoms and clinical conditions are very encouraging. The work about the assessment of an objective quality image is still in progress.

## Computed Tomography dose calculations using a radiation Treatment Planning System

H-E Källman<sup>1,5</sup>, R Holmberg<sup>2</sup>, J Andersson<sup>3</sup>, L Kull<sup>4</sup>, E Traneus<sup>2</sup> and A Ahnesjö<sup>5</sup>

<sup>1</sup>Center for Clinical research, County Dalarna, Falun, Sweden

<sup>2</sup>RaySearch Laboratories, Stockholm, Sweden

<sup>3</sup>Department of Radiation Sciences, Radiation Physics, Umeå University, Umeå, Sweden

<sup>4</sup>Radiation Physics, County Norrbotten, Luleå, Sweden

<sup>5</sup>Medical radiation sciences, Inst. for Immunology, Genetics and Pathology, Uppsala University, Uppsala, Sweden

**Purpose:** Explore the possibility to use a radiation Treatment Planning System (TPS) for CT patient dose calculations.

**Method:** The Kerma distribution and Half Value Layer of the beam on a standard CT (GE Optima 660, GE Healthcare, USA) was determined. The beam data was used to define a source model for Monte Carlo dose calculations in the TPS (Raystation, RaySearch Laboratories, Stockholm, Sweden). DICOM image header parameters and log files from the CT examinations was used to define the movement of the radiation beam relative the patient couch and the modulation of the beam intensity during the movement. The dose calculations were validated in solid water (stationary radiation beam) and in an anthropomorphic phantom (moving radiation beam).

**Major findings:** For a stationary beam, the calculated depth dose in solid water was in close agreement with the dose measured with an ionization chamber.

For a moving beam, the calculated dose in the anthropomorphic phantom was verified using TLD. In this geometry, the movement of the beam was verified and the maximum difference between calculated and measured dose was 15%. Absolute dose comparisons was hampered by the energy dependence of the TLD.

**Conclusions:** Calculation of patient dose with an accuracy that facilitates risk estimates can be done using a TPS. The developed beam model for a CT is specified by measurements that can be performed on any clinical CT. The data in the DICOM header is sufficient to describe the required aspects of the scan, except the beam intensity modulation retrieved from a logfile belonging to the CT examination.

## **A Monte-Carlo simulation framework for joint optimisation of image quality and patient dose in digital paediatric radiography**

**B Menser<sup>1</sup>, D Manke<sup>2</sup>, D Mentrup<sup>2</sup> and U Neitzel<sup>2</sup>**

<sup>1</sup>*Philips Research, Eindhoven, The Netherlands*

<sup>2</sup>*Diagnostic X-ray Advanced Development, Philips Healthcare, Hamburg, Germany*

**Introduction:** In paediatric radiography, the imaging task should be performed with the lowest possible radiation dose according to the ALARA principle. Therefore, it is essential to adapt the acquisition parameters to the body size of the paediatric patient. In this work, we present a Monte-Carlo simulation framework for optimizing the imaging protocols in digital paediatric radiography. In contrast to other dose optimisation approaches described in literature, this framework allows for simultaneous assessment of both patient dose and image quality aspects from the same simulation.

**Simulation framework:** A framework for simulating the image acquisition in digital radiography has been developed. The core components are a proprietary Monte-Carlo engine and a set of anthropomorphic, voxelized patient models based on the XCAT2 phantom library from Duke University. The Monte-Carlo simulation collects the deposited energy for each voxel of the segmented patient model, which enables the calculation of organ dose and effective dose. While the scattered radiation in the image is also obtained with Monte-Carlo methods, the primary radiation is calculated analytically with a high resolution version of the patient model. This results in simulated radiographies that allow for a visual and numerical assessment of image quality aspects.

**Experimental validation:** This work focuses on the experimental validation of the imaging chain simulation. The performance of the Monte-Carlo engine in estimating the patient dose has been investigated in a previous work (Prinsen et al., ECR 2014 – Book of Abstracts, 2014). X-ray images of different technical phantom setups consisting of several PMMA and aluminium plates have been simulated and compared to x-ray images of real phantoms from a DigitalDiagnost 4.0 system (Philips Healthcare). The same quantitative image figures have been determined on both the simulated and real x-ray images. For a wide range of x-ray spectra (40-100kV, with and without pre-filtration) the differences in signal and noise levels are both below 3%, and the errors for simulated contrast and CNR values are generally below 10%.

**Conclusion:** It has been validated experimentally that the simulation framework is able to reproduce both patient dose and figures related to image quality at high accuracy. Therefore, it may be used to optimize the imaging parameters in paediatric radiography.



## Dual-lattice anthropomorphic voxel models for image quality optimization

**N Petoussi-Henss<sup>1</sup>, J Becker<sup>1</sup>, M Greiter<sup>1</sup>, H Schlattl<sup>1</sup>, M Zankl<sup>1</sup> and C Hoeschen<sup>1,2</sup>**

<sup>1</sup>*Research Unit Medical Radiation Physics and Diagnostics, Helmholtz Zentrum München, Neuherberg, Germany*

<sup>2</sup>*Institute of Medical Technology, Department of Electrical Engineering and Information Technology, Otto-von-Guericke University, Magdeburg, Germany*

The purpose is to establish a method to determine the dependence of dose and image quality on imaging settings (e.g., filtration, tube voltage) for various imaging technologies. This method employs simulations of the imaging process using Monte Carlo methods and a combination of a standard and higher resolution voxel models. These combined voxel models (or phantoms) are called “dual lattice”.

A high-resolution model of a lung ((0.11 mm)<sup>3</sup> voxel volume, slice thickness: 114 μ) was fitted into a whole-body voxel model which had initially a lower resolution (in plane resolution: 1.875 mm; slice thickness 5 mm, voxel volume: 17.6 mm<sup>3</sup>). It was shown that this resolution was too coarse in comparison to the lung model and the simulated x-ray image resulted consequently in jagged, step structures, particularly at the edges of the ribs. These steps could eventually cover the fine structures, preventing therefore their recognition.

For this reason the edges of the organs in the body model surrounding the high-resolution organ model were smoothed. This was achieved by creating a NURBS/PM-based representation of the body model and giving a finer resolution of 500 microns for the re-voxelization of the NURBS/PM model. A NURBS/PM model allows easy modification of anatomical features as well as posture and it can be re-voxelized to any resolution. Thorax examinations of different parameters were simulated using the Monte Carlo code EGS4nrc, modified such as to perform dual lattice transport.

It was shown that voxel models of different voxel resolution can be combined – higher resolution in partial body and lower resolution in the rest of the body. The fine structures of the lung were easily recognizable at the simulated images. Thus, the influence of various imaging parameters on the resulting image quality (e.g., contrast-to-noise ratio, MTF or NPS) can be investigated.

## Customization of a Monte Carlo dosimetry tool for dental Cone Beam CT systems

A Stratis<sup>1</sup>, G Zhang<sup>2</sup>, R Jacobs<sup>1</sup>, R Bogaerts<sup>2</sup> and H Bosmans<sup>2</sup>

<sup>1</sup>*Katholieke Universiteit Leuven, Department of Imaging and Pathology, OMFS-IMPACT Research Group, Campus St. Raphael, Leuven, Belgium,*

<sup>2</sup>*University Hospitals of Leuven, Leuven, Belgium*

**Purpose:** To customize, calibrate and validate a Monte Carlo (MC) framework intended to be applied to different dental CBCT systems for dosimetric applications.

**Method:** A previously developed EGSnrc MC framework was adapted to operate based on equivalent source models requiring only energy spectra and filter description measurements. Half Value Layer (HVL) and air kerma measurements across the edge of the detector were performed with an FC65-G Farmer ionization chamber (IC) (IBA Dosimetry, Schwarzenbruck, Germany) to specify the energy spectra and describe the total filtration. The method was initially applied to a Promax 3D Max (Planmeca, Helsinki, Finland) CBCT scanner. A so-called Monte Carlo calibration factor was established to relate the dose in a real scan ( $\mu\text{Gy}/\text{mAs}$ ) to the MC calculated dose ( $\mu\text{Gy}/\text{histories}$ ) in air. For validation, we measured the doses at 4 different positions within a cylindrical water phantom and compared the results against the simulation counterparts. This was achieved by careful voxelisation and subsequent simulation of the phantom and the ion chamber.

**Results:** Unique calibration factors were obtained for each scan protocol. The minimum difference between the measured and the calculated dose values was observed when the IC was placed at the centre of rotation (1.8%). In the same central axial plane of the FOV, the difference was 3% when the IC was shifted towards the detector and positioned at 1 cm inside the boundaries of the FOV. The maximum difference was 6.1% when the ion chamber was positioned along the rotation axis close to the upper edge of the FOV, whereas closer to the lower edge the difference was 4%.

**Conclusion:** A hybrid Monte Carlo simulation tool for dental CBCT was calibrated and validated for dosimetric applications for a Planmeca Promax 3D Max system. This work is part of a larger study in which we aim for a flexible dosimetry tool intended to calculate organ doses in patient specific voxel models and specific system characteristics.

## A method for simulation of spiculated mammographic lesions

P Elangovan<sup>1</sup>, A Rashidnasab<sup>1,4</sup>, R Ferrari Pinto<sup>1</sup>, D R Dance<sup>2,3</sup>, K C Young<sup>2,3</sup> and K Wells<sup>1</sup>

<sup>1</sup>Centre for Vision, Speech and Signal processing, University of Surrey, Guildford, United Kingdom

<sup>2</sup>National Co-ordinating Centre for the Physics of Mammography (NCCPM), Royal Surrey County Hospital, Guildford, Surrey, United Kingdom

<sup>3</sup>Department of Physics, University of Surrey, Guildford, United Kingdom

<sup>4</sup>Department of Imaging and Pathology, KU Leuven, Leuven, Belgium

**Aim:** Our group is developing the use of computational modelling tools for rapid evaluation and comparison of breast imaging systems with virtual clinical trials. Such an approach relies on the simulation of 3D synthetic cancer pathology that is similar in appearance to real breast cancer tumours. In previous work, we used a fractal-growth approach called diffusion limited aggregation (DLA) to simulate masses with ill-defined margin, and subsequently conducted studies involving a team of radiologists to validate their appearance. In this study we aim to extend the model to create masses with realistic spiculations.

**Method:** The spicules were modelled as 3D cubic splines and added to the surface of the core synthetic lesions generated using the DLA method. In order to simulate spicules with realistic curvature, 2D skeletons of spicules were extracted from clinical mammograms containing spiculated lesions. These templates were used as a guideline for appropriate selection of inflection points for generating spicules. A diverse range of realistic spiculated lesions was generated by modifying the input parameters to the model such as the number of spicules, number of spiculated clusters, cluster size and spicule distribution. The spiculated lesions were inserted into normal clinical images using a physics based insertion technique and then shuffled with real spiculated images, and finally presented to a team of radiologists for ranking as to their realism.

**Results:** The preliminary results showed that the observers had difficulty in differentiating simulated spiculated lesions from real spiculated lesions, and radiologists rated spiculated lesions sufficiently greater than DLA masses in realism and malignancy.

**Conclusions:** The results demonstrate the feasibility of this approach and warrant a detailed study which is currently underway.

***Invited speaker*****The use of diagnostic reference levels in optimisation****C J Martin<sup>1</sup>***<sup>1</sup>Department of Clinical Physics, University of Glasgow, Glasgow, United Kingdom*

The concept of diagnostic reference levels (DRLs) was introduced in the UK to aid optimization of radiation protection for diagnostic procedures in the 1990s. Results from surveys of patient doses were used to determine reference doses for which the majority of radiologists considered images were adequate for diagnosis. This allowed medical physicists to compare dose measurements made in their hospitals with recognised standards. The concept of DRLs has since been adopted by ICRP, and the European Basic Safety Standard requires governments to promote establishment of national DRLs and assessment of patient doses as part of the optimization process for medical exposures. National DRLs can be based initially on patient dose surveys in 20-30 large hospitals. Common types of examinations representative of hospital workload should be used, and data collected for 20-30 patients for each examination. Restrictions on patient weight will generally be required, but electronic data collection of larger samples can avoid the need for this restriction. DRLs are defined in terms of measured quantities, namely entrance surface air kerma and kerma-area product for radiographic and fluoroscopic exposures, and for computed tomography (CT) the CT dose index and dose length product. The ICRP proposes that median doses for each type of examination at every hospital be collated and DRLs based on the 3<sup>rd</sup> quartile value of the distribution of medians for all hospitals. In addition the setting of a national achievable dose related to the median value from the distribution is recommended to encourage further optimisation. The setting of DRLs is the first step in a continual process of dose audit and optimisation. Thereafter regular audits of patient dose should be undertaken to collect data from which patient doses can be determined for examinations that reflect the clinical workload and range of equipment used at each hospital. Median doses from the distributions should be compared with relevant DRLs to identify procedures for which further optimisation is required and corrective action taken. This paper describes methods involved in setting DRLs, carrying out patient dose surveys as part of dose audit, and gives examples to illustrate the optimisation process.

## Diagnostic dose levels in paediatric Computed Tomography at the Queen Silvia Children's Hospital, Gothenburg, Sweden

A Thilander-Klang<sup>1,2</sup>, M Hultenmo<sup>1</sup>, S Johansson<sup>3</sup> and H Caisander<sup>3</sup>

<sup>1</sup>Department of Medical Physics and Biomedical Engineering, Sahlgrenska University Hospital, Gothenburg, Sweden

<sup>2</sup>Department of Radiation Physics, Institute of Clinical Sciences, the Sahlgrenska Academy, University of Gothenburg, Gothenburg, Sweden

<sup>3</sup>Department of Paediatric Radiology and Physiology, The Queen Silvia Children's Hospital, Gothenburg, Sweden

**Purpose:** In the optimisation of image quality in Computed Tomography (CT) the knowledge of the radiation dose level is an important factor especially for the examination of children. The aim of this study was to investigate the dose levels from CT examinations at the Queen Silvia Children's Hospital.

**Materials and Methods:** During the time period January 25<sup>th</sup> 2012 to August 11<sup>th</sup> 2013 the Radiation Dose SR objects from all the CT examinations performed on the CT unit [Discovery CT750HD, GE Healthcare] were collected using the DoseWatch software [GE Healthcare]. But here are only the standard (trauma and tumour) examinations of the brain (n=707), thorax (n=149) and abdomen (n=312) included. The values of CTDI<sub>vol</sub> (Computed Tomography Dose Index by volume) and DLP (Dose Length Product) were among the collected data. For comparison only one series is included in the DLP values even if the patient has been exposed to more than one series.

The CT protocols are labelled according to age, but the radiographer takes also into account the body weight of the patient when selecting the protocol to use. The age groups are: 0-6 months, 7-11 months, 1-5 y, 6-10 y, 11-15 y, and adults. The groups corresponds roughly to <7kg, 7-10 kg, 10-20 kg, 20-30 kg, 30-50 kg, and >50 kg in body weight.

**Results:** The most frequent CT examination were the ones of the brain. The average CTDI<sub>vol</sub> = 18 mGy with average DLP = 269 for mGycm patients between 1 and 5 years-old at examination (n=169). The corresponding values were 24 mGy and 359 mGycm for patients between 6-10 years-old (n=196) and 26 mGy and 402 mGycm for patients between 11-15 years-old (n=215). For example CT Abdomen for patients between 11-15 years-old (n=189) the average CTDI<sub>vol</sub> was 3.7 mGy with an average DLP of 154 mGycm.

**Conclusions:** Average CTDI<sub>vol</sub> and DLP values has been determined for 1 168 pediatric CT examinations of the brain, thorax and abdomen examinations of children between 0 and 18 years-old at examination. Local dose reference levels from these CT examinations has been established.

## Multicentre comparison of patient dose for X-ray guided embolizations of arteriovenous malformations in the brain

J E M Mourik<sup>1,2</sup>, M L Overvelde<sup>3</sup>, D Zweers<sup>1</sup> and K Geleijns<sup>1</sup>

<sup>1</sup>*Department of Radiology, Leiden University Medical Center, Leiden, The Netherlands*

<sup>2</sup>*Department of Radiology / Nuclear Medicine, Sint Franciscus Gasthuis, Rotterdam, The Netherlands*

<sup>3</sup>*Medical Physics, Albert Schweitzer Hospital, Dordrecht, The Netherlands*

**Purpose:** Due to the long fluoroscopy times and repeated DSA runs, the threshold entrance skin dose for tissue reactions, such as temporary epilation of the scalp (2–3Gy), is sometimes exceeded during X-ray guided embolization of arteriovenous malformations (AVM) in the brain. Dosimetric benchmarking was performed to investigate entrance skin dose(-rate) and entrance detector dose(-rate) for complex neuroradiological interventions and to identify opportunities for optimization.

**Methods and materials:** A head phantom was developed from Perspex and aluminium. The entrance dose-rate (fluoroscopy) and dose per frame (DSA) were measured with a solid-state dosimeter (RTI Piranha T20) at the phantom surface (entrance skin dose(-rate), ESD) and at the flat panel detector (entrance detector dose(-rate), EDD) at 5 hospitals. Four hospitals were highly experienced in performing very complex embolizations procedures, while one hospital only performed less complex procedures. The acquisition protocols that were used in routine clinical practice were investigated, both for fluoroscopy and DSA, and measurements were performed for all available magnifications. In addition, technical characteristics of the AVM Imaging protocols were recorded and compared.

**Results:** Main differences in protocols involved tube voltage (75–105 kVp), pulse-rate (6.3–15 fr/s) and beam filtration (0.3mm Cu up to 0.9 mm Cu + 1 mm Al). For fluoroscopy, measured ESD and EDD were in the ranges (44–488  $\mu\text{Gy/s}$ ) and (0.3–1.6  $\mu\text{Gy/s}$ ), respectively. For the standard magnifications, higher ESD were measured for hospital E, up to 145% (20 cm) and 168% (31 cm) compared to the other hospitals. For DSA, ESD of 744–3600  $\mu\text{Gy/frame}$  and EDD of 2.6–9.7  $\mu\text{Gy/frame}$  were found. For a magnification >30 cm similar ESD values (dose difference < 25%) were obtained for DSA in all hospitals. For hospital E and magnification of 20 cm, up to 94% higher dose-rates were measured.

**Conclusion:** Large differences in both acquisition protocols and entrance dose were observed between the hospitals. Optimization of pulse-rate, dose per pulse, beam filtration and tube voltage may further improve imaging protocols and lower the patient dose.

## Updated estimations of effective dose for PET radiopharmaceuticals recently published by the ICRP

M Andersson<sup>1</sup>, L Johansson<sup>2</sup>, D Minarik<sup>1</sup>, S Mattsson<sup>1</sup> and S Leide Svegborn<sup>1</sup>

<sup>1</sup>Medical Radiation Physics, Department of Translational Medicine, Lund University, Skåne University Hospital, Malmö, Sweden

<sup>2</sup>Department of Radiation Sciences, Umeå University, Umeå, Sweden

**Aim and background:** The potential risk for stochastic effects of ionising radiation (mainly lethal cancer) to a population is currently estimated by the effective dose. In recent years, there have been a number of revisions and updates influencing the method to estimate the effective dose. This relates both to the phantom used for organ/tissue dose calculations and the organ/tissue weighting factors. The aim of this study was to perform effective dose estimations for <sup>18</sup>F-FET, <sup>18</sup>F-FLT, <sup>18</sup>F-choline, <sup>18</sup>F-fluoride and <sup>11</sup>C-raclopride using the most recent phantoms and weighting factors.

**Material and Methods:** The biokinetic models for the five radiopharmaceuticals were based on the models given in the fourth addendum to ICRP publication 53. A modification of the gastro-intestinal tract was applied in order to incorporate the ICRP human alimentary tract model. The effective dose estimations were made with the ICRP/ICRU computational adult male and female voxel phantoms together with the new tissue weighting factors from ICRP publication 103. The internal dose calculations were performed with the computer program IDAC2.0, which have included these changes and also uses the decay data of ICRP publication 107.

**Results and Conclusion:** The new effective doses per administered activity were calculated to be 0.015, 0.014, 0.0089, 0.020 and 0.0043 mSv/MBq for <sup>18</sup>F-FET, <sup>18</sup>F-FLT, <sup>18</sup>F-fluoride, <sup>18</sup>F-choline, and <sup>11</sup>C-raclopride, respectively. The radiation risk estimations showed a reduction in effective dose for all five radiopharmaceuticals using the updated methods and assumptions compared to the previous ones. The largest difference was for <sup>18</sup>F-fluoride with a reduction of 48% (from 0.017 mSv/MBq to 0.0089 mSv/MBq) compared to the previous estimation.

## **Managing patient's dose in digital x-ray chest screening examinations using an anthropomorphic phantom: comparison between a Russian and a Swedish hospital**

**A V Vodovatov<sup>1</sup>, A A Drozdov<sup>2</sup> and C Bernhardsson<sup>3</sup>**

*<sup>1</sup>St-Petersburg Research Institute of Radiation Hygiene after Professor P.V.Ramzaev, St-Petersburg, Russia*

*<sup>2</sup>St-Petersburg State Mariinsky Hospital, St-Petersburg, Russia*

*<sup>3</sup>Medical Radiation Physics, Department of Traditional Medicine, Malmö, Lund University, Skåne University Hospital, Malmö, Sweden*

An anthropomorphic phantom study was performed in 2013-2014 on conventional x-ray units at two different hospitals, one located in Russia (Mariinsky hospital, St-Petersburg) and one in Sweden (Skåne University hospital, Malmö). The aim of the study was to determine the potential of patient dose (dose-area product and effective dose) reduction in digital x-ray chest screening examinations by changing the tube voltage, additional filtration thickness and grid. It was possible to achieve up to 50% DAP reduction by raising the tube voltage and simultaneously increase the total filtration to the maximum allowed by the x-ray unit. The effective dose decreased by 10-15% with the tube voltage increase and increased by the same value with the increase in the total filtration. Absence of grid allowed to reduce both DAP and effective dose by 50-80%. Comparison between Russian and Swedish x-ray units showed the same trend in DAP and effective dose reduction. However, the absolute dose quantity values were lower by almost a factor of 10 for the Swedish units due to different image receptors and image reconstruction algorithms.



## Iterative scatter correction for grid-less bedside chest radiography: Performance for a chest phantom

D Mentrup<sup>1</sup>, S Jockel<sup>1</sup>, B Menser<sup>2</sup> and U Neitzel<sup>1</sup>

<sup>1</sup>*Diagnostic X-ray Advanced Development, Philips Healthcare, Hamburg, Germany*

<sup>2</sup>*Philips Research, Eindhoven, The Netherlands*

**Purpose:** In clinical practice, using an anti-scatter grid is often avoided for bedside thorax examinations because of dose considerations and a more complicated workflow. The quality of the resulting non-grid chest images is compromised by a significant loss of image contrast caused by scattered radiation. This work demonstrates that the contrast in radiographs of a chest phantom can be restored by software-based scatter correction which involves an iterative model-based estimation of the scatter signal and a grid-like subtraction of the scatter signal.

**Methods:** An algorithm was developed to correct for the scatter background in images acquired without anti-scatter grid (commercial name: *SkyFlow*). The algorithm implies an iterative estimation of the scatter signal employing pre-computed Monte Carlo scatter kernels, and a partial subtraction of the estimated scatter signal using grid calibration data. Radiographs of a thorax phantom were acquired using a portable flat detector both with and without a stationary anti-scatter grid. Three aluminum discs were placed in the lung, the retrocardial and the abdominal areas. The contrast generated by the discs was measured in both images, and the local contrast improvement factors (CIF) achieved by the anti-scatter grid were determined. Additionally, contrasts generated by the discs were measured before and after scatter correction, and the CIFs achieved in this way were calculated.

**Findings:** The CIFs achieved with the software scatter correction were 1.42 in the lung (grid: 1.46), 1.79 in the retrocardial area (grid: 1.79), and 2.41 in the abdomen (grid: 2.46). The CIFs obtained with the grid and with scatter correction are in good agreement. Therefore, the experiment demonstrates quantitatively that software-based scatter correction allows restoring the image contrast of a non-grid image in a manner comparable to an anti-scatter grid. In addition, the visual appearance of the resulting chest phantom images is similar, and scatter correction does not lead to an artificial noise impression.

**Conclusion:** By providing grid-like image contrast for non-grid chest radiographs, software-based scatter correction may have the potential to allow grid-less image acquisition for portable chest radiography.

## **Influence of scout acquisition and scan direction on the dose reducing effect of automatic tube current modulation**

**C Franck<sup>1</sup> and K Bacher<sup>1</sup>**

*<sup>1</sup>Department of Basic Medical Sciences, Ghent University, Ghent, Belgium*

In order to reduce the potential risk for radiation induced malignancies, manufacturers have introduced different CT dose reduction tools, such as automatic tube current modulation (ATCM) systems. We investigated the influence of the scout acquisition and the actual CT scan direction on the dose reducing effect of the ATCM.

Chest CT-scans with ATCM were made of an isocentrically positioned anthropomorphic RANDO<sup>®</sup> phantom, containing thermoluminescent dosimeters (TLD's). We evaluated 4 CT systems: Siemens Somatom Definition Flash and AS, GE Discovery 750 HD and Toshiba Aquilion. Prior to the chest CT, a scout scan was made with the x-ray tube either in the anteroposterior (AP), posteroanterior (PA) or lateral (LAT) direction. The chest CT was acquired in either a caudocranial (CAUD) or craniocaudal (CRAN) scan direction, using ATCM. TLD-readings were converted into effective dose (E), according to ICRP103 (ICRP Publication 103, 2007). Image quality was assessed by calculating noise in roi's within the phantom.

Higher and lower tube currents are selected by the ATCM, when the scan is based on a PA or LAT scout respectively. Compared to AP, tube currents of a PA- and LAT-scan are respectively on average 16% higher and 31% lower. Consequently, E increases with a factor 1.7 with a PA- instead of a LAT-scan. A CAUD scan gives less current to the neck, compared to a CRAN scan based on the same scout. Therefore thyroid dose halves by taking the scan in CAUD direction. Noise values weren't significantly different when changing scan direction or scout acquisition.

Orientation of scout and scan direction influences the dose reducing efficacy of ATCM.

## Characterising the EOS™ slot scan imaging system with using effective Detective Quantum Efficiency

A H Clavel<sup>1,2,3</sup>, P Monnin<sup>1</sup>, J M Létang<sup>2</sup>, F R Verdun<sup>1</sup> and A Darbon<sup>3</sup>

<sup>1</sup>Institute of Radiation Physics, CHUV, Lausanne, Switzerland

<sup>2</sup>CREATIS, CNRS UMR 5220, Inserm U1044, INSA-Lyon, Villeurbanne, France

<sup>3</sup>EOS Imaging, Paris, France

As opposed to classical detective quantum efficiency (DQE), effective DQE (eDQE) is a figure of merit that allows comparing performances of imaging systems in the presence of scatter rejection devices. In particular, it allows comparing the performances of DR and CR systems relying on external anti-scatter grids, with a system such as EOS™.

The EOS™ linear slot scanning system uses a multi-wire proportional X-ray detector allowing images with over 3.104 levels of grey. Its geometry is such that the detector is self-collimated and rejects scattered radiation. In this study, we used the eDQE to characterise the performances of the EOS™ system in imaging conditions similar to those used in clinical practice.

Effective DQEs were computed from acquisitions with a PMMA phantom placed in the X-ray beam, for various tube voltages (70, 90, 120 kVp), phantom thicknesses (15, 20, 25, 30cm) and air kerma at detector entrance (7.5 to 187  $\mu$ Gy). Signal amplification within the EOS™ detector was kept constant. For each configuration, response curves were determined to correct for the detector's non-linearity, before computing the metrics necessary to the eDQE estimation. Scatter fractions were assessed from the images' signal using the beam stop technique.

Scatter fractions were in the range 4-5% for all configurations. EOS™ eDQE maximum values of 8.5%-14% were found around 0.1  $\text{mm}^{-1}$ . These figures have been obtained with a non-optimised setting (Large Focal Spot and Al additional filter), but still over-perform the best DR systems eDQEs (2%-10%) as recently assessed in a recent publication. Furthermore, the eDQE decreasing trend with increasing phantom thicknesses observed in DR systems was not observed with the EOS™ system.

In EOS™ images the scatter fraction is extremely low (4-5%), allowing low dose image acquisitions in clinical routine. Moreover, amplification of the signal within the image detector allows reaching high eDQE at low frequencies, even behind high patient thicknesses.

## System upgrade on Philips Allura FD20 angiography systems: Effects on patient skin dose and static image quality

N Ryckx<sup>1</sup>, M Sans-Merce<sup>1</sup> and F R Verdun<sup>1</sup>

<sup>1</sup>*Institute of radiation physics, CHUV, Lausanne, Switzerland*

**Purpose:** The extensive use of fluoroscopy in vascular interventions can lead to high patient skin doses. This implies an increased risk of deterministic effects such as depilation, skin and subcutaneous tissue damage. To tackle this problem, Philips Healthcare recently commercialized a new software upgrade (Clarity), claiming to reduce patient exposure while maintain sufficient image quality.

**Materials and methods:** We used 5cm PMMA slabs to simulate patient with thicknesses ranging from 5 to 20cm. A 6cc ionization chamber (Radcal, USA) located at 75cm from the focal spot was used to determine patient entrance skin dose. A TOR-CDR phantom (Leeds Test Objects, UK) was used to assess low-contrast detectability (LCD) and spatial resolution. Two Allura FD20 flat-panel angiography systems, one of which was updated with Clarity, were assessed, and the collected data was compared for the main clinical protocols: low, medium and high quality fluoroscopy, abdominal and thigh digital subtraction angiography (DSA).

**Results:** For the fluoroscopy modes, average dose reductions of 25% (low), 44% (medium) and 35% (high) were measured. The dose per image for DSA runs was reduced by 70% (abdomen) and even 84% (thigh). No significant decrease in image quality was observed for both the LCD and the spatial resolution.

**Conclusion:** The Clarity upgrade for Philips angiography systems seems to be an efficient way to reduce patient exposure, and thus radiation risks. Further investigation should be made for two elements. First, the dynamic response should be assessed using a high-contrast moving objet. Second, further effort should be put into estimating the gain in staff exposure.

## Comparison of wireless detectors for digital radiography systems: Image quality and dose

J E M Mourik<sup>1,2</sup>, P van der Tol<sup>1</sup>, W J H Veldkamp<sup>1</sup> and J Geleijns<sup>1</sup>

<sup>1</sup>Department of Radiology, Leiden University Medical Center, Leiden, The Netherlands

<sup>2</sup>Department of Radiology / Nuclear Medicine, Sint Franciscus Gasthuis, Rotterdam, The Netherlands

**Purpose:** Wireless detectors are more frequently used in digital radiography. The advantages of wireless detectors are greater flexibility and better hygiene. The purpose of this study was to compare dose and image quality of wireless detectors for digital chest radiography.

**Materials and methods:** A chest phantom was developed from perspex, aluminium, foam (air) and a contrast-detail phantom (CDRAD). Entrance dose at both the detector (EDD) and phantom (EPD) were measured with a solid-state dosimeter. Dose and image quality (CDRAD) were measured for wireless detectors of 7 different vendors (A-G). Both the actual clinical protocols and a standard reference protocol (120kV, EDD: 4 $\mu$ Gy) were evaluated. For image quality, 6 successive images were acquired for each protocol and analysed with automated software yielding averaged inverse image quality figures (IQFinv). In addition, for each detector and protocol the effective dose was calculated using a Monte Carlo simulation program. As input for the Monte Carlo simulation the measured EDP and the actual radiation quality (tube voltage and total filtration) were used. Geometry (focus-skin distance: 125 cm), beam size (28.3 x 33.3 cm) and patient (adult, length 178.6 cm, weight 73.2 kg) were standardized.

**Results:** All wireless detectors used a CsI scintillator and differed mainly in size [34-43cm] and pixel size [125-200 $\mu$ m]. Main differences in clinical protocols involved tube voltage [90-125kV], tube current [0.5-2.0mAs], the use of a small (C, E and F) or large focus and the use of additional filtration (A, C, F and G). For the clinical protocols, large differences in EDD [A: 1.4; B: 1.8; C: 2.0; D: 4.4; E: 5.6; F: 7.0; G: 11.8  $\mu$ Gy] and EPD [A: 13.9; B: 21.7; C: 17.3; D: 58.3; E: 68.8; F: 54.2; G: 80.2  $\mu$ Gy] were observed. Effective dose varied between 0.005 and 0.036 mSv for the clinical protocol and between 0.011 and 0.014 mSv for the reference protocol.

**Conclusion:** Large differences in acquisition parameters, entrance dose and image quality were observed between the 7 different systems. Although effective dose is low (< 0.04 mSv), further improvement of imaging technology and acquisition protocols is warranted for optimization of wireless digital chest radiography.

## **The process of optimisation of radiological protection – the significance of diagnostic reference levels**

**A Almén<sup>1,2</sup> and M Båth<sup>1,2</sup>**

*<sup>1</sup>Department of Medical Physics and Biomedical engineering, Sahlgrenska University Hospital, Gothenburg, Sweden*

*<sup>2</sup>Department of Radiation Physics, Institute of Clinical Sciences, Sahlgrenska Academy at University of Gothenburg, Gothenburg, Sweden*

The system of diagnostic reference levels in medicine has been presented as a tool to advice on when a local review of the procedures and equipment is warranted in order to determine whether the protection has been adequately optimised. The system is somewhat country specific, presumably due to different national regulations or guidelines, but as a whole relies on the same principles and standards. Diagnostic reference levels are typically set for standardised patients and procedures with minor considerations of the need to manage individual patient characteristics or specific medical tasks in the optimisation process.

Optimisation of radiological protection should involve key aspects influencing the radiation dose to the patients and also include the needs of optimising the protection for each patient individually. The actual given radiation dose to the patient is affected by a number of factors, amongst other things equipment specific features and training of staff performing the examinations. This emphasises the need to take a holistic approach and integrate different clinical processes - e.g. purchasing of equipment or the implementation of new examination protocols in the clinic – in the process of optimisation. Taking this approach gives the opportunity to evaluate the significance of the current system of diagnostic reference levels in the process of optimisation and to identify other reference levels supporting the process of optimisation.

This paper will investigate the optimisation process and identify key instances where reference levels could provide support to the optimisation process. The issue of optimising the individual examination with regard to patient characteristics and medical indication will be specifically addressed.

## Cost-risk-benefit analysis in diagnostic radiology - an economic basis for radiation protection of the patient

B M Moores<sup>1</sup>

<sup>1</sup>*Integrated Radiological Services Ltd, Liverpool, United Kingdom*

In 1973 ICRP Publication 22 recommended that the acceptability of radiation exposure levels for a given activity should be determined by a process of cost-benefit analysis. It was felt that this approach could be used to underpin both the principle of ALARA as well for justification purposes.

The net benefit, B, of an operation involving irradiation was regarded as equal to the difference between its gross benefit, V, and the sum of three components; the basic production cost associated with the operation, P, the cost of achieving the selected level of protection, X, and the cost Y of the detriment involved in the operation:

$$B = V - (P + X + Y)$$

This approach was applied to processes where a practice employing radiation did not involve the direct irradiation of the population, when V and P could be considered to be independent of exposure. However, for medical practices patients are exposed directly to achieve a total benefit so that V and P cannot necessarily be considered to be independent of exposure.

Purely risk based radiation protection strategies have not been robust enough to prevent significant growth in both population and individual patient doses arising from radiological practices and the appropriateness of x-ray examinations is now a major consideration. Consequently, it is worthwhile reconsidering the ICRP cost-benefit analysis concept as a basis for ALARA and justification in medical radiation protection.

This paper presents a theoretical cost-risk-benefit analysis that is applicable to the diagnostic accuracy (level 2), of the hierarchical efficacy model presented by NCRP. This level is concerned with the sensitivity and specificity of an x-ray technique within a defined clinical problem setting. The model proposed assumes two distinct patient populations exist within the referral group. One for whom an examination is deemed to be appropriate (adequately justified) and one for whom an examination could be considered to be inappropriate (unjustified).

The analysis enables the total costs of an examination to be expressed in terms of the sensitivity and specificity arising from any radiological practice expressed as a function of the relative numbers of appropriate/inappropriate examinations. The relevance of economic factors to the fundamental basis for medical radiation protection is discussed for various patient referral and healthcare models.

## **Need for individual cancer risk estimations in x-ray and nuclear medicine imaging?**

**S Mattsson<sup>1</sup>**

<sup>1</sup>*Department of Medical Radiation Physics, Translational Medicine Malmö, Lund University, Malmö, Sweden*

In x-ray and nuclear medicine investigations the primary goal is to produce images of clinically acceptable quality for the individual patient. A second goal is to use the lowest possible radiation dose to get this image quality. To facilitate this real optimization of the investigations, it is necessary that the radiation dose and the potential cancer risk associated with each investigation of each patient can be reported and documented. The current dose-reporting methods are however mostly generic, based on the effective dose (intended for a population of workers, 18-65 years of age). It has the advantage of allowing comparison of radiation dose from different sources using a single quantity. It can also be used to compare the relative dose contributions from different examinations, similar technologies and procedures in different hospitals and countries and the use of different technologies for the same medical examination. Effective dose however ignores body size and hence dose variation from patient to patient is not reflected neither the strong dependence of risk on age and gender.

To estimate the individual cancer risk, there is a need for anatomical description of the patient using individual voxel phantoms (based on CT and/or MR images) or hybrid phantoms as an alternative to stylized mathematically describable phantoms. In nuclear medicine we have gradually to move away from reference biokinetic models and start to describe individual physiologic states and biokinetics. Finally one has to adjust population based cancer risk to the individual depending on age- and gender.

Such efforts are going on for both paediatric and adult CT-investigations, where organ doses have been reconstructed individually and used to evaluate possible risk of leukaemia and solid tumours after CT investigations earlier in life. In mammography even more detailed individual cancer risk estimates are done. The presentation will summarize reasons for individual cancer risk estimates and results of such estimates.



## **A Strategic Research Agenda for Radiation Protection Research Related to Medical Applications of Ionising Radiation – A common proposal of EANM, EFOMP, EFRS, ESR and ESTRO**

**C Hoeschen<sup>1</sup>, S Combs<sup>2</sup>, J Damilakis<sup>3</sup>, W Dörr<sup>4</sup>, G Frija<sup>5</sup>, G Glatting<sup>6</sup>, J McNulty<sup>7</sup>, G Paulo<sup>8</sup>, W Stiller<sup>9</sup>, V Tzapaki<sup>10</sup> and JF Verzijlbergen<sup>11</sup>**

<sup>1</sup>*Institute of Medical Technology, Otto-von-Guericke-University Magdeburg, Germany and Research Unit Medical Radiation Physics and Diagnostics, Helmholtz Zentrum München, Oberschleißheim, Germany*

<sup>2</sup>*Klinik für Radioonkologie und Strahlentherapie, Klinikum rechts der Isar, Technical University Munich, Munich, Germany*

<sup>3</sup>*Department of Medical Physics, Faculty of Medicine, University of Crete, Iraklion, Greece*

<sup>4</sup>*Christian Doppler Laboratory for Medical Radiation Research for Radiation Oncology, Medical University of Vienna, Vienna, Austria*

<sup>5</sup>*Imaging Department, Hôpital Européen Georges Pompidou, Paris, France*

<sup>6</sup>*Department of Medical Radiation Physics/Radiation Protection, Medical Faculty Mannheim of the University Heidelberg, Mannheim, Germany*

<sup>7</sup>*School of Medicine and Medical Science, University College Dublin, Dublin, Ireland*

<sup>8</sup>*Coimbra School of Health Technology, Polytechnic Institute of Coimbra, Coimbra, Portugal*

<sup>9</sup>*Diagnostic Radiology, University Hospital Heidelberg, Heidelberg, Germany*

<sup>10</sup>*Medical Physics Department, Konstantopoulio General Hospital of Athens, Athens, Greece*

<sup>11</sup>*Department of Nuclear Medicine, Erasmus Medical Center, Rotterdam, the Netherlands*

In the past decade the funding scheme of the EC for radiation protection research has been changed. While in the past topics had been identified by the commission and projects had been chosen based on corresponding calls, today, large scale projects are funded which organize the calls for scientific projects themselves. This is based on so called strategic research agendas (SRAs) of corresponding platforms like MELODI, EURADOS, NERIS, ALLIANCE. The European associations dealing with medical applications of ionizing radiation (EANM, EFOMP, EFRS, ESR, ESTRO) do not have a common platform and more important they do not have a common SRA so far. During the large scale EC project the definition of a SRA was initiated together with MELODI and EURADOS. This SRA is currently developed. The main research areas will be ordered in areas like quantification and measurements, optimization and radiation protection, risk and benefit and its communication, radiobiology or similar. This SRA will be presented in a workshop connected to OXMI 2015 and discussed with stakeholders. The result of this discussion will then be presented together with the SRA draft to all interested attendees of the conference and discussed. The results of these discussions within the workshop and the conference will then be reflected by the associations for a first final version of the SRA. This SRA is supposed to be updated regularly and there will be recurrent request for input from the community. It will also be a fundamental step for the building of a common medical platform using ionizing radiation in medical applications.

***Invited speaker*****Eye lens dosimetry for interventional radiologists and cardiologists: Practical approaches to protection and dose monitoring****C J Martin<sup>1</sup>***<sup>1</sup>Department of Clinical Physics, University of Glasgow, Glasgow, United Kingdom*

Interventional radiologists and cardiologists can receive significant radiation doses to their eyes and there is evidence that some have developed lens opacities as a result. The ICRP have proposed a reduction in the occupational annual dose limit for the lens of the eye from 150 mSv to 20 mSv. Doses received by interventional staff depend on the proximity of staff to the X-ray tube and the use made of local shielding. This paper reviews devices that are available for protection of the eye to enable doses to be kept below the new limit. Ceiling suspended shields can reduce doses by factors of 2-7, but positioning is important and interventional clinicians should be trained in their effective use to take full advantage. Disposable radiation absorbing pads (radpads) placed on the lateral aspect of the patient can reduce eye dose by factors of 2-4.5 and should be considered for complex procedures where use of a ceiling suspended shield is problematic. Lead glasses provide an important component of the protection. However, much of the exposure occurs from the side, and this needs to be taken into account. The more common types are wraparound designs with angled lenses or glasses with flat front lenses and protective side shields and most reduce eye doses by factors between 2.5 and 4.5. The proximity to the eyes of tissue on which X-rays are incident is a major factor in determining the dose to the eye lens, so a close fit to the facial contours is important. Effective methods for monitoring eye doses are required to identify potential problems in any facility. Dosimeters worn at the side of the eye adjacent to the X-ray tube or in the middle of the forehead provide the best assessments of eye doses, while an unprotected dosimeter worn at the neck will give an indication of eye dose. If operators wear eye protection, then a protection factor of 0.5 can be applied to take account of the dose reduction. Potential requirements for protective devices and dose monitoring can be determined from risk assessments using generic values for dose linked to examination workload.

## Optimisation of radiological protection in a complex hybrid environment using detailed dose rate information

C Lundh<sup>1,2</sup>, M Båth<sup>1,2</sup> and A Almén<sup>1,2</sup>

<sup>1</sup>*Department of Radiation Physics, Institute of Clinical Sciences, Sahlgrenska Academy at The University of Gothenburg, Gothenburg, Sweden*

<sup>2</sup>*Department of Medical Physics and Biomedical Engineering, Sahlgrenska University Hospital, Gothenburg, Sweden*

**Purpose:** Physicians performing image-guided interventions are exposed to one of the highest radiation risk levels in healthcare. Hybrid environments combine the imaging technology of the image-guided interventions with operation environments, engaging more medical specialties to the use of advanced imaging devices. This complicates the risk management of radiological protection. The aim of this study was to explore the possibilities of using dose rate data for risk assessment in a multi-purpose hybrid room.

**Method:** Dose rate data was collected for three types of image guided interventions in a hybrid room at Sahlgrenska University Hospital. The three procedure types studied were EndoVascular Aortic Repair (EVAR), Transcatheter Aortic Heart Valve (TAVI) and an orthopedic procedure of the back (Ort Back). Dose rate data for scattered radiation was collected using an active dosimeter system, giving dose rate data with a time resolution of 1 second in a fixed unshielded point on the C-arm. Data was analysed and visualized as histograms.

**Results:** The dose rates varied substantially between the three types of procedures studied. The median dose rates were 2.3 mSv/h (EVAR), 1.4 mSv/h (TAVI) and 0.1 mSv/h (Ort back). During EVAR-procedures the absolute majority of the dose rates were between 1 and 10 mSv/h while it during Ort Back-procedures was dominated by dose rates below 0.1 mSv/h.

**Conclusions:** A multi-purpose hybrid room have dose rates that vary substantially between the different areas of use, both regarding dose rate levels and dose rate distribution. The use of dose rate information adds important information that can improve the management of risk in these environments.

## The effect of low kV on staff dose during CT guided interventions

P van der Tol<sup>1</sup>, J E M Mourik<sup>1,2</sup>, K Y E Leung<sup>1,3</sup> and J Geleijns<sup>1</sup>

<sup>1</sup>*Department of Radiology, Leiden University Medical Center, Leiden, The Netherlands*

<sup>2</sup>*Department of Radiology / Nuclear Medicine, Sint Franciscus Gasthuis, Rotterdam, The Netherlands*

<sup>3</sup>*Department of Medical Physics, Albert Schweitzer Hospital, Dordrecht, The Netherlands*

**Purpose:** The radiation exposure to the staff during CT guided interventions is high compared to regular fluoroscopy guided interventions. Lead aprons protect the staff against scattered radiation and the attenuation of the lead apron increases rapidly at lower photon energies. This study evaluates the feasibility of dose reduction for the staff during CT guided interventions by using a low tube voltage at either constant patient dose or constant image quality.

**Method:** All measurements were performed at a Toshiba Aquilion CT system equipped with CT fluoroscopy. A CTDI body phantom ( $\varnothing 32$ cm cylindrical PMMA) was placed in the gantry, and a 600 cc ionization chamber (Keithley) positioned at 1 m from the isocenter of the scanner at chest height, was used to measure the absorbed dose. The absorbed dose was taken as a measure of staff dose after a correction for the attenuation of 0.5 mm Pb at the different tube voltages. First, the CTDI used for the routine CT fluoroscopy protocol at 120 kV was taken as the reference. The tube voltage was lowered to 80 kV and CTDI was kept constant by changing the tube current. Second, image quality expressed as the standard deviation (SD) of Hounsfield units in images acquired at 120 kV was taken as the reference. The noise (SD) at 80 kV was kept equal to the noise at 120 kV by increasing the tube current.

**Results:** By fixing the CTDI while lowering the tube voltage, a dose reduction of 75% was achieved when behind a lead apron of 0.5 mm lead equivalent thickness. Keeping the noise constant while lowering the tube voltage resulted in a dose reduction of 55% when behind 0.5 mm Pb.

**Conclusions:** Lowering the tube voltage during CT fluoroscopy while maintaining the patient dose will result in a lower dose behind the lead apron and decreased image quality. It is also feasible to lower the tube voltage while maintaining image quality. This will result in less reduction of the dose behind the lead apron, higher patient dose and more scattered radiation. In this case care should be taken to avoid high patient skin dose and metal artefacts.

## Accurate KAP meter calibration as a prerequisite for optimization in projection radiography

A Malusek<sup>1</sup>, M Sandborg<sup>1</sup> and G Alm Carlsson<sup>1</sup>

<sup>1</sup>*Medical Radiation Physics, Department of Medical and Health Sciences and Center for Medical Image Science and Visualisation, Linköping University, Linköping, Sweden*

A general consensus in diagnostic radiology is that optimization is worth of consideration if the resulting reduction in patient dose is 10-15% or larger at maintained image quality. In projection radiography the patient dose can be estimated from the kerma area-product,  $P_{KA}$ . Owing to (i) high energy dependence of some KAP meters measuring this quantity and (ii) requirements of IEC that the uncertainty in  $P_{KA}$  measurements should be lower than 25% ( $k=2$ ), some clinical x-ray units report  $P_{KA}$  whose bias is up to the limit of this uncertainty. Clearly, such high bias can adversely affect the optimization procedure as this uncertainty propagates into the uncertainty of the derived patient dose when the tube voltage is used as a parameter of the optimization function. To fix this problem, the current practice of using energy independent calibration coefficients for KAP meters should be abandoned. However before manufacturers implement the energy dependent calibration coefficients, medical physicists may work around the problem by determining corresponding correction factors.

In this work, we describe two approaches based on the tandem calibration method for clinical KAP meters. In the first method, a computational model of the clinical KAP meter is created and used to calculate beam quality correction factors to a calibration coefficient determined at a standards laboratory. In the second method, the first method is used for the calculation of the beam quality correction factor transferring a beam quality at the standards laboratory to a clinical reference beam quality. Beam quality correction factors transferring from the clinical reference beam quality to a user beam quality at the x-ray unit (used in the patient examination) are measured with an energy independent ionization chamber. The methods were used for the Siemens Aristos FX (radiography) and Siemens Artis Zee (fluoroscopy) x-ray units. Biases in reported  $P_{KA}$  were up to 25% and 9%, respectively. These results show that active measures have to be taken to fulfil the recommendations of IAEA and ICRP that measurement uncertainties should be less than 7% ( $k=2$ ) in diagnostic radiology.

## Effect on relative KAP meter energy dependence of heavily filtered beams used in X-ray systems

L Herrnsdorf<sup>1</sup> and H Petersson<sup>1</sup>

<sup>1</sup>*Medical Radiation Physics, Department of Translational Medicine Malmö, Lund University, 205 02 Malmö, Sweden*

Today it is common with more than 1 mm copper filtration in the collimator of X-ray systems. The collimator filter disc may change automatically based on kV selection. Due to the inherent design, KAP meters have a large energy dependence even for lightly filtered beams (RQR IEC beam quality standard 61267). The present standard IEC 60580 states an accuracy of 20% for KAP meters based on RQR. The aim of this work is to investigate the relative energy dependence for heavily filtered beams (RQC) for several types of KAP meters.

A 30 cm<sup>3</sup> ion chamber (NE2530) was calibrated at the primary standard calibration laboratory at PTB for RQR and RQC for 50, 70 and 100 kV. The laboratory for the investigation used an Arco Ceil (Mediel, Mölndal, Sweden) for which the accuracy of the true voltage and total filtration was checked with a Barracuda S/N BC1-02090063.

The relative energy dependence of the internal KAP meter, a Diamentor M4 (PTW, Braunschweig, Germany) KAP meter and a Barracuda R100 dose detector (RTI, Mölndal, Sweden) was determined relative to NE2530 ionisation chamber. The true KAP value was calculated with a Nova X-ray beam analyser (RTI, Mölndal, Sweden) and the R100 placed in the middle of the field.

The Penelope Monte Carlo code and a KAP model were used as an alternative method for determining the relative energy dependence. Simulations were made for photon energies between 10 and 100 keV in step of 0.5 keV and weighed with RQR and RQC spectra generated with SpekCalc software.

Our result shows increased relative energy dependence for KAP meters for the heavy filtered beams used in X-ray system, which make the use of the data more questionable. In fact, the built-in KAP meter that can correct for the effect of the moveable filter in the collimator may be a better solution for this type of beams.

## Benchmarking of CT to patient exposure optimization

D Racine<sup>1</sup>, A H Ba<sup>1</sup>, J G Ott<sup>1</sup>, N Ryckx<sup>1</sup>, F O Bochud<sup>1</sup> and F R Verdun<sup>1</sup>

<sup>1</sup>*Institute of Radiation Physics, CHUV, Lausanne, Switzerland*

Patient dose optimization in Computed Tomography (CT) has to be done using clinically relevant tasks when dealing with image quality assessments. We will report the performances of more than 50 CT units installed in Switzerland, using a model observer (MO) that mimics human detection of low contrast targets.

A dedicated phantom (QRM, Moehrendorf, Germany) containing spheres (5 and 8 mm diameter; 10 and 20 HU at 120kV) was scanned on 53 CT units, at a CTDIvol level of 15 mGy. Images were reconstructed with a nominal thickness of 2.5 mm or 2mm and using only filtered back-projection and assessed using a MO. We used the Channelized Hotelling Observer (CHO) with dense difference of Gaussian channels. The results were computed by performing Receiver Operating Characteristics (ROC) analysis and using the area under the curve (AUC) as a figure of merit (FOM).

Our results showed a small disparity depending on the CT units. For the 8 mm target the average of the AUCs were  $0.998 \pm 0.006$  at 20HU, and  $0.945 \pm 0.027$  at 10HU. For the 5 mm target the averaged AUCs were  $0.967 \pm 0.031$ , and  $0.719 \pm 0.071$  respectively 20 and 10 HU contrast.

Because of the robustness of the CHO, this investigation opens the way for CT benchmarking, when varying the dose settings or reconstruction strategies especially when switching units and/or adapting protocols. In the future, a FOM which represents an expected level of low contrast detectability should be issued to ensure that dose reduction does not impair diagnostic quality.

## Dosimetry on a mobile intraoperative CT system

P van der Tol<sup>1</sup>, J E M Mourik<sup>1,2</sup> and J Geleijns<sup>1</sup>

<sup>1</sup>Department of Radiology, Leiden University Medical Center, Leiden, The Netherlands

<sup>2</sup>Department of Radiology / Nuclear Medicine, Sint Franciscus Gasthuis, Rotterdam, The Netherlands

**Purpose:** A mobile intraoperative CT system (AIRO) coupled with a navigation system (Brainlab) allows surgeons to track surgical instruments real-time in the operating room. For diagnostic CT examinations patient dose is expressed as the computed tomography dose index (CTDI) and the dose length product (DLP). A helical acquisition on the mobile intraoperative CT is achieved by movement of the gantry, instead of translation of the table which is common for diagnostic CT systems. The DLP cannot be calculated for this system according to the current definition of DLP since it combines both axial and helical acquisitions during one CT scan. This study describes how DLP can be measured and calculated for this system.

**Method:** The intraoperative CT starts the acquisition with a partial axial acquisition, followed by translation of the gantry, as a helical acquisition, and is continued again with a partial axial acquisition. The rotations during the helical acquisition provide the coverage of the planned scan, the axial rotations will be referred to as over-rotations and they are required for reconstruction of the study at the borders of the planned scan. Dose measurements free in air ( $CTDI_{free-in-air}$ ) were performed with a 10 cm CT ionisation chamber (Keithley) for different scan lengths with a fixed pitch. From these measurements, the total number of rotations and the number of over-rotations per acquisition could be calculated. The  $CTDI_w$  was measured in the standard CT dose phantom. From these results combined with the nominal beam width, the DLP was calculated and compared to the DLP as displayed on the system console.

**Results:** From the measurements it was found that the intraoperative CT system uses 1.7 over-rotations: at the start and end of each helical acquisition 0.85 additional axial rotations are performed. These rotations are not taken into account in the system DLP, and therefore the system underestimates the DLP. For short scan lengths, the DLP can be up to 80% higher than shown on the system.

**Conclusions:** On a moving gantry system the additional dose from over-rotations should be taken into account for the DLP to prevent underestimation of the radiation exposure of the patient.



## Clinical audit of image quality in radiology using visual grading characteristics analysis

E Tesselaar<sup>1</sup>, N Dahlström<sup>2</sup> and M Sandborg<sup>3</sup>

<sup>1</sup>Medical Radiation Physics, County Council of Östergötland, Linköping University, Linköping Sweden

<sup>2</sup>Radiology, Department of Medical and Health Sciences and Center for Medical Image Science and Visualisation, Linköping University, Linköping Sweden

<sup>3</sup>Medical Radiation Physics, Department of Medical and Health Sciences and Center for Medical Image Science and Visualisation, Linköping University, Linköping Sweden

Clinical audit is a multi-professional activity and required by Swedish national enactment. The aim of this work was to assess whether an audit of clinical image quality could be efficiently implemented by introducing visual grading techniques as a part of the curriculum in a national training course in radiological protection.

Lumbar spine, bedside chest and abdomen CT examinations of adult patients of both gender were selected, each with twenty images or image series. For each examination, the image data was divided into two sets with different image acquisition techniques. In bedside chest, a modern DR system replaced an old CR system. In lumbar spine, the sensitivity class of the DR system's automatic exposure control (AEC) was increased from 400 to 560. In abdomen CT, iterative reconstruction with a 30% reduction in  $CTDI_{vol}$  was compared to filtered back-projection. The images were randomly and blindly assessed with a visual grading technique using 5-6 specific image criteria based on European Guidelines. Between 12 and 33 observers took part in the audit. The results were analysed using visual grading characteristics (VGC) where a VGC-score of 0.5 indicates that the two sets have equal image quality. Inter-rater reliability was assessed using Gwet's coefficient.

The results show that increasing the AEC sensitivity class in lumbar spine AP radiography significantly reduced image quality ( $VGC=0.35\pm 0.04$ ). Using a modern flat-panel DR system in bedside chest AP radiography significantly improved image quality ( $VGC=0.61\pm 0.03$ ). Image quality was maintained ( $VGC=0.51\pm 0.04$ ) in abdominal CT with iterative reconstruction compared to filtered back-projection in spite of reducing the  $CTDI_{vol}$  with the iterative reconstruction by 30%. The inter-rater reliability was moderate to good, with some positive correlation ( $r^2=0.47$ ) between a high inter-rater reliability and better perceived image quality. Median observation time per image or image series was between 0.5 and 1.5 minutes.

We conclude that using image criteria to assess the quality of radiographs can serve as a rapid method for performing audit in a clinical environment, however methods to improve the inter-rater reliability may need to be developed to improve precision in the audit.

## Dutch quality control of Radiology imaging equipment: a unified approach for protocols and software

A A Becht<sup>1</sup>, W K J Renema<sup>2</sup> and J E M Mourik<sup>3</sup>

<sup>1</sup> *Department of Medical Technology, Gelre ziekenhuizen, Apeldoorn, The Netherlands*

<sup>2</sup> *Department of Radiology and Nuclear Medicine, Radboud UMC, Nijmegen, The Netherlands*

<sup>3</sup> *Department of Radiology and Nuclear Medicine, Sint Franciscus Gasthuis, Rotterdam, The Netherlands*

**Purpose:** In literature several protocols are available for acceptance testing and quality control of Radiology imaging equipment. However, it is not always evident which protocol has to be used or where to find it. Furthermore, cut-off values for parameters to fail or pass the test are not always rationalized, as even the rationale of the test itself is not clearly stated. It is clear that a lot of colleagues involved with testing are unnecessarily reinventing the wheel. Therefore, an expert group of Dutch medical physicist experts decided to set up a quality control system, called 'WAD', consisting of both comprehensive and practical tests for all radiology imaging equipment.

**Method:** A group of medical physics experts assessed the literature on quality testing in the domains MRI, CT, US, Fluoroscopy, Conventional X-ray and Display devices. Combined with their own professional experience they deduced protocols for (acceptance) testing. It was ensured that the format of the protocols were uniform. Furthermore, the protocols had to be constructed in such a way that minimally a medical physicist trainee could perform them. As a part of the protocol set, a dedicated vendor independent software platform was developed to process, analyse and store the results of the tests.

**Results:** Protocols for the above mentioned modalities were constructed and can be downloaded from the member site of the Dutch Society for Medical Physics (NVKF). Explicit disclaimers and explanations were provided as well as specific spreadsheets for measurements and calculations. The developed software platform has got a DICOM input and a webbased interface where test results can be retrieved from a database. The modular design enables a continuous expansion and improvement of new processing algorithms.

**Conclusions:** The derived protocols are used in the majority of hospitals in the Netherlands. Every Dutch medical physicist has now access to protocols and spreadsheets for testing of radiology imaging equipment. Feedback forms provide input for continuous improvement. The next version will include, among other things, tests to verify Dutch DRL's.

## Individualized calculation of tissue imparted energy in breast tomosynthesis

N Geeraert<sup>1,3</sup>, R Klausz<sup>2</sup>, S Muller<sup>2</sup>, I. Bloch<sup>3</sup> and H Bosmans<sup>1</sup>

<sup>1</sup>*Department of Radiology, KU Leuven, Leuven, Belgium*

<sup>2</sup>*GE Healthcare, Buc, France*

<sup>3</sup>*Telecom ParisTech, CNRS LTCI, Paris, France*

**Purpose:** In a previous study we demonstrated the limitations of the Average Glandular Dose (AGD) for the quantification of the individual irradiation in mammography, and proposed to use Glandular Imparted Energy (GIE) instead. We describe here a method to estimate the GIE based on quantification and localization of the glandular content in the breast in digital breast tomosynthesis (DBT).

**Method:** A set of ten digital phantoms made of glandular spheres of different diameters and positions in an adipose background and a digital anthropomorphic phantom (Carton, 2014) all with known Volumetric Breast Density (VBD) are defined. They are projected then reconstructed in conditions simulating GE SenoClaire DBT equipment. The histogram of the voxel values of the DBT volume is computed, and the voxels labelled as adipose (below threshold) or glandular tissue (above threshold). The threshold value is set to maintain the fraction of glandular voxels equal to the VBD. Finally, the GIE is calculated by Monte Carlo (MC) computation for both the original phantoms and the labelled, reconstructed volumes.

**Major Findings:** For nine out of the ten phantoms with spheres the computed glandular masses differ by 8 to 13% from the real value. For half of these phantoms the GIE obtained from DBT is within 20% of the value computed on the original phantom. The largest relative deviations were observed for phantom thicknesses small or large compared to the spheres diameters, or when the VBD or GIE value was low. For the anthropomorphic phantom the computed glandular mass was overestimated by 23% and the GIE underestimated by 25%. The accuracy of the results is mainly limited by the z-resolution of DBT.

**Conclusions:** The proposed method allows the estimation of the individual GIE from a single DBT acquisition. It should now be better characterized on a variety of anthropomorphic phantoms

## Thoracic spine imaging: A comparison between radiography and tomosynthesis using visual grading characteristics

E Ceder<sup>1</sup>, B Danielson<sup>1</sup>, P Kováč<sup>1</sup>, H Fogel<sup>1</sup> and M Båth<sup>2,3</sup>

<sup>1</sup>*Department of Radiology, Sahlgrenska University Hospital, Gothenburg, Sweden*

<sup>2</sup>*Department of Medical Physics and Biomedical Engineering, Sahlgrenska University Hospital, Gothenburg, Sweden*

<sup>3</sup>*Department of Radiation Physics, Institute of Clinical Sciences, Sahlgrenska Academy at the University of Gothenburg, Gothenburg, Sweden*

**Background:** Conventional radiography (CR) is the most-often used modality in imaging of the thoracic spine, as primary examination as well as follow-up of known pathology. However, the ability of radiography to clearly depict thoracic vertebrae is limited, mostly due to overlying structures. Digital tomosynthesis (DTS) has in other parts of the body – most notably in chest imaging – been shown to increase conspicuity of relevant pathology where overlying structures is an issue. DTS has not yet been evaluated as an imaging modality of the thoracic spine.

**Purpose:** To compare the ability of CR and DTS to depict relevant structures of the thoracic vertebrae.

**Materials and Methods:** In this prospective visual grading study, 23 patients referred in 2014 for elective radiographic examination of the thoracic spine were examined using CR and DTS in the sagittal plane. The lateral projections of the CR and DTS images were read in random order by four radiologists evaluating the ability of the modalities to present a clear reproduction of nine specific relevant structures of vertebrae T3, T6 and T9. The data were analyzed using Visual Grading Characteristics (VGC) analysis.

**Results:** In terms of clear reproduction, VGC analysis revealed that there was a statistically significant difference ( $p < 0.05$ ) between CR and DTS in favor of the latter, for all evaluated structures apart from the anterior vertebral edges and lower end plates of T6 and T9. The differences were most striking in T3. No structures were evaluated as being more clearly reproduced by CR.

**Conclusion:** The study indicates that most vertebral structures of the thoracic spine are perceived as more clearly reproduced by DTS than by CR, suggesting that detection of pathology would be improved by the use of DTS.

## Visibility of structures of relevance for patients with cystic fibrosis in chest tomosynthesis – influence of anatomical location and observer experience

C Meltzer<sup>1,2</sup>, M Båth<sup>3,4</sup>, S Kheddache<sup>1,2</sup>, H Ásgeirsdóttir<sup>5,6</sup>, M Gilljam<sup>5,6</sup> and Å A Johnsson<sup>1,2</sup>

<sup>1</sup>Department of Radiology, Institute of Clinical Sciences, The Sahlgrenska Academy at University of Gothenburg, Gothenburg, Sweden

<sup>2</sup>Department of Radiology, Sahlgrenska University Hospital, Gothenburg, Sweden

<sup>3</sup>Department of Radiation Physics, Institute of Clinical Sciences, The Sahlgrenska Academy at University of Gothenburg, Gothenburg, Sweden

<sup>4</sup>Department of Medical Physics and Biomedical Engineering, Sahlgrenska University Hospital, Gothenburg, Sweden

<sup>5</sup>Gothenburg CF-center, Sahlgrenska University Hospital, Gothenburg, Sweden

<sup>6</sup>Department of Respiratory Medicine, Institute of Medicine, The Sahlgrenska Academy at University of Gothenburg, Gothenburg, Sweden.

**Purpose:** To assess visibility of pulmonary structures of relevance for patients with cystic fibrosis on digital tomosynthesis (DTS) images in comparison to computed tomography (CT) images and to investigate if visibility is affected by anatomical location and observer experience.

**Methods:** Twenty-one patients with cystic fibrosis were examined by DTS and helical CT within 90 minutes. Tube voltage of both modalities was 120kV. Nominal slice thickness of the coronal section images of DTS was 5 mm and slice thickness of the transverse CT images was 1-1.25 mm. In each patient 30 pulmonary structures, primarily bronchiectasis, mucus plugging and vessels, were identified in predefined regions at four different anatomical levels of the CT examination, resulting in a total of 630 structures for head to head comparison between the modalities.

Three observers, with varying experience both regarding DTS and patients with cystic fibrosis, independently evaluated visibility of the structures in DTS on a scale from 0 to 5 using the transverse CT images as reference and coronal CT images (thickness 4mm / increment 3mm) for anatomical guidance. The observers' responses were analyzed using visual grading characteristics (VGC) analysis.

**Results:** Visibility in DTS in comparison to CT was reported as equal in 34%, inferior in 52% and superior in 14 % of the structures. The visibility of structures in the central and peripheral lateral regions of the lungs received higher scores compared to the peripheral regions anteriorly, posteriorly and around the diaphragm ( $p \leq 0.001$ ). There were no significant differences between the central regions of the different anatomical levels. The most experienced observer reported higher visibility scores than the two less experienced observers ( $p \leq 0.01$ ).

**Conclusion:** The results indicate that the perceived visibility of specific anatomical structures in DTS is generally inferior to CT and dependent on both anatomical location and observer experience.

## Effect of radiation dose on pulmonary nodule size measurements in chest tomosynthesis

C Söderman<sup>1</sup>, Å A Johnsson<sup>2,3</sup>, J Vikgren<sup>2,3</sup>, R Rossi Norrlund<sup>2,3</sup>, D Molnar<sup>2,3</sup>, A Svallkvist<sup>1,4</sup>, L G Månsson<sup>1,4</sup> and M Båth<sup>1,4</sup>

<sup>1</sup>Department of Radiation Physics, Institute of Clinical Sciences, Sahlgrenska Academy, University of Gothenburg, Gothenburg, Sweden

<sup>2</sup>Department of Radiology, Institute of Clinical Sciences, Sahlgrenska Academy, University of Gothenburg, Gothenburg, Sweden

<sup>3</sup>Department of Radiology, Sahlgrenska University Hospital, Gothenburg, Sweden

<sup>4</sup>Department of Medical Physics and Biomedical Engineering, Sahlgrenska University Hospital, Gothenburg, Sweden

**Objective:** For chest tomosynthesis, a general reduction of the standard radiation dose may be considered for implementation in clinical praxis due to that previous studies have shown remained levels of detection of pulmonary nodules at lower radiation doses. If, at the same time, chest tomosynthesis is to be considered for use in pulmonary nodule follow up, it is important to investigate the effect of a reduced radiation dose on nodule size assessment. The aim of the present study was to investigate the dependency of the accuracy and precision of nodule diameter measurements on the radiation dose level in chest tomosynthesis.

**Methods:** Artificial ellipsoid shaped nodules with known dimensions were created and inserted in clinical chest tomosynthesis. The volume of the nodules corresponded to that of a sphere with a diameter of 4, 8 or 12 mm. Each size group included 27 nodules. Noise was added to the images in order to simulate different examination doses using a previously described method. Four thoracic radiologists were given the task of measuring the longest diameter of the nodules. The study was restricted to nodules located in areas of the tomosynthesis images not noticeably affected by high density structures such as the heart or diaphragm since measurements on nodules in these areas have been shown to suffer from low accuracy.

**Results:** The measurement accuracy, in terms of mean measurement error, as well as the intraobserver variability, showed little or no dependency on radiation dose level. There was as a tendency of increasing interobserver variability with decreasing radiation dose level for the smallest nodules. Of the smallest nodules, the observers found 6 – 11 of the nodules non measurable due to poor visibility at the standard dose level. This number increased slightly with decreasing radiation dose level.

**Conclusion:** A dose reduction in chest tomosynthesis may be possible without significantly affecting the accuracy and precision of nodule diameter measurements. The increasing number of nonmeasurable nodules with decreasing radiation dose for small nodules may raise some concerns regarding an applied general dose reduction in the clinical praxis for chest tomosynthesis examinations, although small nodules are of less clinical importance.

## Finding role for Digital Tomosynthesis (DTS) in chest imaging

Á Horváth<sup>1</sup>, G Horváth<sup>2</sup> and K Szondy<sup>3</sup>

<sup>1</sup>*Innomed Medical Inc, Budapest, Hungary*

<sup>2</sup>*Budapest University of Technology and Economics, Budapest, Hungary*

<sup>3</sup>*Semmelweis University Department of Pulmonology, Budapest, Hungary*

**Background:** Innomed deals with x-ray imaging system development since the early 2000 but it has 25 years experiences in manufacturing medical devices. In the last ten years we developed our own PACS system and Chest X-Ray CAD system. But we saw the limitations of our digital X-Ray imaging techniques.

Lung cancer has the highest mortality rate among all cancer types regardless of sex and it has especially high occurrence in Hungary. We know that there is evidence since 2012 that lung cancer mortality can be decreased by 20% with LDCT screening.

In 2012 we started to develop our own DTS system with which we might achieve the same rate. We decided to create also CAD system for DTS images.

**Methods:** Our DTS device is in fact a full featured tilting table. Its main attributes are 100-180cm SID, using movable dynamic detector from THALES with JPI grid. This device is suitable for DTS imaging but also for fluoroscopy and spot imaging. DTS examination takes 10 seconds and makes 60 images from +/- 20 degrees and results 140 slices in 1.5kx1.5k resolution. We focus on chest imaging in our project to make as good slices as possible for the radiologist/pulmonologist just as for our developing CAD solution.

**Results:** For the image reconstruction we have developed special MITS like algorithm in cooperation with the Budapest University of Technology and Economics (BUTE). With the first two DTS prototypes we have two ongoing studies at the two largest Pulmonology in Hungary for different purposes: lung cancer screening, lung cancer follow up and large airways stenosis detection. The result images are convincing based on feedback from different specialist, like pulmonologists, radiologist, oncologists, surgeon, etc.

**Conclusion:** Based on physicians feedback it looks like DTS can substitute CT for follow-ups in many cases and might be a good alternative for LDCT in screening. It has a promising use in detecting large airways stenosis as well. As physicians start to use DTS, every month a new area of usage is found. Using DTS images we will finish our lung CAD system development at the end of Q2 2015.

## Clinical use of chest tomosynthesis - after five years with the new modality

C Petersson<sup>1</sup>, M Båth<sup>2,3</sup>, J. Vikgren<sup>1,4</sup> and Å A Johnsson<sup>1,4</sup>

<sup>1</sup>*Department of Radiology, Sahlgrenska University Hospital, Gothenburg, Sweden*

<sup>2</sup>*Department of Radiation Physics, Institute of Clinical Sciences, The Sahlgrenska Academy at University of Gothenburg, Gothenburg, Sweden*

<sup>3</sup>*Department of Medical Physics and Biomedical Engineering, Sahlgrenska University Hospital, Gothenburg, Sweden*

<sup>4</sup>*Department of Radiology, Institute of Clinical Sciences, The Sahlgrenska Academy at University of Gothenburg, Gothenburg, Sweden*

**Purpose:** To investigate the use of chest tomosynthesis (CTS) five years after its introduction in clinical praxis at a tertiary center and to explore to which extent CTS could replace computed tomography (CT) and should substitute chest radiography (CR).

**Methods:** A study of examinations performed 24 to 28 months prior to the survey was performed using the radiology information system and picture archiving and communication system. Every posteroanterior CR, CT and CTS examination completed during office hours (07-17) the third week of each month from August to December 2012 was included in the study. By means of predefined criteria it was decided if a CTS would have been appropriate instead of the performed CR and if CTS could have replaced the implemented CT. Regarding the CTS it was judged if CT would have been performed had CTS not been available and whether the use of CTS had resulted in an adverse event (i.e. missed pathology).

**Results:** A total of 2172 examinations had been completed; 1433 CR (714 women, 12-96 years), 523 CT (288 women, 16-95 years) and 216 CTS (125 women, 18 -92 years). It was judged that CT would have been performed in 63% of the CTS cases if CTS had not been available. Regarding the CT examinations, CTS could have served as an alternative in 8% of the cases and concerning the CXR examinations, CTS had been appropriate in at least 14 % of the cases. One adverse event was noted. It was a case where CT examinations prior to and after the intervening follow-up with CTS showed the same ground glass opacities that could not be identified by the CTS examination.

**Conclusions:** The results of the present study indicate that the use of CTS 5 years after its introduction in clinical praxis has not reached its full potential in optimizing the use of CT resources and increasing diagnostic accuracy in chest radiography. CTS may be a viable alternative to CT in approximately 25% of clinical cases and should substitute CR more frequently than today.



## Iterative reconstruction: different solutions- different effects

M A Staniszevska<sup>1</sup> and D Chruściak<sup>2</sup>

<sup>1</sup>*Department of Medical Imaging Techniques, Medical University of Lodz, Poland*

<sup>2</sup>*Holy-cross Oncology Centre, Kielce, Poland.*

CT scan procedures are constantly perceived as providing high doses of radiation to patients. Solutions that enable reduction of the dose while maintaining good diagnostic value of images are being intensively investigated. An “iterative reconstruction” (IR) algorithm has been the leading alternative for last five years. Different solutions for the IR algorithm were elaborated by the main vendors and they compete with each other at the level of possible dose reduction (more than 50% has been declared). The aim of the study was to compare the benefits from IR algorithms offered by the main four vendors, while applying the same exposure parameters. Investigations were performed for modern multislice CT scanners (64 rows and more). The measurements consists of:

- image quality indicators (using Catphan phantom) and
- dosimetric indicators of exposure (DLP and CTDI<sub>vol</sub>).

DLP was measured using traditional 5-hole PMMA phantom and dosimeter Barracuda (RTI, Sweden). CT scanner results for the particular level of IR algorithm and the Filtered Back Projection (FBP) algorithm were compared. (Both algorithms were installed independently in CT computer and could be chosen according to user preferences.)

The results of the Catphan images obtained for the IR (and FBP) algorithms implemented in CT scanners of main four vendors were analyzed. As a result of the same exposure parameters the values of CTDI<sub>vol</sub> were nearly the same for all the scanners. Despite of that were some differences to the visualization of the low-contrast Catphan objects and signal-to-noise ratios.

The main conclusion from image analysis is as follows: at higher levels of the IR algorithm (i.e. more repetitions of iterative loop) a higher signal-to-noise ratio should be observed together with a better visualization of low-contrast objects, but the end result is not always consisted. This means that patient dose may be lower but the image quality may be insufficient for diagnosis. A realistic approach to dose reduction should be tested by phantom measurements for the CT scanner.

## Assessment of clinical image quality in paediatric abdominal CT examinations – dependency on level of Adaptive Statistical iterative Reconstruction (ASiR) and type of convolution kernel

J Larsson<sup>1,2</sup>, M Båth<sup>1,3</sup>, K Ledenius<sup>4</sup>, H Caisander<sup>5</sup> and A Thilander-Klang<sup>1,3</sup>

<sup>1</sup>*Department of Radiation Physics, Institute of Clinical Sciences, Sahlgrenska Academy, University of Gothenburg, Gothenburg, Sweden*

<sup>2</sup>*Section of Diagnostic Imaging and Functional Medicine, NU-Hospital Group, Trollhättan, Sweden*

<sup>3</sup>*Department of Medical Physics and Biomedical Engineering, Sahlgrenska University Hospital, Gothenburg, Sweden*

<sup>4</sup>*Department Radiology, Skaraborg Hospital, Skövde, Sweden*

<sup>5</sup>*Department of Paediatric Radiology and Physiology, The Queen Silvia Children's Hospital, Gothenburg, Sweden*

**Purpose:** The purpose of this study was to investigate the effect of combinations of convolution kernel and level of Adaptive Statistical iterative Reconstruction (ASiR) on diagnostic quality and visualisation of anatomical structures for paediatric abdominal CT examinations.

**Materials and Methods:** Thirty five patients (mean age 10 years-old, range; 2 to 15 years-old) undergoing routine abdominal CT on a 64 slice MDCT scanner (Discovery CT750 HD, GE Healthcare) were included in the study. Raw data was retrospectively reconstructed into 5 mm thick and interval 2.5 mm transaxial image stacks at levels of 30%, 50%, 70%, 90% and 100% ASiR, all in combination with three kernels; Soft, Standard and Detail. In a blinded randomized visual grading study, four paediatric radiologists with different experience rated a question of diagnostic quality and 6 questions related to anatomical structures, using a four point rating scale. Data were analysed in comparison with 30% ASiR with kernel Soft (the settings used clinically prior to the study) using a method for paired ordinal data that identifies and measures systematic shift in rating distributions. The shift is expressed as the Relative Position (RP).

**Results:** A clear dependency on type of convolution kernel was seen for the relationship between ASiR level and image quality. For the Soft and Standard kernels, the optimal diagnostic quality was obtained at 70% ASiR. For the Detail kernel, the diagnostic quality increased with ASiR level, but at no ASiR level for this kernel a better diagnostic quality than at 30% ASiR with kernel Soft was obtained. The visibility of the extra hepatic part of the portal vein was best delineated at 70% ASiR with kernel Soft (RP -0.12; 95% CI -0.20 to -0.04).

**Conclusions:** This study shows that for paediatric abdomen CT examinations the clinical image quality at a given ASiR level is dependent on the convolution kernel and that a more edge enhancing kernel can benefit from a higher ASiR level. For the acquisition settings used in the present work, the optimal combinations of ASiR level and convolution kernel was 70% ASiR with kernel Soft or Standard.

## **Overview, practical tips and potential pitfalls using automatic exposure control in CT – Siemens CARE Dose 4D**

**M Söderberg<sup>1</sup>**

*<sup>1</sup>Medical Radiation Physics Malmö, Department of Translational Medicine, Lund University, Skåne University Hospital, Malmö, Sweden*

Automatic exposure control (AEC) in computed tomography (CT) systems, operating with tube current modulation, is routinely used today. However, for optimal use there are several aspects of an AEC system that needs to be considered. The purpose of this study was to give an overview of Siemens AEC system CARE Dose 4D and discuss and exemplify practical tips and potential pitfalls.

Three anthropomorphic phantoms (adult torso phantom, adult chest phantom and paediatric whole body phantom) have been examined using two different Siemens CT systems, Definition Flash and Sensation 16. Examination parameters were chosen according to recommendations from the manufacturer or as routinely used in the clinic. To illustrate the importance of the localizer to the tube current modulation process, some key aspects have been investigated; patient centring, projection angle and scanning outside the localizer. In addition, the influence of scanning direction, scan protocol (organ characteristic), adaptation strengths, metal implants and use of protective devices have been evaluated.

The localizer is fundamental for the AEC system to obtain information of the patient's attenuation. Inappropriate centring can increase both image noise and radiation dose. For an adult CT scan of the thorax, 5 cm off-centring may result in approximately 15% dose increase. Beyond the localizer no tube current modulation will occur and CARE Dose 4D will adapt the tube current based on the latest available localizer information. The tube projection angle of the localizer has a major impact of the radiation dose. When scanning the thorax, changing from the default setting anterior-posterior (AP) to posterior-anterior increased the radiation dose 13%, and performing both AP and lateral decreased the radiation dose 20%. To achieve optimal tube current modulation the scan protocol that fits to the region to be scanned should always be selected. User-specific modifications of image quality or radiation dose to the patient cohort can be obtained by selecting appropriate adaptation strengths. The dynamics of the tube current modulation will also depend on the scanning direction since the online angular tube current modulation is based on 180 degrees pre-projection data.

When attempting strategies to optimise CT radiation dose and image quality there are several aspects of the AEC system that requires special attention to obtain optimal outcome.

## Methods for determination of CTDI

E Bąbel<sup>1</sup> and M A Staniszewska<sup>1</sup>

<sup>1</sup>*Department of Medical Imaging Technique Medical University of Lodz, Lodz, Poland*

**Purpose:** The volume computed tomography dose index (CTDI<sub>vol</sub>) is usually determined based on dose derived from measurements made on cylindrical phantoms PMMA. This method is no perfect solution because human body is different from the circle-shaped phantom. For this reason, introducing the elliptical phantoms to measurements of CTDI<sub>vol</sub> was proposed. The elliptical phantom is designed to better imitate the human body shape. Thanks to this, determination of CTDI<sub>vol</sub> should be more accurate. The aim of the study was to assess impact of the phantom shape on the result of determination of CTDI<sub>vol</sub>.

**Method:** PMMA phantom with a diameter of 16 centimeters and two elliptical CIRS phantoms were used to measurements of DLP. Elliptical phantoms with dimensions 11.5/14 centimeters and 14/18 centimeters were made of tissue equivalent material. Studies were carried out on the GE CT scanner. Phantom studies consistent in measuring the dose depending on the shape of the phantom. Each phantom was scanned using the same exposure parameters for the two CT protocols designed to the study of the head and abdomen. On the basis of measurements were determined CTDI<sub>vol</sub> for each of phantoms, for both protocols of examination.

**Major findings and conclusions:** Comparing the values CTDI<sub>vol</sub> which was determined for PMMA phantom and greater elliptical phantom, (the size of this phantom is similar to PMMA phantom) CTDI<sub>vol</sub> value in both protocols was lower for the elliptical phantom. In the case of the smaller elliptical phantom determined CTDI<sub>vol</sub> value was comparable with value determined for PMMA phantom for both protocols. It should be emphasized that this phantom is much smaller than the PMMA phantom. The obtained results allow to conclude that the shape of the phantom affect on the final outcome of the determination of CTDI<sub>vol</sub> and it is worth do the further studies of this issue.

## Implications of patient centering on organ dose in Computed Tomography examinations - A comparison between TLD measurements and CT Expo simulation

**B Kataria**<sup>1,2,4</sup>, **M Sandborg**<sup>2,3</sup> and **J Nilsson-Althén**<sup>2,3</sup>

<sup>1</sup>Radiology Department/University Hospital Linköping, Linköping, Sweden

<sup>2</sup>Department of Medical & Health Sciences/Linköping University, Linköping, Sweden

<sup>3</sup>Radiation Physics, Region Östergötland, Linköping University, Linköping, Sweden

<sup>4</sup>Center for Medical Image Science & Visualization, CMIV/ Linköping, Sweden

Modern Computed Tomography (CT) scanners provide several features that facilitate optimization of radiation dose such as Automatic exposure control (AEC) systems. The use of AEC demands appropriate patient centering in the gantry as off-centering affects both image quality and radiation dose.

The aim of this experimental study was to measure variation in organ and abdominal surface dose during CT examinations of the head, neck/ thorax and abdomen at isocenter and two off-center positions in the vertical plane and to compare the results of physical thermo luminescence dosimeter (TLD) measurements at isocenter to CT Expo simulation calculations to ascertain the degree of agreement between measured and simulated absorbed organ doses. CT dose Profiler was used to measure dose variation due to x-ray tube start position. Atom anthropomorphic male phantom was used and TLD's were loaded into five radiation sensitive organs to measure organ dose and 7 dosimeters were taped to the phantom to measure surface dose. The phantom was then scanned using clinical head, neck/thorax and abdomen protocols on a 128 slice Siemens Definition AS scanner at isocenter and two off-center positions.

The ventrally placed organs and ventral surface received less dose compared to values at isocenter when off-centered 3cm above isocenter. Similarly dorsal placed organs and dorsal surface dose values were lower compared to reference levels at 5 cm off-centering below isocenter. The breasts received a higher dose compared to isocenter when the phantom was off-center below the isocenter. The results in ventral surface dose variation due to vertical centering were confirmed by CT Dose Profiler measurements which also showed variation in dose due to start position of the tube. The CT-Expo dose calculations were somewhat lower but still in agreement with dose levels at isocenter.

Patient off centering in the vertical plane affects organ doses in CT examination of the head, neck/thorax and abdomen. Correct patient positioning in the gantry isocenter is critical especially in the vertical position to maintain optimal patient dose.

## **Dosimetric measurements using the TG 200 phantom – a comparison of dosimetric techniques with application in CT and CBCT**

**M Gunnarsson<sup>1</sup>, L Herrnsdorf<sup>1</sup>, P Törnqvist<sup>2</sup> and M Söderberg<sup>1</sup>**

<sup>1</sup>*Medical Radiation Physics, Department of Translational Medicine, Lund University, Malmö, Sweden*

<sup>2</sup>*Department of Hematology and Vascular Diseases, Vascular Center, Malmö, Sweden*

A well-known problem with the currently used dose metrics in CT (CTDI, DLP) is that many of today's modern scanners use nominal beam widths that are wider than the extent of the 100 mm pencil ionization chamber and the 150 mm long CTDI phantom used to measure the CTDI. This results in an underestimation of the measured dose due to the fact that the scattered "dose-tails" from the phantom are not included/covered in the measurement. Efforts by AAPM Task Group (TG) 111 has led to the development of new methodologies for dose measurements and a phantom (AAPM TG 200) that will more accurately reflect scanner output. In addition, the International Electrotechnical Commission (IEC) has proposed adjustments to the CTDI methodology for wider beam widths (IEC 60601-2-44).

The purpose of this study was to use the suggested AAPM dose descriptors and measurement methods in comparison with the currently used dose metrics (CTDI, DLP and DAP). This was achieved by using the AAPM TG 200 phantom and performing measurements on CT and CBCT in different clinical situations.

In this study, a point dose detector, CT dose profiler (RTI, Mölndal, Sweden) was used to measure the equilibrium dose ( $D_{eq}$ ) and dose profiles. The detector was pulled through the AAPM TG 200 phantom by a mover (RTI, Mölndal, Sweden) and the dose signal was sampled and analysed by using Cobia and Ocean (RTI, Mölndal, Sweden). The obtained dose profiles and  $D_{eq}$  from the measurements showed as expected that the dose contribution from a significant part of the scattered dose-tails were not included in the traditional CTDI measurements.

In conclusion, this study shows the importance of introducing the suggested new method to obtain better dose estimation for modern CT and CBCT with wide beams.

## Comparison of effective dose estimates of paediatric conventional X-ray and computed tomography examinations of the cervical spine

M Hultenmo<sup>1</sup> and A Thilander-Klang<sup>1,2</sup>

<sup>1</sup>Department of Medical Physics and Biomedical Engineering, Sahlgrenska University Hospital, Gothenburg, Sweden

<sup>2</sup>Department of Radiation Physics, Institute of Clinical Sciences, Sahlgrenska Academy, University of Gothenburg, Gothenburg, Sweden

**Purpose:** The aim of the study was to compare effective dose estimates of paediatric cervical spine examinations performed with either conventional X-ray or computed tomography (CT) technique.

**Materials and Methods:** Data from 13 paediatric conventional X-ray examinations and 19 paediatric CT examinations of the cervical spine were analysed. The conventional examinations were performed on an Arcoma Arco unit (Mediel, Sweden) and the CT examinations were performed on a 64-slice Discovery CT750 HD scanner (GE Healthcare), both located at the Queen Silvia Children's Hospital, Gothenburg, Sweden. Age dependent protocols were used for both modalities. Effective doses from the conventional X-ray examinations with five standard projections - frontal, lateral, frontal open mouth, and oblique lateral dx and sin, respectively - were estimated by using the Monte Carlo based software PCXMC 2.0 (STUK – Radiation and Nuclear Safety Authority, Finland). In the PCXMC program each patient and projection was simulated individually with regard to phantom size, radiation field size, exposure parameters and the registered KAP (air kerma-area-product) value. Effective doses from the CT examinations were estimated by using the software CT-Expo V2.3 (G. Stamm and H. D. Nagel, Germany). Only four phantom sizes were available (baby, child, Eve and Adam) and the phantom that best matched the body weight of each patient was used. Individual scan parameters from the CT examinations were used in the program, but the tube current was adjusted so that the  $CTDI_{VOL}$  (CT dose index by volume) and DLP (dose-length-product) calculated by the program matched the ones given in the dose report of the examination.

**Results:** Effective doses of the CT cervical spine examinations varied between 0.2 and 0.7 mSv, generally increasing with body weight. Corresponding values for conventional X-ray examinations varied between 0.1 and 0.2 mSv, and decreased with body weight. The effective dose values for smaller patients (10-25 kg) were approximately 1 to 4 times higher for CT examinations than for the conventional examinations. For larger patients (50-70 kg) the differences in effective dose depending on modality increased and CT resulted in 2 to 8 times higher effective dose values.

**Conclusions:** It is important to justify the need of improved diagnostic information when choosing CT instead of conventional X-ray technique for paediatric cervical spine examinations, since the former can result in up to 8 times higher effective dose estimates.

## Computed tomography dose index and dose length product for 4-slice scanner at a densely populated city of northern Nigeria

I Garba<sup>1</sup>, M Yahuza<sup>2</sup>, M Barde<sup>1</sup> and M Abba<sup>1</sup>

<sup>1</sup>Department of Medical Radiography Bayero University Kano, Kano State, Nigeria

<sup>2</sup>Department of Radiology Bayero University Kano, Kano State, Nigeria

**Aim:** The study aimed to investigate the radiation dose values patients' received while undergoing head CT with a view of proposing DRLs.

**Background:** Modern CT scanners now offer a lot of clinical opportunity. However, these clinical capabilities have not been without a price, namely a major source of medical diagnostic radiation exposure. Therefore, to allow CT investigation to continue without unnecessarily exposing patients to ionizing radiation, dose optimization strategies have been developed. One of such strategies is the use of Diagnostic Reference Levels (DRLs) for different CT examinations, which serves as a platform upon which radiation workers operate and manage radiation dose to the patient.

**Methods:** This was a prospective study conducted in a densely populated centre located in Northern Nigeria. Data was collected from all consented patients that presented for a routine head CT. All the scans were done on a 4-slice GE Brightspeed scanner. The scanner is equipped with dose description parameters namely the CTDI and DLP. Also, the scanner is calibrated by a medical physicist, and has duly signed acceptance certificates. The collected data was classified based on patient's age. The measured radiation doses in the present study were compared with reported data from the international communities where there are established DRLs. The data was analysed using SPSS version (16) statistical software to determine the mean and third quartile values at the 95% confidence interval.

**Results:** The 3<sup>rd</sup> quartile values of CTDI and DLP for head CT obtained were: <1 year (27 mGy and 345 mGy\*cm), 1-5yrs (48 mGy and 699 mGy\*cm), 6-10 yrs (61 mGy and 1011 mGy\*cm), 11-15 yrs (65 mGy and 1085 mGy\*cm) and >16 yrs (51 mGy and 805 mGy\*cm). The values compared well with data reported in the literature from UK, Germany, & Belgium.

**Conclusion:** The study has established radiation dose values for head CT that compared well with reported data in the literature. Therefore, could be used to propose DRLs for Nigerian population.



## A first step to defining DRLs for CT-examinations in Russia

L. Chipiga<sup>1, 2</sup>

<sup>1</sup>*Research Institute of Radiation Hygiene, St. Petersburg, Russia*

<sup>2</sup>*Federal North-West Medical Research Centre, St. Petersburg, Russia*

Computed Tomography (CT) is one of the most efficient but also a high-dose diagnostic tool available. There is a growing need of optimization in this field due to the rapid increase in number of CT units and availability of CT-examinations in Russia. The Belgorod Region of Russia was chosen as a representative region to develop proper optimization procedures. The work consisted of several steps: to survey of protocol parameters, collection of patient information and dosimetric parameters; to identify dosimetric parameters distribution and to define the most suitable value for the DRL. In 2014, dose audits of CT-examinations were performed at each CT unit across the Belgorod Region. This was done for CT-examinations with intravenous contrast and CT-examinations without contrast, using data collection and analysis methods. The results show that the highest doses were observed for chest, abdomen and pelvic examinations using intravenous contrast agents. The effective dose reached 120 mSv (DLP = 6130 mGy\*cm) per CT-examination. Abnormally high patient doses may be explained by that each CT-examination with contrast consists of several phases (several scans). The dose distributions were approximately log-normal and the median identified in the Belgorod Region were higher than same value in St. Petersburg. The most suitable value for defining the DRL is the DLP. It is important to specify in detail both the clinical task associated with the procedure and the body organs scanned, as differences between similar procedures may affect patient dose and hence DRL values.

## Exposure of the Swiss population by X-ray diagnostic imaging: Results of the 2013 intermediate survey

R LeCoultre<sup>1</sup>, J Bize<sup>2</sup>, M Champendal<sup>1</sup>, D Wittwer<sup>3</sup>, N Ryckx<sup>2</sup> and F R Verdun<sup>2</sup>

<sup>1</sup>University of Health Sciences HESAV, HES-SO, Lausanne, Switzerland

<sup>2</sup>Institute of Radiation Physics, CHUV, Lausanne, Switzerland

<sup>3</sup>Swiss Federal Office of Public Health, Bern, Switzerland

**Introduction:** According to EURATOM 97/43, and more recently EURATOM 2013/59, nationwide surveys on radiation dose to the population from medical radiology are recommended in order to follow the trends in population exposure. An extensive national survey was conducted in Switzerland in 1998 and the annual dose was estimated to be 1.0 mSv per inhabitant. An update of this survey was performed in 2008 and showed a 20% increase. The goal of the 2013's survey was to investigate the present exposure of the population in a context where the radiological practice is rapidly evolving.

**Materials and methods:** The invoice coding information were collected in the five University Hospitals for the whole year allowing to get a very high level of detail concerning the radiological procedures performed together with the population age and gender information. For all other practices (general practitioners, dentists, private radiological practices) a website was used to collect the data ([www.RADDOSE.ch](http://www.RADDOSE.ch)) and a 30% answer rate of the chosen sample was obtained.

**Results:** The projection of the results at the national level gave the following results: on average we estimate 1.3 radiological examinations per year and per inhabitant (including dental radiographs). Among this, CT examinations represent 8.5%, general radiographs 38% and dental radiographs 50%. The average annual dose was, in 2013, 1.4 mSv per inhabitant; CT representing 72% of that dose. Thus, from 2008 to 2013 the average dose has increased from 1.2 to 1.4 mSv with an increase of 15% in the number of CT examinations.

**Conclusion:** This study will be completed by studying the effect of iterative reconstruction in CT using dose data collected by software such as DoseWatch or Radimetrics available in several University hospitals. The use of such software will allow a major improvement of reliability of the dose vectors used for these kinds of surveys.

## Exploring Dual Energy Computed Tomography images for radiotherapy treatment planning of patients with metal implants

E Pettersson<sup>1</sup>, U Lindencrona<sup>2</sup>, N Drugge<sup>2</sup> and A Thilander-Klang<sup>1,2</sup>

<sup>1</sup>*Department of Radiation Physics, Institute of Clinical Sciences, The Sahlgrenska Academy at The University of Gothenburg, Gothenburg, Sweden*

<sup>2</sup>*Department of Medical Physics and Biomedical Engineering, Sahlgrenska University Hospital, Gothenburg, Sweden*

**Purpose:** Image artefacts caused by metal implants such as hip prostheses in computed tomography (CT) images for radiotherapy treatment planning reduces the ability to delineate structures between the prostheses, and also to form the correct electron density map of the patient used for the determination of absorbed dose. The aim of this study were to explore the use of Dual Energy CT (DECT) images as input for radiotherapy treatment planning.

**Materials and Methods:** CT images of a phantom [062A electron density phantom, CIRS] with bilateral metal inserts of titanium and steel, respectively, were acquired with a polychromatic CT [Aquilion LB, Toshiba] and with a DECT [Discovery CT 750HD, GE Healthcare]. The DECT generated virtual monoenergetic (VME) CT images and they were used with and without GE's metal artefact reduction software (MARS). All the images were compared with regards to visibility of structures and electron density conversion between and of the metal inserts themselves.

**Results:** The visibility in the VME images of Titanium inserts without MARS is dependent on the VME energy, and have an optimal photon energy near 110 keV. Additional streaking appears in these images when MARS is applied. Steel inserts eliminates visibility at all VME energies. But with the use of MARS it is possible to delineate structures between the two steel inserts. When MARS is applied the CT numbers of the titanium and steel inserts are identical.

**Conclusions:** For a patient with bilateral hip prostheses of unknown metal two sets of VME images, photon energy of 110 keV, should be reconstructed: one with MARS to delineate structures between steel prostheses, and one without MARS to reduce streaking from titanium prostheses and to acquire the electron density for the prosthesis material.

## Quantitative dual-energy computed tomography using the base material decomposition in projection and image space

M Magnusson<sup>1,2</sup>, D Ballesterro<sup>1,2</sup>, M Sandborg<sup>1</sup>, G Alm Carlsson<sup>1</sup> and A Malusek<sup>1</sup>

<sup>1</sup>Medical Radiation Physics, Department of Medical and Health Sciences and Center for Medical Image Science and Visualisation, Linköping University, Linköping, Sweden

<sup>2</sup>Computer Vision Laboratory, Department of Electrical Engineering, Linköping University, Linköping, Sweden

Quantitative dual-energy computed tomography (QDECT) may help to improve the specificity of computer aided diagnostics for the following reasons: (i) Computers are especially good at analysing absolute values of well defined physical quantities characterizing the imaged tissues. (ii) The material-specific data from QDECT may be combined with data from other modalities (e.g. MRI) to provide diagnostic tests that are more specific than individual-modality tests.

QDECT can, among others, provide information about material composition of the imaged object. Existing methods can be divided into (i) projection-based basis material decomposition (PBBMD) like the Alvarez-Macovski method, and (ii) image-based basis material decomposition (IBBMD) like the two- and three-material decomposition methods. The Alvarez-Macovski method provides beam hardening artefact free images, but the resulting material composition data are often biased. The two- and three-material decomposition methods give approximate results unless the CT numbers are unbiased. Therefore they may benefit from model-based iterative reconstruction (MBIR) algorithms like DIRA from the authors or Veo from GE. The aim of this work is to evaluate a novel approach where the Alvarez-Macovski method is combined with the two- and three-material decomposition methods.

First, we implemented the Alvarez-Macovski method. Two different bases were investigated, the photoelectric effect and Compton scattering cross sections (PC) as well as water and compact bone (WB). The limit of only two bases lead to biased material composition since coherent scattering was neglected in the PC base and other body materials contributing to the attenuation coefficients were neglected in the WB base. To mitigate the problem, we used the a priori knowledge that the object consisted of soft and bone tissue only and performed an IBBMD procedure: three-material decomposition into water, protein and lipid for soft tissue and two-material decomposition into bone, bone marrow and mass density for bone. To do so, a connection between the different base materials was established in a calibration procedure.

The results showed that the combined method suppressed beam hardening artefacts and provided unbiased material composition for a 2D pelvic phantom. We expect that further improvement can be achieved by including the presented method in an MBIR algorithm like DIRA.

## Parallelization of the model-based iterative reconstruction algorithm DIRA

A Örtenberg<sup>1</sup>, M Magnusson<sup>1,2</sup>, M Sandborg<sup>1</sup>, G Alm Carlsson<sup>1</sup> and A Malusek<sup>1</sup>

<sup>1</sup>*Medical Radiation Physics, Department of Medical and Health Sciences and Center for Medical Image Science and Visualisation, Linköping University, Linköping, Sweden*

<sup>2</sup>*Computer Vision Laboratory, Department of Electrical Engineering, Linköping University, Linköping, Sweden*

Recent technological developments in computer hardware like the introduction of graphical processing units (GPUs) and coprocessors supporting massively parallel computing open new approaches to image reconstruction, analysis and optimization as computations that originally took hours can now take seconds. Codes that were used in research environments only can now reach execution times that are acceptable in clinics. The authors have developed such a code—a model-based iterative image reconstruction algorithm in dual-energy computed tomography DIRA, which provides unbiased CT numbers by reconstructing images at specific photon energies. Such images are beam hardening artefact free and can be used for instance to determine elemental composition of imaged tissues, which is an important information for radiation treatment planning systems. The aim of this work is to show how the parallelization can be done and what speedups can be achieved.

The parallelization was shown on the DIRA code. The most CPU demanding routines were converted from Matlab to C and parallelized via the OpenMP and OpenCL frameworks. The performance of the original single threaded code was compared to the performance of the parallelized versions for the task of image reconstruction of a single male pelvis slice. Computations were done on a computer with two Intel Xeon E5-2660 CPUs (16 cores) and a computer with the AMD R7 Series 260X GPU (896 cores). It was found that OpenMP-optimized code (excluding I/O routines) executed 8.6 times faster on the 16-core system; the total execution time was shortened from 121 to 11 seconds. The major speedup was achieved in the calculation of the forward and back projections (10.9 and 11.3, respectively) where individual photon energies or projections can be processed in parallel. Only the routine computing polychromatic projections was parallelized via OpenCL. The speedup was 9.9 compared to the C version. Other routines did not use the GPU effectively because of large data transfers and needed synchronization. Only several weeks of work of a skilled programmer were needed to significantly improve the performance of the code. This fact should be considered when optimization tasks are hampered by slow computer codes.

## Patient dose assessment after interventional cardiology procedures: A multi-centric approach to trigger optimization

N Ryckx<sup>1</sup>, J J Goy<sup>2</sup>, J C Stauffer<sup>2</sup> and F R Verdun<sup>1</sup>

<sup>1</sup>Institute of Radiation Physics, CHUV, Lausanne, Switzerland

<sup>2</sup>Cardiology Department, Fribourg Hospital, Fribourg, Switzerland

**Purpose:** As the number and complexity of fluoroscopically-guided interventions increase, a serious effort has to be put on the optimization of the X-ray dose delivered to the patient. In order to set up this optimization process, the clinical practice for a given cardiology center has to be analyzed with great statistical power and compared to the data at local or national level.

**Materials and methods:** The data of eight Swiss cardiology centers has been collected using CardioReport (CVX Medical, France). The following interventions have been collected: Coronary angiography (CA, 24,261), coronary angioplasty (PTCA, 1,099), CA+PTCA (18,797), transcatheter aortic valve implantation (221), shunt closure (622), myocardial biopsy (73), electrophysiology (210), defibrillator implantation (281), pacemaker implantation (300), radio-frequency ablation (720) and alcohol septal ablation (7). The collected dose indicators were cumulated air kerma, cumulated kerma-area product (KAP), fluoroscopy time and number of images per procedure. Data analysis was performed using an in-house software solution (Memoviz, Switzerland) in terms of the first, second and third quartile (Q1, Q2 and Q3) of the dose indicator distributions.

**Results:** The Q3 of the KAP for CA was at 69.41 Gy cm<sup>2</sup>. For comparison, the lowest Q3 was at 49.95 Gy cm<sup>2</sup> (-28%), whereas the highest Q3 was at 89.97 Gy cm<sup>2</sup> (+30%). In terms of fluoroscopy time however, the aforementioned centers yielded values of respectively 8.9 and 9.6 minutes. The highest (12.3 minutes) and lowest (6.0 minutes) Q3 for fluoroscopy time came from two completely different centers than the first two ones. Thus, practice harmonization could start with an extra effort towards optimal beam collimation.

**Conclusion:** This kind of large scale analysis can trigger the first discussions on practice optimization. Extra care has thus to be taken towards a correct classification of the respective procedures, in order to compare comparable practices. Further care has to be taken on the reliability of the respective dose indicators, thus implying extra efforts by medical physicists in the characterization of the dose monitors of the respective imaging units.

## Skin dose, effective dose and related risk in TAVI procedures– Is the cancer risk acceptable for younger patients?

A Karambatsakidou<sup>1</sup>, A Omar<sup>1</sup>, B Chehrazi<sup>1</sup>, A Rück<sup>2</sup> and J Scherp Nilsson<sup>1</sup>

<sup>1</sup>Department of Medical Physics, Karolinska University Hospital, Stockholm, Sweden

<sup>2</sup>Department of Cardiology, Karolinska University Hospital, Stockholm, Sweden

**Purpose:** Transcatheter treatments of valve disease are almost solely performed in elderly patients where the skin injury is the main issue, as regard to radiation effects. The aim of this study was to estimate conversion factors for both maximum entrance skin dose (MESD) and effective dose for patients undergoing transcatheter aortic valve implantation (TAVI) procedures at Karolinska University Hospital in Stockholm. The risk of exposure-induced cancer death (REID) for prospectively younger patients subjecting the same procedures has been evaluated as well.

**Material and method:** The effective dose and the risk estimations were performed with the software PCXMC 2.0 together with Euro-American mortality and cancer incidence data taken from ICRP 103, for 22 patients (11 female, 11 male). The REID was determined at 40-, 50-years and at age of exposure, respectively. Further, the skin dose was estimated for a subgroup of 15 patients with gafchromic films, which in turn were calibrated on site.

**Results:** The conversion factor for skin dose ( $CF_S = \text{MESD} / \text{kerma-area-product (KAP)}$ ) was  $9.7 \pm 1.5 \text{ mSv/Gycm}^2$  and the corresponding conversion factor for effective dose ( $CF_E = \text{effective dose} / \text{KAP}$ ) was  $0.24 \pm 0.02 \text{ mSv/Gycm}^2$ . The REID for this patient cohort was between 1:9900 and 1:1400. Furthermore, decreasing the age at exposure to 40- and 50 years will result in the increase of REID by 91% and 84% in females and 45% and 43% in males, respectively.

**Conclusions:** Currently, the REID is not an issue due to the relatively high patient age but so is the radiation induced skin injury and may require patient follow-up. The risk of cancer induction has to be highlighted when these procedures pass to the next level, when examining younger and lower-risk patients.

## **Skin doses of the patients undergoing interventional radiological examinations**

**S Sarycheva<sup>1</sup> and V Golikov<sup>1</sup>**

*<sup>1</sup>Institute of Radiation Hygiene, St. Petersburg, Russia*

The aim of this study was to evaluate the risk of deterministic secondary health effects of patients undergoing main interventional radiological (IR) examinations. Quantitative characteristic of the probability of occurrence of deterministic effects in the skin is the maximum value of the absorbed dose in the most exposed area of skin – maximum skin dose (MSD).

The data relevant to the IR examinations were collected in St. Petersburg hospitals. More than 400 procedures were under investigation. The basic patterns of the dose distribution on the surface of the patient's skin were studied for the main types of IR procedures. The assumptions about the MSD localization areas and concentration value were modeled based on the statistical distribution of the geometric parameters of IR procedures. The conservative values of conversion coefficients from dose area product (DAP) to MSD depending on field of view (FOV) were calculated.

The real measurements of absorbed dose in the patient's skin were carried out with the Gafchromic XR-RV3 film (43 pcs). These measurements allowed evaluating the actual dose distribution on the skin surface and verifying the obtained dose coefficients. The data obtained with the film dosimetry are found in good agreement with the modeled results and the data from the literature.

The conversion coefficients from DAP to MSD as well as DAP threshold reference values depending on FOV are suggested in order to avoid of deterministic radiation effects in skin.



## Verification of indicated skin entrance air kerma in cardiac x-ray guided intervention using Gafchromic film

J Nilsson Althén<sup>1</sup> and M Sandborg<sup>2</sup>

<sup>1</sup>Medical Radiation Physics, County Council of Östergötland, Linköping University, Linköping, Sweden

<sup>2</sup>Medical Radiation Physics, Department of Medical and Health Sciences and Center for Medical Image Science and Visualization, Linköping University, Linköping, Sweden

Modern interventional x-ray systems indicate the maximum entrance air kerma at the interventional reference point (IRP) and keep track of the different projections used during the x-ray guided procedure in order to assess the spatial distribution of air kerma at the skin.

The aim of this work was to verify the indicated maximum entrance air kerma on the skin for an Innova IGS 520 (GE Healthcare) interventional x-ray system and to find a suitable entrance air kerma action level that can be used to decide if a patient needs follow up procedure regarding potential skin injuries. Temporary skin erythema can occur for skin dose larger than 2 Gy.

Gafchromic films were placed on the couch just below the patient for twenty patients to monitor the spatial distribution of air kerma during the interventional procedure. The film was then scanned in a flatbed scanner and the maximum signal determined by placing ROI:s in the image. The signal from the scanned Gafchromic film was calibrated to air kerma at the film using a T20 Piranha probe (RTI Electronics AB, Mölndal) in the range 0-2 Gy. Data on the total and maximum accumulated air kerma at the reference point from the x-ray equipment was obtained from the PACS dose report for each patient.

Comparisons between measured (film) and indicated dose data (dose report) shows that the measured data is  $1.9 \pm 0.3$  (mean  $\pm 1$  standard deviation) higher than indicated data. This is partly due to scattered (backscattered and forward scattered) radiation not included in the indicated entrance air kerma at the reference point. An additional factor that influences the measured skin dose is the actual distance between the skin and the focal spot that is typically unknown. The corresponding ratio between measured air kerma with the film and the total accumulated air kerma for the whole procedure is  $0.8 \pm 0.3$ .

The action dose level for patient follow-up regarding skin injury was therefore set to 1 Gy as these measurements suggests that the maximum skin dose is approximately two times higher than the maximum indicated dose in the dose report.

## **Correlation between scatter radiation dose at the height of the operator's eye and dose to patient for different angiographics projections.**

**F Leyton<sup>1,2</sup>, M S Nogueira<sup>2</sup>, E Vano<sup>3</sup>, L Gubolino<sup>4</sup>, Maycon<sup>4</sup> and C Ubeda<sup>5</sup>**

<sup>1</sup>*Radiological Sciences Center, Health Sciences Faculty, Tarapacá University, Arica, Chile and Faculty of Medicine, Diego Portales University, Santiago, Chile*

<sup>2</sup>*Centro de Desenvolvimento da Tecnologia Nuclear - CDTN/CNEN, Belo Horizonte, Brazil*

<sup>3</sup>*Department, Complutense University and San Carlos Hospital, Madrid, Spain*

<sup>4</sup>*INCORPI, Hospital Forneceadores de Cana, Piracicaba, Brazil*

<sup>5</sup>*Radiological Sciences Center, Health Sciences Faculty, Tarapacá University, Arica, Chile*

Cases of radiation induced cataract among cardiology professionals have been reported in studies. In view of evidence of radiation injuries, the ICRP recommends limiting the radiation dose to the lens to 20 mSv per year for occupational exposure. The aim of this work was to report scattered radiation doses to the eye lens of the interventionalist from procedures performed without use of ceiling suspended screens, correlated with different angiographic projections.

Measurements were made in a cardiac laboratory with an angiography X-ray system General Electric Innova 2100 IQ equipped with flat-panel detector. Polymethylmethacrylate plates of 30x30x5 cm were used to simulate a patient with a thickness of 20 cm. A 20-cm field of view was used. Two fluoroscopy modes (low and medium, 15 frame/s), cine mode 15frame/s. Four angiographic projections anterior posterior (AP), lateral (LAT), left anterior oblique caudal (spider) and left anterior oblique cranial (LAOCRA) and a cardiac protocol for patient between 70 to 90 kg was used.

Measurements of phantom entrance doses rate and scatter doses rate were performed with two Unfors Xi plus, model 8202031-HXi and 8202062-CXi survey detector. The focus to detector phantom entrance distance was 55 cm and focus to flat panel detector distance was 100 cm. The detector measuring scatter radiation was positioned at the usual distance of the cardiologist's eyes during working conditions (1m from the isocenter and 1.7 m from the floor).

There is a good linear correlation between phantom entrance doses rate and scatter dose rate to AP projection. There is a good linear correlation between the kerma-area product and scatter dose at the lens,  $R^2$  0.9986 and 0.9988 for AP and LAT projection, respectively. An experimental correlation factor of 2.3 and 17.6  $\mu\text{Sv}$  per  $\text{Gy}\cdot\text{cm}^2$  has been found for the AP and LAT projections, respectively.

The entrance dose of PMMA for fluoroscopy low, medium and cine was 13, 39 and 282 mGy/min, respectively to AP. The highest dose rate in the lens was 60.19 mSv/h at projection LAOCRA in cine mode. Interventional operator can easily exceed the dose limit for lens if radiation protection tools are not used.

## Assessing the usefulness of the quasi-ideal observer for quality control and dose optimisation in fluoroscopy and interventional radiology

E Tesselaa<sup>1</sup> and M Sandborg<sup>2</sup>

<sup>1</sup>Medical Radiation Physics, County Council of Östergötland, Linköping University, Linköping, Sweden

<sup>2</sup>Medical Radiation Physics, Department of Medical and Health Sciences and Center for Medical Image Science and Visualisation, Linköping University, Linköping, Sweden

Image quality in quality assurance tests on fluoroscopy systems are often evaluated by subjective visual methods which suffer from low sensitivity and precision. The aim of this work was to evaluate measurements of the square of the signal-to-noise ratio rate,  $\text{SNR}_{\text{rate}}^2$  on a modern fluoroscopy system to assess its potential for quality control and dose optimisation.

The quasi-ideal model observer (Med. Phys., 31, 2564-2576, 2004) was used to measure  $\text{SNR}_{\text{rate}}^2$  in phantom images acquired with a Siemens Axiom Artis Zee MP. The phantom consisted of a 2 mm Cu filter and a 5 cm thick acrylic phantom containing low contrast details of aluminium and plastic. The dose rate, pulse rate and the thickness of the Cu filter at the x-ray tube were varied to measure the effect on the  $\text{SNR}_{\text{rate}}^2/P_{\text{KA},\text{rate}}$  ( $P_{\text{KA},\text{rate}}$  being the kerma-area product rate), i.e. the dose-efficiency. Repeated measurements were made to assess the precision of the method for quality control tests.

The variation in  $\text{SNR}_{\text{rate}}^2/P_{\text{KA},\text{rate}}$  over 4 consecutive weekly measurements was 5% (%CV) for the 5 mm Al contrast detail, whereas lower thickness contrast details showed substantially higher variations over consecutive measurements. The  $\text{SNR}_{\text{rate}}^2/P_{\text{KA},\text{rate}}$  was strongly dependent on the thickness of the contrast detail as expected. An increase in the  $\text{SNR}_{\text{rate}}^2/P_{\text{KA},\text{rate}}$  of 80% was observed when the low dose rate mode was used compared with normal and high dose rate modes. This is due to the use of much thicker additional 0.9 mm Cu used in the low dose rate mode compared to 0.2-0.3 mm Cu used in the other two modes.  $\text{SNR}_{\text{rate}}^2/P_{\text{KA},\text{rate}}$  decreased with increasing phantom thickness (1-3 mm Cu) since the photons that contribute most to the dose-efficiency are attenuated more in the thicker phantom. Finally, only a 5% variation in  $\text{SNR}_{\text{rate}}^2/P_{\text{KA},\text{rate}}$  was seen between different pulse rates (10-30 pps).

Measurements of  $\text{SNR}_{\text{rate}}^2$  make it possible to reproducibly measure image quality, provided that the SNR of the contrast detail in the phantom is sufficiently high. The  $\text{SNR}_{\text{rate}}^2/P_{\text{KA},\text{rate}}$  varied with dose rate and phantom thickness, but was independent of pulse rate. These results indicate that  $\text{SNR}_{\text{rate}}^2/P_{\text{KA},\text{rate}}$  measurements offer better sensitivity and precision for quality control tests and dose optimisation, compared to visual assessment.

## Multicentre comparison of image quality for low contrast objects and micro-catheter tips in X-ray guided treatment of arteriovenous malformation in the brain

J E M Mourik<sup>1,2</sup>, M L Overvelde<sup>3</sup>, I HernandezGiron<sup>4</sup>, W J H Veldkamp<sup>1</sup>, D Zweers<sup>1</sup> and K Geleijns<sup>1</sup>

<sup>1</sup>Department of Radiology, Leiden University Medical Center, Leiden, The Netherlands

<sup>2</sup>Department of Radiology / Nuclear Medicine, Sint Franciscus Gasthuis, Rotterdam, The Netherlands

<sup>3</sup>Medical Physics, Albert Schweitzer Hospital, Dordrecht, The Netherlands

<sup>4</sup>Medical Physics, Universitat Rovira i Virgili, Tarragona, Spain

**Purpose:** Treatment of arteriovenous malformations (AVM) can be performed as a minimally invasive X-ray guided procedure during which a micro-catheter is used to reach the treatment site. This procedure requires acquisition protocols that provide a high level of image quality and consequently a relatively high entrance skin dose (ESD) for the patient. The high level of image quality is required to visualize the very small micro-catheters in the contrast enhanced vessel and against the anatomical background of the skull. Purpose of this study was to investigate the relation between image quality and ESD for large low contrast objects and small micro-catheter tips.

**Materials and methods:** Images of the Leeds TOR CDR phantom and 5 micro-catheter tips (0.40, 0.50, 0.57, 0.60 and 0.63mm) were acquired in combination with a PMMA head phantom at 4 hospitals (referred to as hospital A, B, C, D) with the acquisition protocols for fluoroscopy and DSA that were implemented in clinical practice. The TOR CDR phantom contains 17 large ( $\varnothing$  11mm) circular objects with decreasing contrast. Contrast-to-noise ratios (CNR) were calculated for all circular objects of the TOR CDR ( $CNR_{TOR}$ ) and the tips ( $CNR_{TIP}$ ). In addition, ESD was measured on the head phantom using a solid-state dosimeter.

**Results:** For fluoroscopy, the highest ESD-rate was found for hospital B (137 $\mu$ Gy/s). Up to 78% lower ESD-rates were found for the other three hospitals (A: 120, C: 77, D: 67 $\mu$ Gy/s). Only small differences (< 8%) in ESD for DSA were found [1.5–1.7mGy/frame]. The ranking of the hospitals, from higher to lower  $CNR_{TOR}$  was B-A-D-C for DSA and fluoroscopy. For DSA, although ESD values were similar, relative differences (expressed as the highest  $CNR_{TOR}$  obtained in (B) for the largest nominal contrast in the phantom (0.075)) were 43% (A), 77% (C) and 58% (D), respectively. For fluoroscopy, these relative differences were 3% (A), 66% (C) and 47% (D). The same ranking of image quality was obtained for the catheter tips. For fluoroscopy, relative differences in  $CNR_{TIP}$  were up to 39% (A) and 71% (C and D), respectively. For DSA, these relative differences were up to 73% (A), 72% (C) and 69% (D).

**Conclusion:** For fluoroscopy a correlation between ESD and CNR was found. Although only small differences in ESD-rate were observed for DSA ESD, differences in CNR were large. Differences may be due to differences in imaging protocols (e.g. kV, filtration, pulse rate) and post processing. These results can be used to optimize the acquisition protocols for treatment of AVM in the brain.

## Breast density assessment in breast tomosynthesis using the central projection image

P Timberg<sup>1,2</sup>, K Lång<sup>3,4</sup>, H Sartor<sup>3</sup>, M Dustler<sup>1</sup> and S Zackrisson<sup>3,5</sup>

<sup>1</sup> Medical Radiation Physics, Lund University, Malmö, Sweden

<sup>2</sup> Skåne University Hospital, Region Skåne, Lund, Sweden

<sup>3</sup> Diagnostic Radiology, Lund University, Malmö, Sweden

<sup>4</sup> Unilabs breast clinic, Malmö, Sweden

<sup>5</sup> Skåne University Hospital, Region Skåne, Malmö, Sweden

Breast tomosynthesis (BT) is gaining more ground in the field of mammography. Still, it faces several challenges and one of them is breast density assessment. Breast density is an independent risk factor for developing breast cancer. An objective, rigid and automatic method for its quantification is nowadays in increased demand. Volpara is a well-established robust method for breast density assessments in digital mammography (DM) but has not yet been adapted to conform to 3D images. The aim of this study was to investigate the possibility to quantify breast density in BT projection images. As an initial step we investigated the possibility to quantify breast density in the central BT projection image (which resembles a low dose DM image) using Volpara. In the following step we compared density measures in BT with DM using the same cases. In total 1000 consecutive cases (MLO projections in BT and DM) were included from the Malmö breast screening trial (MBTST). Our results showed that Volpara overestimated the density in higher angular projection images due to ray path length, as Volpara is currently configured to operate at a constant breast thickness. The noise present in the low dose BT projection image did not notably impair the quantification. Hence the central projection image was used for the assessment. In summary, it is possible to use Volpara to quantify the breast density in the central projection BT image. We have found a high agreement in breast density assessment between DM and BT based on preliminary findings.

Results are preliminary and may be subject to change.

## **Validation of a simulation procedure for generating breast tomosynthesis projection images**

**H Petersson<sup>1</sup>, L M Warren<sup>2</sup>, A Tingberg<sup>1</sup>, M Dustler<sup>1</sup> and P Timberg<sup>1</sup>**

<sup>1</sup>*Medical Radiation Physics, Department of Translational Medicine, Lund University, Malmö, Sweden*

<sup>2</sup>*National Coordinating Centre for the Physics of Mammography, Royal Surrey County Hospital, Guildford, United Kingdom*

Breast tomosynthesis (BT) is an imaging technique that recently have been introduced as an alternative or complement to standard mammography in breast cancer screening. In BT, a set of projection images of the breast are acquired over a limited angular range. The projection images are then reconstructed to form a 3D image volume. The method depends on the choice of several acquisition parameters such as angular range, number of projections, projection distribution and dose distribution among the projections. In order to achieve optimal performance for detection of lesions such as microcalcifications and low contrast masses, the acquisition geometry has to be optimized. A way of evaluating many different acquisition parameters without development of physical prototypes or human radiation exposure is to use Monte Carlo simulations.

A simulation procedure, based on the Monte Carlo code system Penelope and the geometry of a Siemens MAMMOMAT Inspiration BT system, has been developed to generate BT projection images of a digital breast phantom. The procedure uses analytical ray tracing to produce scatter and noise free images, Monte Carlo to simulate scatter contribution and measured values from flatfield image acquisitions to model system noise.

The aim of this work is to validate the developed simulation procedure. This will be done by comparing simulated images with real images acquired with the modelled Siemens BT system. A test phantom, with corresponding digital phantom, consisting of gold discs and aluminium foil placed between PMMA slabs will be used for measurements of contrast-to-noise ratio and sharpness of the real and simulated images. This comparison will indicate the validity of the used simulation procedure.

## Influence of in-plane artifact on pulmonary nodule size measurements in chest tomosynthesis

C Söderman<sup>1</sup>, Å A Johansson<sup>2,3</sup>, J Vikgren<sup>2,3</sup>, R Rossi Norrlund<sup>2,3</sup>, D Molnar<sup>2,3</sup>, A Svallkvist<sup>1,4</sup>, L G Månsson<sup>1,4</sup> and M Båth<sup>1,4</sup>

<sup>1</sup>Department of Radiation Physics, Institute of Clinical Sciences, Sahlgrenska Academy, University of Gothenburg, Gothenburg, Sweden

<sup>2</sup>Department of Radiology, Institute of Clinical Sciences, Sahlgrenska Academy, University of Gothenburg, Gothenburg, Sweden

<sup>3</sup>Department of Radiology, Sahlgrenska University Hospital, Gothenburg, Sweden

<sup>4</sup>Department of Medical Physics and Biomedical Engineering, Sahlgrenska University Hospital, Gothenburg, Sweden

**Objective:** In tomosynthesis imaging, a halo-like artifact can appear around structures in the reconstructed section images. This is due to the limited angular range of the tomosynthesis scan, leading to an incomplete sampling of the frequency space. The artifact is generally more prominent in the scan direction. In the case of chest tomosynthesis, the appearance of the artifact around pulmonary nodules may have an effect on the accuracy of nodule diameter measurements such that it might not be obvious if the artifact should be included or not in the measurement. The aim of the present study was to investigate how the halo-like artifact should be managed when measuring pulmonary nodules in chest tomosynthesis images in order to achieve a high level of accuracy in nodule size assessment.

**Methods:** An analysis of measurements of the longest diameter of artificial ellipsoid shaped nodules with known dimensions inserted in clinical chest tomosynthesis images was performed. The measurements were done as part of a previous study investigating nodule measurement accuracy. Before the simulated nodules were inserted in the images a rotation was applied to them such that the longest diameter lied in different directions in the image plane relative to the tomosynthesis scan direction. The amount of rotation for each nodule was chosen randomly. Measurements were made by four thoracic radiologists. The analysis of the data for the present study included an investigation of a possible dependency of measurement error on the amount of rotation of the nodules.

**Results:** All radiologists chose not to include the artifact in their measurements. The measurement error of the longest diameter of the nodules was at a constant level regardless of in which direction the longest diameter of the nodule lied relative to the scan direction.

**Conclusion:** The results indicate that the halo-like artifact visible around pulmonary nodules in chest tomosynthesis images should not be included when measuring the diameter of the nodules.

## Evaluation of an improved implementation of a method of simulating pulmonary nodules in chest tomosynthesis

F Svensson<sup>1</sup>, C Söderman<sup>2</sup>, A Svalkvist<sup>1,2</sup>, R Rossi Norrlund<sup>3,4</sup>, J Vikgren<sup>3,4</sup>, ÅA Johnsson<sup>3,4</sup> and M Båth<sup>1,2</sup>

<sup>1</sup>*Department of Radiation Physics, Institute of Clinical Sciences, Sahlgrenska Academy at University of Gothenburg, Gothenburg, Sweden*

<sup>2</sup>*Department of Medical Physics and Biomedical Engineering, Sahlgrenska University Hospital, Gothenburg, Sweden*

<sup>3</sup>*Department of Radiology, Institute of Clinical Sciences, Sahlgrenska Academy at University of Gothenburg, Gothenburg, Sweden*

<sup>4</sup>*Department of Radiology, Sahlgrenska University Hospital, Gothenburg, Sweden*

**Purpose:** At the previous Malmö Conference on Medical Imaging, Svalkvist et al presented a method of simulating the presence of pulmonary nodules in chest tomosynthesis images through using computer simulations. The method was later evaluated in an observer study that revealed that although the artificial lung nodules had similar detectability as real nodules, experienced thoracic radiologists to some extent were able to distinguish them from real nodules. Recently, an error was found in the code used to generate the simulated nodules in the evaluation study. This error has now been corrected. The purpose of the present work was to perform a thorough evaluation of the corrected implementation of the nodule simulation method for chest tomosynthesis, comparing the detection rate and appearance of the artificial nodules with those of real nodules in an observer performance experiment.

**Material and methods:** A cohort consisting of 64 patients, 38 patients with a total of 129 identified pulmonary nodules and 26 patients without identified pulmonary nodules, was used in the study. Simulated nodules, matching the real clinically found pulmonary nodules by size, attenuation, and location, were created and randomly inserted into the tomosynthesis section images of the patients. Three thoracic radiologists reviewed the images in an observer performance study divided into two parts. The first part included nodule detection and the second part included rating of the visual appearance of the nodules. The results were evaluated using a modified receiver-operating characteristic (ROC) analysis.

**Results and conclusions:** The data collection is not complete and the final results will be presented at the conference. A preliminary analysis indicates that the corrected code increases the similarity between the artificial nodules and real nodules and that the validity of the implemented method thus has increased.



## Image fusion of two FBP-reconstructed digital tomosynthesis volumes from frontal and lateral acquisitions

J Arvidsson<sup>1</sup>, C Söderman<sup>2</sup> and M Båth<sup>1,2</sup>

<sup>1</sup>*Department of Medical Physics and Biomedical Engineering, Sahlgrenska University Hospital, Gothenburg, Sweden*

<sup>2</sup>*Department of Radiation Physics, Institute of Clinical Sciences, Sahlgrenska Academy, University of Gothenburg, Gothenburg, Sweden*

**Purpose:** Digital tomosynthesis (DTS) has been used in chest imaging as a low radiation dose alternative to computed tomography (CT). DTS can to a certain degree separate overlapping anatomical structures at different depth levels using traditional filtered back projection (FBP) reconstruction schemes. However, the spatial resolution remains limited in the out-of-plane dimension. The aim of this work was to investigate if utilizing information from both a frontal and lateral DTS acquisition will give a more accurate 3D representation of the examined object.

**Method:** As a first indication of whether a dual-view DTS data acquisition can yield a fair resolution in the three spatial dimensions, a manual registration between two reconstructed DTS volumes, one being a frontal data acquisition and the other a lateral one, was performed. An anthropomorphic chest phantom was scanned using a linear DTS acquisition in frontal and lateral directions, at 120 kVp. The two corresponding volumes were reconstructed, downsampled to a lower resolution and manually co-registered. Being manual, the registration step was subjective and thus included identifying suitable landmarks that could be used to ensure that the correct rigid transformation between the two volumes was found. Finally a CT examination of the phantom, used as a ground truth 3D representation, was manually co-registered to the DTS data. The reconstruction, downsampling and co-registering was performed using both commercial and freely available software.

**Major Findings:** The resulting co-registered volume gave a more accurate isotropic 3D representation of the examined object than the two original reconstructions. Oblique planes were more accurately reproduced by the co-registered volume whereas coronal and sagittal planes were better reproduced by the original frontally and laterally reconstructed volumes.

**Conclusions:** The proposed method shows that fusing frontally and laterally reconstructed DTS volumes is possible and yields a more accurate isotropic 3D representation of the examined object than original DTS reconstructions. By utilizing a dual-view DTS acquisition geometry some advantages of including DTS data from orthogonal projection angles were illustrated. The findings are encouraging for further work on reconstruction algorithms using a dual-view DTS acquisition geometry.

## Effective dose to patients from thoracic spine examinations with tomosynthesis

A Svallkvist<sup>1,2</sup>, C Söderman<sup>2</sup> and M Båth<sup>1,2</sup>

<sup>1</sup>*Department of Medical Physics and Biomedical Engineering, Sahlgrenska University Hospital, Gothenburg, Sweden*

<sup>2</sup>*Department of Radiation Physics, Institute of Clinical Sciences, the Sahlgrenska Academy at University of Gothenburg, Gothenburg, Sweden*

Tomosynthesis, which refers to the principle of collecting low-dose projections of the patient at different angles and using these projections to reconstruct section images of the patient, is an imaging technique recently introduced to healthcare. Phantom evaluations have indicated that the effective dose of a thoracic spine examination using tomosynthesis is about twice the dose from a conventional radiological thoracic spine examination (including four projections), but no detailed description of actual patient doses has been published. The aims of the present work were to calculate the average effective dose to patients from clinical use of tomosynthesis for lateral thoracic spine examinations and to determine a conversion factor between kerma-area product (KAP) and effective dose for the examination.

The GE Discovery XR656 system with VolumeRAD option (GE Healthcare, Chalfont St. Giles, UK) was used to perform thoracic spine tomosynthesis examinations on 17 patients. The examinations included both patients standing up and patients laying down. The recorded dose data consisted of the registered KAP for each of the 60 projection radiographs collected in a tomosynthesis examination and by examining the image data, the field size for each projection radiograph was obtained. These data, together with information of the patient height and weight, were used in the Monte Carlo program PCXMC 2.0 (STUK – Radiation and Nuclear Safety Authority, Helsinki, Finland) to calculate the effective dose for each projection radiograph, using the conversion factors given in ICRP 103. The total effective dose for the tomosynthesis examinations were finally obtained by adding the effective doses from the 60 projection radiographs included in each examination. Based on a comparison between the total registered KAP of the tomosynthesis examination and the calculated effective dose, a conversion factor between total KAP and effective dose was determined.

The results revealed that the mean effective dose for the thoracic spine examinations was 0.47 mSv (range, 0.24-0.81 mSv). Using the mean total KAP of the examinations and the mean calculated effective dose a conversion factor of 0.092 mSv/Gycm<sup>2</sup> was obtained. The obtained conversion factor agrees well with the conversion factor of 0.091 mSv/Gycm<sup>2</sup> previously reported for conventional radiological lateral thoracic spine examinations (Wall et al., Report HPA-CRCE-028, Health Protection Agency, UK, 2011).

## Retrospective estimation of patient dose-area product in thoracic spine tomosynthesis performed using VolumeRAD

M Båth<sup>1,2</sup>, C Söderman<sup>2</sup> and A Svalkvist<sup>1,2</sup>

<sup>1</sup>*Department of Medical Physics and Biomedical Engineering, Sahlgrenska University Hospital, Gothenburg, Sweden*

<sup>2</sup>*Department of Radiation Physics, Institute of Clinical Sciences, Sahlgrenska Academy at University of Gothenburg, Gothenburg, Sweden*

**Purpose:** For a tomosynthesis examination performed using the VolumeRAD system (GE Healthcare, Chalfont St. Giles, UK), the scout image is normally the only image stored in the picture archiving and communication system (PACS) that contains dose data in the digital imaging and communications in medicine (DICOM) header. Recently, a method of retrospectively estimating the patient dose-area product (DAP) of a chest tomosynthesis examination performed using the VolumeRAD system from DICOM data available in the scout image was presented (Båth et al, Med Phys 2014). The purpose of the present work was to evaluate the application of the method to thoracic spine tomosynthesis.

**Material and Methods:** DICOM data for the projection radiographs acquired during the examination were retrieved directly from the modality for 17 patients undergoing thoracic spine tomosynthesis with VolumeRAD. Using information about how the exposure parameters for the tomosynthesis examination are determined by the scout image, an estimated DAP for the tomosynthesis examination was determined from DICOM data in the scout image. Based on comparing the estimated DAP with the actual DAP registered for the projection radiographs acquired during the tomosynthesis examination, a correction factor for the adjustment in field size with projection angle was determined.

**Results:** The field-size correction factor for thoracic spine tomosynthesis was determined to 0.92. Applying this factor to the DAP estimated retrospectively from the scout image, the maximum difference between the estimated DAP and the actual DAP was smaller than 3% for all patients.

**Conclusions:** The previously developed method of retrospectively estimating the DAP of a chest tomosynthesis examination performed using the VolumeRAD system from DICOM data in the scout image can be applied also to thoracic spine tomosynthesis. The method may thus be of value for retrospectively estimating patient dose in clinical use of thoracic spine tomosynthesis.

## **Image quality assessment in chest x-ray using an anthropomorphical phantom**

**A A Drozdov<sup>1</sup>, A V Vodovatov<sup>2</sup> and C Bernhardsson<sup>3</sup>**

<sup>1</sup>*St-Petersburg State Mariinsky Hospital, St-Petersburg, Russia*

<sup>2</sup>*St-Petersburg Research Institute of Radiation Hygiene after Professor P.V.Ramzaev, St-Petersburg, Russia*

<sup>3</sup>*Medical Radiation Physics, Department of Translational Medicine, Malmö, Lund University, Skåne University Hospital, Malmö, Sweden*

The current system of diagnostic image quality assessment (designed for conventional film-based x-ray systems) should be /modernized as there is an almost complete shift to digital x-ray technologies, even in developing countries. In this study, the European chest PA x-ray image quality criteria were revised in order to consider digital imaging capabilities. Also, a methodology of expert image quality assessment, based on VGA and ICS methods, was developed. The methodology used is based on an anthropomorphic chest phantom (Kyoto Kagaku, Japan) survey that was tested in two major University Hospitals (St. Petersburg, Russia). The survey focused on the comparison of digital images that were acquired on a range of tube voltages, using AEC on different digital x-ray units with different detector types. This approach is preferable as it primary considers professional opinions and the needs of the end-users (diagnostic radiologists and referring physicians).

## Evaluation of dose reduction potentials of a novel scatter correction software for bedside chest X-ray imaging

V Toth<sup>1</sup>, C Brieskorn<sup>2</sup>, B Renger<sup>1</sup>, D Mentrup<sup>3</sup>, S Jockel<sup>3</sup>, F Lohöfer<sup>1</sup>, M Schwarz<sup>1</sup>, E J Rummeny<sup>1</sup> and P B Noël<sup>1</sup>

<sup>1</sup>Institute of Diagnostic and Interventional Radiology, Klinikum Rechts der Isar, TU Munich, Germany

<sup>2</sup>Institute for Biomedical Technique and Informatics, TU Ilmenau, Germany

<sup>3</sup>Diagnostic X-ray Systems, Philips Healthcare, Hamburg, Germany

**Aims and Objectives:** Bedside chest X-rays (CXR) for catheter position control may add up to a considerable radiation dose in ICU patients. Suboptimal imaging circumstances often impair image quality, which may be mitigated by an anti-scatter grid; however, grids have several drawbacks (workflow burden, problems with beam alignment). The aim of this study was to evaluate image quality and dose reduction potentials of a novel scatter correction software (SkyFlow, Philips Healthcare, Hamburg, Germany) developed to increase the contrast of gridless CXRs.

**Materials and Methods:** CXRs of a „Lungman“ (Kyoto Kagaku) thoracic phantom with a Portacath system, a central venous line and a dialysis catheter were performed in an experimental setup using a mobile X-ray system (MobileDiagnost wDR 2.0, Philips Healthcare) with multiple kV and mAs settings without and with an anti-scatter grid. Images with diagnostic Exposure Index (EI<sub>s</sub> 250-500) were evaluated for the difference in applied mAs with and without anti-scatter grid. Three radiologists assessed image quality of grid and non-grid images, the latter with and without scatter correction processing.

**Results:** The application of an anti-scatter grid implied twice as high mAs in order to reach diagnostic EI<sub>s</sub>. SkyFlow significantly improved the diagnostic quality of images acquired without grid. CXR with grid provided better image quality than gridless imaging with scatter correction.

**Conclusion:** The evaluated scatter correction software significantly improved image quality of gridless CXR. Even though its image quality does not reach that of CXR with anti-scatter grid, the significant reduction in patient dose advocates the use of such algorithms for bedside CXR imaging.

## **Estimation of organ doses for the patients undergoing X-ray examination by use of physical human phantoms**

**V Golikov<sup>1</sup>, A Barkovsky<sup>1</sup>, E Wallström<sup>2</sup> and Å Cederblad**

*<sup>1</sup>Institute of Radiation Hygiene, St. Petersburg, Russia*

*<sup>2</sup>Dept. of Radiology, Trollhättan Hospital - NÄL, Trollhättan, Sweden*

The results of phantom experiments performed with the purpose of organ doses estimation for the patients undergoing X-ray examination are presented. In experiments were used physical phantoms of the adult man (Alderson Rando) and child of five years old ("ATOM Ltd" production). For both phantoms were simulated chest and urography examinations with parameters typical for their running in Russia and Sweden (tube voltage 80 – 140 kV, filtration 4 – 4.5 mm Al, focus to film distance 100 – 150 cm). Average organ doses (inside phantoms), surface doses and dose in free air were measured using TL-detectors (TLD-100, Harshaw). The experimental values of organ doses were compared with the data obtained by calculation methods. In the calculations were used mathematical Cristy's phantoms representing adult and child of five years old. In general reasonable agreement is obtained between the two sets of the results. As a rule for organs inside primary field of radiation doses agree to within 30%. The larger differences in organ doses are observed for organs located close to the edge of the beam of primary radiation.

## Comparison of the accuracy in kidney activity concentration estimates by the conjugate view and posterior view methods

T Magnander<sup>1,2</sup>, J Svensson<sup>3</sup>, M Båth<sup>1,2</sup>, P Gjertsson<sup>4</sup>, E Forssell-Aronsson<sup>1,2</sup> and P Bernhardt<sup>1,2</sup>

<sup>1</sup>*Department of Radiation Physics, Institute of Clinical Sciences, Sahlgrenska Academy at University of Gothenburg, Gothenburg, Sweden*

<sup>2</sup>*Department of Medical Physics and Biomedical Engineering, Sahlgrenska University Hospital, Gothenburg, Sweden*

<sup>3</sup>*Department of Oncology, Institute of Clinical Sciences, Sahlgrenska Academy at University of Gothenburg, Gothenburg, Sweden*

<sup>4</sup>*Department of Clinical Physiology, Institute of Medicine, Sahlgrenska Academy at University of Gothenburg, Gothenburg, Sweden*

**Purpose:** In nuclear medicine the conjugate view method (CV) is the most common method for activity quantifications in planar images. The advantage with the CV method is its depth independence, i.e. the activity concentrations can be calculated from two opposite planar images without the knowledge of depth. However, one disadvantage of the method that the signal to background ratio is dependent on the location of the object. This effect might increase the inaccuracy in the activity concentration estimates. Therefore, the activity in off-center objects might be better estimated by the camera projection with the shortest camera to object distance. The aim of the present study was to compare the CV method with a posterior-anterior (PA) projection method for estimation of <sup>177</sup>Lu activity concentrations in the kidneys.

**Methods:** The two methods were used to retrospectively determine and compare the left and right kidney activity concentration in 20 patients treated with <sup>177</sup>Lu-DOTA-octreotate at Sahlgrenska University Hospital. The kidney was segmented in the SPECT or CT image using an appropriate segmentation algorithm. An attenuation map for <sup>177</sup>Lu was created from the CT. Attenuated planar AP and PA projections were created from the SPECT and the attenuation map. The kidney VOI was projected onto the AP and PA projections. The activity concentration in the kidney was calculated using both the PA projection method (AC<sub>PA</sub>) and the CV method (AC<sub>CV</sub>) and the results were compared to the concentration in the kidney VOI in the SPECT.

**Results:** The mean ratio between AC<sub>CV</sub> and the SPECT determined activity concentration was 1.99 with a standard deviation (SD) equal to 1.03 and the mean ratio between AC<sub>PA</sub> and the SPECT determined concentration was 1.66 with SD=0.80. Both methods demonstrated that the main problems with activity estimates from planar images are the influences of attenuation and the activity concentration in the under and overlying tissues.

**Conclusions:** The present study shows that a true background estimate cannot be accurately performed with neither the CV nor the PA method and that the difficulties in obtaining a true background affect the CV method more than the PA method. The study indicates that the PA method gives a more accurate estimate of the kidney activity concentration than the CV method.

## Evaluation of image quality parameters in PET/CT using the MADEIRA and NEMA NU-2 2001 phantoms

L Chipiga<sup>1, 2</sup>, M Sydoff<sup>3</sup>, I Zvonova<sup>1</sup> and C Bernhardsson<sup>4</sup>

<sup>1</sup>*Research Institute of Radiation Hygiene, St. Petersburg, Russia*

<sup>2</sup>*Federal North-West Medical Research Centre, St. Petersburg, Russia*

<sup>3</sup>*Department of Radiation Physics, Skane University Hospital, Lund, Sweden*

<sup>4</sup>*Department of Radiation Physics, Skane University Hospital, Malmö, Sweden*

Positron Emission Tomography combined with computed tomography (PET/CT) is a quantitative technique which can be used for diagnosing a number of different diseases and also for monitoring treatment response for different types of tumors. However, the accuracy of the data is limited by the spatial resolution of the PET system. This causes a “smearing” of the signal from inside a lesion out into the neighbouring voxels, thereby causing an underestimation of the apparent activity in the lesion, the so-called Partial Volume Effect (PVE). The most common types of phantoms used for activity quantification in PET utilizes fillable sphere inserts in an elliptical or circular cylinder made of polymethyl methacrylate (PMMA), for example the NEMA NU-2 2001 phantom. The aim of this study was to investigate the influence of lesion size and tumor-to-background activity concentration ratio (TBR) on image quality and system recovery using a new MADEIRA phantom that includes PMMA cones instead of spheres, developed within the collaborative project “”. The results from these measurements were then compared with the results from similar measurements using the NEMA phantom. Measurements were done on four different PET/CT systems (Siemens Biograph 16, Philips Gemini, Philips Gemini ToF and GE Discovery 690) and the results from the measurements with the two different phantoms were compared. For all investigated PET/CT systems, the activity concentration obtained from the reconstructed images were closest to the true activity concentration at low values of TBR (less than 10). At higher TBR (30-35) the reconstructed activity values were reduced to 50-60% of the true activity values. The MADEIRA phantom allows for a wide range of possibilities in measuring image quality parameters and the results obtained from measurements with this phantom show good agreement with the results obtained from measurements with the NEMA NU-2 2001 phantom.



**Portable scintillation detector for lung activity measurements prior to V/P<sub>SPECT</sub>****M Larsson<sup>1</sup>, J Himmelman<sup>2</sup> and J Dalmo<sup>2</sup>**<sup>1</sup>*Department of Radiation Physics, Institute of Clinical Science, Göteborg, Sweden*<sup>2</sup>*Sahlgrenska University Hospital, Göteborg, Sweden.*

Ventilation and perfusion SPECT (V/P<sub>SPECT</sub>) is a tomographic imaging method using <sup>99m</sup>Tc labeled carbon particles (technegas) and <sup>99m</sup>Tc-macro aggregated albumin (MAA), respectively, for examination of the lungs. The primary purpose of V/P<sub>SPECT</sub> is to diagnose pulmonary embolism (PE). Today in Sahlgrenska University Hospital, the gamma camera is used for determination of enough inhaled technegas before the ventilation SPECT, a sufficient activity in the lungs are 20- 30 MBq. To economize with camera time and eliminate the risk of contamination of the camera detector system it would be advantageous to use a portable detector in a preparation room to ensure an adequate count rate. The aim of this study was to find a method to use a portable scintillation detector for estimation of inhaled technegas in lung tissue before V/P<sub>SPECT</sub> and to validate the method for clinical use.

A scintillation detector (SSL Radhound with SS404 Al probe, Southern Scientific UK, Gamma Data AB, UK), was positioned over and/or laterally of the patient lying on a bed in supine position. The patient inhaled technegas and the countrate of the portable detector was compared to the total counts from the ventilation SPECT images.

The scintillation detector count statistics showed potential to replace the gamma camera measurements of the inhaled lung activity. The detected counts by scintillation detector showed good correlation to the number of counts in the SPECT images.

In conclusion, the scintillation measurements can replace the method using a gamma camera for the activity uptake measurement before ventilation SPECT in the clinic.

## **A phantom for determination of calibration coefficients and minimum detectable activities using a SPECT/CT for internal contamination monitoring following radiation emergency situations**

Ü Ören<sup>1</sup>, M Andersson<sup>1</sup>, C L Rääf<sup>1</sup> and S Mattsson<sup>1</sup>

<sup>1</sup>Medical Radiation Physics, Department of Translational Medicine, Lund University, Skåne University Hospital, Malmö, Sweden

There is a risk for internal contamination of individuals following nuclear or radiological events. Rapid investigations and screening of potentially contaminated people are desirable to quickly estimate the contamination levels. The purpose of this on-going study was to derive calibration coefficients (in terms of cps kBq<sup>-1</sup>) and minimum detectable activities, MDA, (in terms of kBq) for a SPECT/CT-study for *in-vivo* internal contamination measurements in radiation emergency situations.

A cylindrical-conical PMMA-phantom with diameter sizes in the range of 10-30 cm was developed in order to simulate different body parts and patients of different sizes. A series of planar gamma camera investigations were conducted using a SPECT/CT modality with the collimators removed for <sup>131</sup>I and <sup>137</sup>Cs; radionuclides potentially associated with radiation emergencies. Energy windows of 337-391 keV and 490-690 keV were selected for <sup>131</sup>I and <sup>137</sup>Cs respectively.

The measurements show that the calibration coefficients for <sup>137</sup>Cs range from 10 to 19 cps kBq<sup>-1</sup> with MDA values in the range of 0.29 kBq to 0.55 kBq for phantom diameters of 10-30 cm. The corresponding values for <sup>131</sup>I are 12 to 37 cps kBq<sup>-1</sup> with MDA values of 0.08 to 0.26 kBq. In addition, a measurement was performed with an Alderson phantom containing a <sup>137</sup>Cs source placed on the lung in order to verify the derived calibration coefficients. The anterior-posterior distance of the Alderson phantom is 23 cm and the corresponding calibration coefficient was used. The results showed that the value of the estimated activity was 29 % higher than the true activity. This simple method for the determination of calibration coefficients and MDA levels can be implemented within the emergency preparedness plans in hospitals with nuclear medicine departments. The derived data will help to roughly estimate the internal contamination of humans following radiation emergencies.

## Can an energy compensated solid-state x-ray detector be used for radiation protection applications at higher energies?

Ü Ören<sup>1</sup>, L Herrnsdorf<sup>1</sup>, M Gunnarsson<sup>1</sup>, S Mattsson<sup>1</sup> and C L Rääf<sup>1</sup>

<sup>1</sup>*Medical Radiation Physics, Department of Translational Medicine, Lund University, Skåne University Hospital, Malmö, Sweden*

Conventional personal radiation monitoring techniques, such as thermoluminescent dosimeters (TLD) and film badges, are time-consuming in preparation and assessment, and do not provide real time information about exposure. The main objective of this study was to investigate the characteristics of a solid-state detector commonly available at hospitals for parallel use as a real-time personal radiation monitor following radiological or nuclear emergency situations.

A solid-state detector probe (R100, RTI Electronics AB, Mölndal, Sweden), dedicated for quality assurance in diagnostic x-ray applications, was chosen for evaluation. The R100 has a built-in energy correction filter allowing the detector to automatically compensate for different photon energies in the energy range of conventional diagnostic X-rays. The energy dependence and the linearity in signal response for the solid-state detector were now examined for a broader photon energy range. The solid-state detector was exposed to X-ray beams using a conventional X-ray unit with effective energies ranging between 28.5-48.9 keV and to  $\gamma$ -rays: 662 keV from <sup>137</sup>Cs and 1.17 and 1.33 MeV from <sup>60</sup>Co. A cylindrical ionization chamber (10x5-6 Radcal, Monrovia, Ca, USA) was used for reference measurements. Both the R100 detector and the ionization chamber were coupled to an electrometer (Barracuda, RTI Electronics AB, Mölndal, Sweden) and the measured charge in terms of nC was recorded and used for dosimetric evaluation. All measurements with the solid-state detector were performed in the photovoltaic mode.

The solid-state detector exhibited approximately 1.8 times over-response at the X-ray energies compared to gamma photons from the <sup>60</sup>Co source. A linearity test showed that the detector demonstrated a linear response ( $R^2=1$ ), given by the charge versus air kerma, when irradiated with <sup>60</sup>Co to air kerma values in the range of approximately 20-200 mGy. We conclude that high energy photons such as those from <sup>60</sup>Co can be detected by the R100 and that the detector can provide real-time dose measurements following nuclear or radiological events.

## **Evaluation of the ionization chamber and solid state detector for a radiometric survey at radiodiagnostic facilities. Preliminary results metrology laboratory**

**F Leyton<sup>1</sup>, M Navarro<sup>1</sup>, E Matos<sup>1</sup> and I Garcia<sup>1</sup>**

*<sup>1</sup>LABPROSAUD, Instituto Federal de Bahia, Salvador, Brazil*

The radiometric survey (RS) is critical to the quality assurance program at radiodiagnostic facilities because it ensures that individuals occupationally exposed and the public are not exposed to levels exceeding doses required by law. In radiodiagnosics the radiological techniques use exposure times of the order of 0,001 to 1 second and energies between 15-150 keV. Ionization chambers and detectors used for radiometric survey should consider these restrictions. Some protocols recommend performing the RS with exposure times of at least 1 s, however, the detector response time sometimes is not indicated by the manufacturer. For these reasons, the aim of this study was to compare the response of two ionization chambers and a solid state detector in rate and integrated mode for different exposure times (1, 2, 3 & 5 s) for different kV (30 , 60, 80 and 100). For 30 kV (mammography) the current 0.1, 1 and 10 mA was used. An X-ray generator (Philips) high frequency was used. The results showed significant differences between the readings of dose rate and exposure time used for different kV, mA and modes. The factors correlate dose rates (rate mode) for different times varied between 0.95 to 2.08 times. For integrated mode, dose rates were calculated for different times and the variation was between 0.81 to 1.51. The average factor for all reads dose rate (rate mode) was 1.37 and the dose rate calculated (integrated mode) was 1.03. The factor of 2.08 was between dose rate measurements 1 to 5 s to 100 kV for an ionization chamber 230 cc. The ionization chamber 180 cc not detected dose rate for less than 3 s and no record readings to 30 kV. Conclusions: The dose rate (rate mode) underestimates the dose to less than 3 seconds. The results suggested measure integrated mode.

## Noninvasive method for the calibration of the peak voltage (kVp) meters

E Matos<sup>1</sup>, C de Navarro<sup>1</sup>, M Navarro<sup>1</sup>, F Leyton<sup>1</sup> and I Garcia<sup>2</sup>

<sup>1</sup>LABPROSAUD, Instituto Federal de Bahia, Salvador, Brazil

The risks associated with the interaction of X-rays with human body makes the diagnostic radiology an area that demands a strict quality control program (QC). The peak voltage (kVp) is an important parameter regularly evaluated within the quality assurance programs because affecting heavily the image quality and absorbed dose to patient. Therefore, the calibration kVp meters are significant to maintain a metrological reliability and thus more accurate and precise measurements. The aim of this work was to propose the implementation of the magnitude peak voltage calibration methodology (kVp) through the substitution method using non-invasive standard meter at LABPROSAUD-IFBA. The reference instrumentation has traceability to primary standards. A X-rays generator (Philips) high frequency was used. The required radiation qualities and the arrangement for calibration comply with the requirements of reference standards IEC 61676. Five kVp meters were evaluated. Comparison between the results of this work with the data of the last calibration of the kVp meters showed a good performance with maximum difference of 4%, which are within the range of uncertainty of the calibration. The estimation of measurement uncertainty was 3.4% with  $k = 2$ , for the non-invasive method complies with the requirement of the IAEA TRS 457 and IEC 61676, which must be less than 5%. Compared to another studio that used the same method was estimated a 3.12% uncertainty with  $k = 2$ . Hence, the implementation of non-invasive method was effective, bringing forward to the society a new option for the calibration and maintenance of the metrological reliability to kVp meters.

## Variations of optical properties of photon irradiated nPAG, nMAG and VIPET polymer dose gels

N Vaiciunaite<sup>1</sup> and D Adliene<sup>1</sup>

<sup>1</sup>*Department of Physics, Kaunas University of Technology, Kaunas, Lithuania*

Application of polymer gels in external radiotherapy is well known since irradiated gels may represent a three dimensional view of absorbed dose distribution. However if polymer gels are sensitive enough they also might be used for patient dose measurements and dose distribution visualization in high dose gradient fields. The purpose of this work was to compare the sensitivity of differently irradiated polymer gels based on N-Vinylpyrrolidone, metacrylic acid and acrylamide investigating their optical properties.

Series of samples (bottles filled with polymer gels: nPAG, nMAG and VIPET) were prepared in the laboratory conditions and irradiated to different doses in teletherapy unit ROKUS-M with <sup>60</sup>Co source, linear medical accelerator Clinac (Varian), X-ray device Siemens Multix PRO and HDR brachytherapy unit microSelectron v2 (Nucletron) with <sup>192</sup>Ir source. Light absorbance, reflectance and transmittance of samples before and after their irradiation were evaluated from spectral data obtained using UV-VIS spectrometer Ocean Optics USB 400. Since the dose response mechanism relies on the production of light-scattering polymer nano/micro-particles in the gel at each site of radiation absorption, optical characteristics and some polymerization parameters were evaluated at different gel depths step by step covering the whole gel volume and reconstructing the whole image at the end. Variation of optical properties due to radiation induced polymerization processes was observed in all investigated gels. It was found that optical properties of N-Vinylpyrrolidone based polymer gel was less sensitive to dose and dose rate variations than of nPAG, nMAG type gels. The highest response to irradiation/the highest polymerization rate was observed in metacrylic acid based gel samples. The results of performed optical measurements are used to discuss the enhancement of gel's sensitivity to dose variations in high gradient dose field when adjusting the gel composition and concentrations of its constituents.

## Simple surface plasmon resonance based dosimeter

D Adliene<sup>1</sup> and B G Urbonavicius<sup>1</sup>

<sup>1</sup>*Kaunas University of Technology, Kaunas, Lithuania*

The interest to application of various surface plasmon resonance (SPR) based sensors for the investigation of chemical and biological processes in thin layers deposited on the grating's surface/media is growing up. Characterization of processes as well as specimen's features might be performed analysing variations of optical properties (refraction index) of these thin layers. SPR sensors by default are characterized by high resolution and small uncertainties, measurements might be performed in situ. The aim of this work was adaptation of the SPR method for dose registration in post irradiated dose gels that change their optical properties due to radiation induced polymerization processes.

Taking into account that an adjusted periodic surface structure is a crucial feature for the surface plasmon resonance media, thin layers of nPAG and nMAG type gels were deposited by spin coating method onto commercially available grating structures (CDs). Prior to deposition, non-exposed gel samples from the same batch were irradiated to the certain doses and dose calibration curves were established. Series of prepared experimental dose sensors were placed on the PMMA phantom in the central position of the irradiation field of the X-ray unit GULMEY D3225 and were irradiated to different doses using 10x10 cm applicator. Special constructed experimental set up was used for the evaluation of refraction index of irradiated samples.

It was possible to distinguish between refraction indexes of every two samples irradiated to different doses up to 2Gy. The results obtained from the refraction index measurements using SPR based dose registration method are provided alongside with the discussion on applicability of this method for dosimetry purposes.

## Automatic segmentation of male pelvis for brachytherapy of prostate

M Kardell<sup>1</sup>, M Magnusson<sup>1,2</sup>, M Sandborg<sup>1</sup>, G Alm Carlsson<sup>1</sup> and A Malusek<sup>1</sup>

<sup>1</sup>Medical Radiation Physics, Department of Medical and Health Sciences and Center for Medical Image Science and Visualisation, Linköping University, Linköping, Sweden

<sup>2</sup>Computer Vision Laboratory, Department of Electrical Engineering, Linköping University, Linköping, Sweden

Early diagnosis and treatment of cancer, which is one of the leading causes of death in developed countries, are of great importance. Recent technological development in CT and MRI allow a synthesis of data from both modalities. Diagnostic value of such images is yet to be determined: the novel approaches need to be tested on a large number of patients and optimization of corresponding diagnostic procedures needs to follow. We focus on the development of the model-based iterative image reconstruction algorithm in dual-energy computed tomography (DECT) DIRA, which improves image quality by better suppressing beam hardening and scatter artefacts. By providing unbiased CT numbers and automatic elemental decomposition of tissues, DIRA can also be used in radiation therapy. Early versions of DIRA automatically segmented tissues into bones and soft tissue. Though this approach improved the accuracy of CT numbers compared to the classical filtered backprojection, it was obvious that better results could be achieved by an automatic segmentation that would identify individual organs and tissues in the DECT data. To address this problem we developed a 2D fully automatic algorithm (MK2014) for the segmentation of male pelvis to bone, subcutaneous fat, muscle, prostate and remaining soft tissues. It uses the following techniques: (i) Bone: histogram matching, thresholding, region growing and combined thresholding and region growing. (ii) Subcutaneous fat: histogram matching, thresholding and region growing. (iii) Muscle: histogram matching, affine registration and a deformable model. (iv) Prostate: histogram matching, affine registration and deformable model. The aim of this work is to present this algorithm.

The MK2014 algorithm was tested on 5 CT images. Ground truth was determined for 1 of those images by a radiologist. The resulting Dice similarity coefficients were 0.957, 0.911, 0.900 and 0.932 for bones, adipose tissue, muscle and prostate, respectively. The algorithm was sufficiently robust. Its disadvantage was the need for correct positioning of the patient as the atlas image strongly depended on slice position. Since this problem can be mitigated by using a 3D segmentation an extension to 3D and a validation on a larger sample of patients are planned.



## Image guided radiotherapy with heavy elements: proofs of concept

C Le Loirec<sup>1</sup>, D Chambellan<sup>1</sup> and D Tisseur<sup>1</sup>

<sup>1</sup>CEA, LIST, F-91191 Gif-sur-Yvette, France

Historically CT has been used for imaging high Z materials using dual energy CT (Eur. Radiol. 17: 1510-1517 and Med. Phys. 36: 1359-1369) and K-edge imaging in which photons with energies above the K edge of high Z agents are used for image reconstruction. However, absorption based imaging is not a dose efficient way of detecting very low concentration of high Z tracers. In contrast, as well known from Non Destructive Testing, imaging of the X-ray fluorescence of high Z elements can provide a very high sensitivity. Gold has a high Z number and a relative ease of excitation; that is why gold nanoparticles (GNPs) are commonly used as the excitation target. The  $K_{\alpha}$  fluorescent X-ray energies of gold are 66.99 and 68.80 keV; both of which are able to escape a body when high energy polychromatic X-rays are used. Tumors that accumulate GNPs can be observed as active-emission targets under high energy X-ray exposure. In vivo determination of location and quantities of GNPs can be quantified if the spatial distribution and the amount of fluorescence within a region of interest can be quantified.

XRF is a promising imaging technique for the diagnosis of tumors and the control of treatments using the photo-activation of heavy elements (Br. J. Radiol. 84: 526-33, Phys. Med. Biol. 55: 3045-3059, Phys. Med. Biol. 53: 5635-5651). Various approaches were already proposed in the literature to determine the organic-distribution and the quantity of GNPs in a tumor and other critical bodies (Phys. Med. Biol. 55: 647-62, J. Biomed. Opt. 16: 066014-1 – 066014-7, IEEE Transactions on medical imaging 31: 1620-1627, Phys. Med. Biol. 56: 3719-3730, Medical Physics 40: 051901, Med. Phys. 40: 030701, X-Ray Spectrom 38: 439-445, Med. Phys. 41: 031902). We propose to develop a new experimental device associated with dose computation software which could be used to diagnosis tumors and/or control treatment in real time. The new set-up has been validated by performing measurements and simulations. The results prove that the 2  $K_{\alpha}$  fluorescent peaks of gold can be observed and used to reconstruct the tumoral volume.

## **Optimisation conventional spin echo sequence for echo-planar diffusion-weighted (SE-EPI-DW) MRI of the Achilles tendon using high-field 3T MR scanner in clinical setting**

**M Al-Mulla<sup>1</sup>, L A Rainford<sup>1</sup> and A McGee<sup>1</sup>**

*<sup>1</sup>Department Diagnostic Imaging, School of Medicine & Medical Science, Health Sciences Centre, University College Dublin (UCD), Dublin, Ireland*

**Objective:** The aim of this study is to use advanced MR scanning techniques to develop an Echo-planar diffusion-weighted (EPI-DW) sequence capable of delineating the Achilles tendon (AT) and surrounding ankle anatomy using a high field 3T scanner in clinical setting.

**Materials and Methods:** Four volunteer ankles underwent DWI at 3T to facilitate sequence optimisation. The ankle joint, including the Achilles tendon, of 19 healthy volunteer ankles were scanned using an optimised SE-EPI-DW sequence followed by three standard FSE-based sequences with the following parameters: TR, TE, NEX and matrix respectively Axial SE-EPI-DW (2030 ms, 30 ms, 12, 112 x 526); Sagittal T1W-SE (400 ms, 12 ms, 4, 256 x 320); Axial T2W-FSE (4500 ms, 81 ms, 4, 218 x 320) and Sagittal STIR (3800 ms, 46 ms, 4, 269 x 384). An expert musculoskeletal radiologist performed visual grading analysis on a defined quality score on the MR images. OSIRIX software was used to generate ADC maps and calculate ADC values for all the ATs.

**Result:** Images acquired with different advanced techniques, enhanced diffusion image quality display, also, showed fewer image artefacts (i.e. blurring, ghosting, distortion) and inhomogeneity effects compared to optimised DWI of the AT. An expert reviewer verified AT visibility within each SE-EPI-DWI acquired and graded 79% of the data as diagnostically acceptable. This study produced novel ADC values of normal AT, found to be of the order  $0.091 \times 10^{-3} \text{ mm}^2/\text{s}$  and 95% CI: 65.92 % to 83.99 %.

**Conclusion:** SE-DW-EPI sequence acquired at 3T generates a number of artefacts due to a number of difficulties created by using DW and EPI. Using the right combination of MR techniques image quality was improved enabling imaging of body structure (AT) qualitatively and quantitatively (i.e. ADC values).

## **VGC Analyzer – a software for statistical analysis of multiple-reader multiple-case visual grading characteristics (VGC) studies**

**M Båth<sup>1,2</sup> and J Hansson<sup>1,2</sup>**

*<sup>1</sup>Department of Radiation Physics, Institute of Clinical Sciences, Sahlgrenska Academy at University of Gothenburg, Gothenburg, Sweden*

*<sup>2</sup>Department of Medical Physics and Biomedical Engineering, Sahlgrenska University Hospital, Gothenburg, Sweden*

Visual grading characteristics (VGC) analysis is a non-parametric rank-invariant method for analysis of visual grading data. In VGC analysis, image quality ratings for two different systems are compared by producing a VGC curve, similar to how the ratings for normal and abnormal cases in receiver operating characteristic (ROC) analysis are used to create an ROC curve. The use of established ROC software for the analysis of VGC data has therefore previously been proposed. However, ROC analysis is based on the assumption of independence between normal and abnormal cases. In VGC analysis this independence cannot always be assumed, e.g. if the ratings are based on the same patients imaged with both systems. The purpose of the present work was therefore to develop a software that takes possible dependencies between ratings into account in the statistical analysis of a VGC study. A computer program that performs a statistical analysis of rating data from a fully-crossed multiple-reader multiple-case VGC study was written in IDL (Research Systems, Inc., Boulder, CO). The software – VGC Analyzer – determines the area under the VGC curve ( $AUC_{VGC}$ ) averaged over the readers and applies non-parametric methods for the statistical tests: a bootstrapping resampling technique to determine the confidence interval of the  $AUC_{VGC}$  and a permutation resampling technique to determine the p-value for testing the null hypothesis that the two compared systems are equal ( $AUC_{VGC}=0.5$ ). A paired resampling is used if there is a dependency between the ratings for the two modalities. Analyses are performed both based on the trapezoidal and the binormal VGC curves and results are given both for the fixed-reader and the random-reader situations. VGC Analyzer can be obtained freely from the authors, and can hopefully simplify the use of VGC analysis in evaluations of image quality.

## Reanalysis of visual grading characteristics (VGC) data using VGC Analyzer

J Hansson<sup>1,2</sup>, L G Månsson<sup>1,2</sup> and M Båth<sup>1,2</sup>

<sup>1</sup>*Department of Medical Physics and Biomedical Engineering, Sahlgrenska University Hospital, Gothenburg, Sweden*

<sup>2</sup>*Department of Radiation Physics, the Sahlgrenska Academy, University of Gothenburg, Sweden*

**Purpose:** Visual grading studies have a weak point in that the statistical evaluation of collected data is often performed in a questionable manner. The introduction of visual grading characteristics (VGC) analysis in 2007 aimed at an improvement by presenting a non-parametric rank-invariant method of comparing visual grading data from two modalities. The resulting figure-of-merit, the area under the VGC curve ( $AUC_{VGC}$ ), was initially proposed to be determined using standard software for receiver operating characteristics (ROC) analysis. However, due to different properties of ROC and VGC data, it can be assumed that the uncertainty of the  $AUC_{VGC}$  is not determined correctly using ROC software. A novel developed software tool (VGC Analyzer) for statistical analysis of VGC data using non-parametric resampling methods has recently been verified on simulated data. The purpose of the present work was to reanalyse data from previously published VGC studies using VGC Analyzer in order to evaluate the validity of the reported results of the previous studies and to investigate the behaviour of VGC Analyzer on real data.

**Method:** Visual grading data from previously performed studies on optimisation of x-ray examinations were reanalysed using VGC Analyzer. The outcome (the mean and 95% confidence interval (CI) of the  $AUC_{VGC}$  and the p-value) was compared with previously reported data from the studies where single reader adapted ROC software had been used and rating data from multiple readers had been pooled. The studies included both paired and non-paired data and were analysed using both fixed readers and random readers.

**Major findings:** The results showed good agreement between the  $AUC_{VGC}$  determined with VGC Analyzer and the previously used methods. However, on non-paired data, narrower CIs were reported by previous studies compared to VGC Analyzer whereas in one study with paired data the reported CIs were similar or even broader using ROC software. Significance testing based on the CI and the p-value from VGC Analyzer in most cases gave the same result, but sometimes led to different results in statistically weak studies when the random reader approach was used. In these cases a p-value  $< 0.05$  was obtained although the CI of the  $AUC_{VGC}$  included 0.5.

**Conclusions:** The results of the present work indicate that studies using single reader adapted ROC software for analysing VGC data may, especially in non-paired data studies, underestimate the uncertainty of the obtained  $AUC_{VGC}$ , leading to an increased risk of Type I errors. On the other hand, incorrect use of ROC software for analysis of paired data may overestimate the uncertainty of the obtained  $AUC_{VGC}$ , leading to increased risk of Type II errors.

## **MedXViewer: An extensible web-enabled software package for flexible, collaborative and remote medical imaging viewing, perception studies and reader training.**

**P Looney<sup>1</sup>, K C Young<sup>1,2</sup> and M D Halling-Brown<sup>3</sup>**

<sup>1</sup> *National Coordinating Centre for the Physics of Mammography, Medical Physics, Royal Surrey County Hospital, Egerton Road, Guildford, United Kingdom*

<sup>2</sup> *Department of Physics, University of Surrey, Guildford, United Kingdom*

<sup>3</sup> *Scientific Computing, Medical Physics, Royal Surrey County Hospital, Egerton Road, Guildford, United Kingdom*

**Purpose:** Remote, collaborative reading training and perception studies are challenging due to heterogeneity of workstations and PACS. MedXViewer (Medical Extensible Viewer) is an application designed to allow workstation-independent, PACS-less, manufacturer-independent viewing and interaction with medical images.

**Methods and Materials:** MedXViewer has been used in a number of perception studies to date and has been extended to support reader training and data collection. The large collection of mammograms and associated data in the OPTIMAM Image database provides a rich resource of data for training or performance monitoring using digital mammograms and digital breast tomosynthesis images. Data sets can be constructed depending on conspicuity, lesion type or other parameters. The images and application can be downloaded from our centralised server. The extensible nature of the design allows for other functionality and hanging protocols to be available for each study or training session. Panning, windowing, zooming and moving through slices are all available while modality-specific features can be easily enabled.

**Results:** MedXViewer can integrate with a web-based image database allowing results from training and studies to be stored centrally. Alternatively, the software can run without a network connection where the images and results can be encrypted and stored locally. Feedback can be provided immediately or centralised and processed by a nominated administrator and accessed via a web interface.

**Conclusions:** Due to the advanced workstation-style functionality, the simple deployment on heterogeneous systems over the internet without a requirement for administrative access MedXViewer provides a useful tool for research, training or performance monitoring.

## **ViewDEX: a status report**

**A Svallkvist<sup>1,2</sup>, S Svensson<sup>1</sup>, M Håkansson<sup>2,3</sup>, M Båth<sup>1,2</sup> and L G Månsson<sup>1,2</sup>**

<sup>1</sup>*Department of Medical Physics and Biomedical Engineering, Sahlgrenska University Hospital, Gothenburg, Sweden*

<sup>2</sup>*Department of Radiation Physics, Institute of Clinical Sciences, Sahlgrenska Academy at University of Gothenburg, Gothenburg, Sweden*

<sup>3</sup>*Department of Diagnostic Radiology, Södra Älvsborgs Sjukhus, Borås, Sweden*

ViewDEX is an image viewer and task manager suitable for research and optimisation tasks in medical imaging. The software has undergone continuous development during more than a decade and has during this time period been used in numerous studies. ViewDEX is DICOM compatible and the features of the interface (tasks, image handling and functionality) are general and flexible. The setup of a study is determined by altering properties in a text-editable file, enabling easy and flexible configuration. ViewDEX is developed in Java and can run from any disc area connected to a computer. It is free to use for non-commercial purposes and can be downloaded from <http://www.vgregion.se/sas/viewdex>.

ViewDEX was originally presented at the Second Malmö Conference on Medical X-ray Imaging in 2004 (Börjesson et al, *Radiat Prot Dosimetry* 114:45-52, 2005) and at the Third Malmö Conference on Medical Imaging in 2009, a thorough evaluation of the efficiency of the software and the expenditure of time for different types of observer studies was presented (Håkansson et al, *Radiat Prot Dosimetry* 139:42-51, 2010). The purpose of the present contribution is to describe the development in recent years and report the present status of ViewDEX. Participants at the conference will also be offered the opportunity for hands-on demonstration of the software.

## Determining the chronological age of breast cancer with $^{14}\text{C}$ bomb-pulse dating and its correlation to collagen SAXS-pattern

K Lång<sup>1</sup>, A Rosso<sup>2</sup>, M Bech<sup>3</sup>, S Zackrisson<sup>1</sup>, D Graubau<sup>4</sup>, K Eriksson-Stenström<sup>5</sup> and S Mattsson<sup>6</sup>

<sup>1</sup>Department of Diagnostic Radiology/ Translational Medicine Malmö, Lund University, Malmö, Sweden

<sup>2</sup>Epidemiology and Register Centre South, Skåne University Hospital, Lund, Sweden

<sup>3</sup>Department of Medical Radiation Physics/Clinical Sciences Lund, Lund University, Malmö, Sweden

<sup>4</sup>Department of Pathology/Clinical Sciences Lund, Lund University, Lund, Sweden

<sup>5</sup>Department of Physics, Division of Nuclear Physics, Lund University, Lund, Sweden

<sup>6</sup>Department of Medical Radiation Physics/Translational Medicine Malmö, Lund University, Malmö, Sweden

**Purpose:** To establish whether it is possible to determine breast cancer age with  $^{14}\text{C}$  bomb-pulse dating and to correlate tumour age with collagen structure characterised with small angle X-ray scattering (SAXS).

**Method:** From 11 women with breast cancer, frozen and paraffin embedded tissues from 1983 were retrieved from Swedish biobanks. The frozen tissue was graphitized and the  $^{14}\text{C}/\text{C}$ -ratio was analysed with accelerator mass spectrometry.  $\delta^{13}\text{C}$  and  $\delta^{15}\text{N}$  analyses were performed to obtain dietary and metabolic information through carbon and nitrogen isotope fractionation information. The paraffin embedded samples were cut and stained with haematoxylin and eosin. Areas of cancer and healthy tissue from each patient were localised microscopically and 30  $\mu\text{m}$  thick and 200  $\mu\text{m}$  thick samples were cut. Synchrotron radiation SAXS patterns were measured for each cancer/healthy tissue pair per patient at the I911-SAXS beamline (wavelength 0.91  $\text{\AA}$ ,  $q$ -range 0.01–0.3  $\text{\AA}^{-1}$ ) at MAX-Lab, Lund University. Also, clinical data including patient history, histology and TNM-status was gathered. The feasibility of the age determination was evaluated by comparing it with clinical data.

**Major findings:** The data collection and analysis are in progress. Our first results indicate that the majority of the SAXS patterns displayed a clear difference in intensity between healthy and cancer-invaded tissue, as has been observed in earlier studies and explained by changes in the collagen structure caused by the cancer. The possible correlation between such structural changes and age of tissue will be analysed and presented.

## **Introducing the silicon photomultiplier (SiPM) technology: A flexible, modular kit for sensor testing and education at postgraduate level**

**L Herrnsdorf<sup>1</sup> and S Mattsson<sup>1</sup>**

*<sup>1</sup>Medical Radiation Physics, Department of Translational Medicine, Lund University, Skåne University Hospital, Malmö, Sweden*

The purpose is to promote education and research to improve development in the field of new radiation measurement equipment based on solid-state detectors. Silicon photomultipliers (SiPM) are attractive candidates for the replacement of the conventional PMTs since they provide high gain with low voltage and fast response. They are very compact and magnetic field compatible.

SiPM are silicon single photon sensitive devices built from an avalanche photodiode (APD) array on common Si substrate. The idea behind this device is the detection of single photon events in sequentially connected Si APDs. The dimension of each single APD can vary from 20 to 100  $\mu\text{m}$ , and their density can be up to 1000 per  $\text{mm}^2$ . Every APD in SiPM operates in Geiger-Müller mode and is coupled with the others by a polysilicon quenching resistor. Although the device works in digital/switching mode, the SiPM is an analog device because all the microcells are read in parallel making it possible to generate signals within a dynamic range from a single photon to 1000 photons for just a single  $\text{mm}^2$  area device.

Special priority is to increase knowledge when it comes to detectors for radiation protection of patients, staff and population, applications in diagnostic radiology, mammography, nuclear medicine, CT, PET, PET/MR, nuclear waste handling, radiological and nuclear accidents, etc.

The goal is to run a detector course at the postgraduate level of approximately 3-5 Hp to be held yearly starting autumn 2015 in Malmö/Göteborg. The courses will be planned in cooperation with MIT-university in Sundsvall (Electronic Design Division) and ERDIT "European Radiation Detection and Imaging Technology Platform", ref <http://www.erdit.eu/>



## Conference sponsors



**Göteborgs  
Stad**



**REGION  
VÄSTRA GÖTALAND**